Doctoral Dissertation (Censored)
博士論文 （要約）

Molecular mechanism of stress induced cellular reprograming
(ストレスによる細胞リプログラミング誘導機構の解析)

A Dissertation Submitted for the Degree of Doctor of Philosophy
February 2020
令和二年二月博士（理学）申請

Department of Biological Sciences, Graduate School of Science,
The University of Tokyo
東京大学大学院理学系研究科生物科学専攻

COLEMAN, Duncan Peter
コールマン・ダンカン・ピーター

•

Chapter 3 will be submitted for publication mid 2020 to an appropriate journal

•

Chapter 4 is under submission for publication with Plant Physiology

Acknowledgements

Over three or so years at Riken and The University of Tokyo I have received extensive guidance and assistance from a great number of people. I firstly want to share my extreme gratitude and appreciation to my supervising professor, Dr. Keiko Sugimoto, who has shown me what it means to be a great scientist, leader and mentor. Her optimism is contagious and her belief in students is invaluable. I wish to sincerely thank the amazing people in the Sugimoto Laboratory, who have assisted me with experiments, writing, and helped me develop skills to grow as a budding scientist. Additionally, I thank to the skillful technicians in our laboratory who have greatly helped my experiments run smoothly. I wish to thank Dr. Takamasa Suzuki (Chubu University) for performing sequencing and bioinformatics for the RNA-sequencing analysis. I am also very grateful to my examination committee, Dr. Munetaka Sugiyama, Dr. Hirokazu Tsukaya, Dr. Kyoko Ohashi-Ito and Dr. Tetsuji Kakutani for taking time to read and provide helpful feedback on this thesis. I also wish to thank my family, Hilary and Hamish, for their kind support while studying aboard. I was supported financially by the Ministry of Education, Culture, Sports, Science and Technology (MEXT) scholarship.

Table of Contents

•

Chapter 3 will be submitted for publication mid 2020 to an appropriate journal

•

Chapter 4 is under submission for publication with Plant Physiology

List of gene names

Gene Name	Annotation
ABI5	*ABA INSENSITIVE 5*
ABI5	*ABA INSENSITIVE 5*
ALF4	*ABERRANT LATERAL ROOT FORMATION 4*
ARF	*AUXIN RESPONSE FACTOR*
ARR	*ARABIDOPSIS RESPONSE REGULATOR*
ASA1	*ANTHRANILATE SYNTHASE A1*
CDPK	*CALCIUM DEPENDENT PROTEIN KINASE*
COI1	*CORONATINE INSENSITIVE 1*
CUC1	*CUP SHAPED COTYLEDON 1*
DORN1	*DOES NOT RESPOND TO NUCLEOTIDES 1*
DREB2A	*DEHYDRATION-RESPONSIVE ELEMENT BINDING PROTEIN 2A (DREB2A)*
ERF115	*ETHYLENE RESPONSE FACTOR 115*
ERS2	*ETHYLENE RESPONSE SENSOR 2*
ESR1	*ENHANCER OF SHOOT REGENERATION*
HSFA1	*HEAT SHOCK FACTOR A1*
HSFA2	*HEAT SHOCK FACTOR A2*
IAA3	*INDOLEACETIC ACID-INDUCED PROTEIN 3*
IPT5	*ISOPENTENYLTRANSFERASE 5*
JAZ6	*JASMONATE ZIM 6*
LBD	*LATERAL ORGAN BOUNDARY DOMAIN*
LEC	*LEAFY COTYLEDON*
MAPK	*MITOGEN ACTIVATED PROTEIN KINASE*
MMS2/HPY2	*METHYL METHANESULFONATE-SENSITIVE 21 / HIGH PLOIDY2*
MP/ARF5	*MONOPTEROS / AUXIN RESPONSE FACTOR 5*
MYB51	*MYB DOMAIN PROTEIN 51*
OBP4	*OBF BINDING PROTEIN 4*
PAT1	*PHYTOCHROME A SIGNAL TRANSDUCTION 1*
PHB	*PHABULOSA*
PHV	*PHAVOLUTA*
PLT	*PLETHORA*
PSK5	*PHYTOSULFOKINE 5*
RAB18	*RESPONSE TO ABA 18*

RAP2.6L	*RELATED TO AP2 6L*
RBOHD	*RESPIRATORY BURST OXIDASE HOMOLOG D*
REV	*REVOLUTA*
SNC1	*SUPPRESSOR OF NPR1-1, CONSTITUTIVE 1*
SCR	*SCARECROW*
SCZ/HSFB4	*SCHIZORIZA/ HEAT SHOCK FACTOR B4*
SIZ1	*SAP AND MIZ 1*
STM	*SHOOT MERISTEMLESS*
SUM1	*SMALL UBIQUITIN-LIKE MODIFIER 1*
UBQ10	*UBIQUITIN 10*
VSP1	*VEGETATIVE STORAGE PROTEIN 1*
WIND1	*WOUND INDUCED DEDIFFERENTIATION 1*
WOX5	*WUSCHEL RELATEDHOMEOBOX 5*
WUS	*WUSCHEL*
YUC	*YUCCA*

List of abbreviations

CIM	Callus inducing media
SIM	Shoot inducing media
HSR	Heat stress reponse
LRP	Lateral root primordia
TDR	Temperature dependent repression
JA	Jasmonic acid
SA	Salicyclic acid
ABA	Abscisic acid
2,4D	2,4-dichlorophenoxyacetic acid
OG	Oligogalacturonide
IAA	Indole-3-acetic acid
2-IP	2-isopentenyladenine

List of figures

Chapter 3 will be submitted for publication mid 2020 to an appropriate journal

Chapter 4 is under submission for publication with Plant Physiology

Chapter 1 Introduction

Plants follow an indeterminant developmental pathway and maintain meristematic tissue at the tips of growing roots and shoots (Scheres, 2007). As such, they have evolved the ability to repair damaged tissues and even regenerate whole organs after excision and injury (Bloch, 1941; Birnbaum and Alvarado, 2008; Ikeuchi et al., 2019). Remarkably, plants are sometimes able to produce new meristem and regenerate new organs in response to damage. This process, known as *de novo* organogenesis, and often involves some degree of cellular reprograming, or change in cell fate (Sena et al., 2009; Sugimoto et al., 2011; Ikeuchi et al., 2016; Kareem et al., 2016; Ikeuchi et al., 2019). Cellular reprograming is tightly regulated in plants and requires strong stimuli such as abiotic stresses and/or exogenous hormone application to initiate. Ability to regenerate differs greatly between plant species, mosses such as *Physcomitrella* and semi-aquatic plants such as *Rorippa aquatica* utilize *de novo* regeneration as a rapid colonization mechanism but other species such as rice and maize are relatively recalcitrant to regeneration (Ishikawa et al., 2011; Ikeuchi et al., 2019). While our understanding of molecular mechanisms regulating cellular reprograming during regeneration has improved greatly recently (Ikeuchi et al., 2019), key questions remain as to how external ques, such as wounding, are perceived and interact with developmental pathways.

1.1 Hormone-induced *in vitro* shoot regeneration

External application of plant hormones cytokinin and auxin induces cellular reprograming in many plant tissues. The advent of biotechnology and transformation of plant tissue *via* Agrobacterium transfection or particle bombardment has meant tissue culture methods have become a valuable tool to obtain genetically modified plants following transformation (Walden and Wingender, 1995). A well-established method of inducing shoot organogenesis from explants is a two-step system, whereby explants are firstly incubated on auxin-rich callus inducing medium (CIM), and then transferred to cytokinin-rich shoot inducing medium (SIM) which promotes shoot formation from callus (Valvekens et al., 1988). The molecular mechanism of this process has been partially elucidated in the model plant species *Arabidopsis thaliana* (Arabidopsis) (Fig. 1-1). One major finding is that, upon incubation of explants on CIM, auxin triggers callus formation by activating the lateral root formation pathway (Figs.

1-1 and 1-2A). It was first shown that mutation of *ABERRANT LATERAL ROOT FORMATION 4* (*ALF4*), a gene required for the initial divisions during lateral root formation, completely blocks auxin-induced callus formation (Sugimoto et al., 2010)., Auxin-activated AUXIN RESPONSE FACTOR (ARF7) and ARF19, also required for lateral root formation, induce expression of *LATERAL ORGAN BOUNDARY DOMAIN 16* (*LBD16*)*, LBD18 and LBD29*, which then promote cell proliferation during callus formation (Fan et al., 2012) (Fig. 1-1). Following this, root meristem regulators *WUSCHEL-RELATED HOMEOBOX 5* (*WOX5*), *WOX7*, *PLETHORA 1* (*PLT1*) and *PLT2* are broadly expressed in callus cells (Atta et al., 2009; Sugimoto et al., 2010). This gain of root meristem-like-identity within callus cells is crucial for the acquisition of shoot regeneration competency, as illustrated by the requirement of *PLT3/5/7*, *LBD16,* and *WOX5/7/14* for shoot formation (Kareem et al., 2015; Kim et al., 2018; Liu et al., 2018a).

Transfer to SIM induces further reprogramming of pluripotent callus, allowing the acquisition of shoot meristem identity (Figs. 1-1 and 1-2). A key molecular event underlying this cell fate transition is the transcriptional activation of a homeobox gene *WUSCHEL* (*WUS*), which is induced in the promeristem within the first few days after transfer to SIM (Atta et al., 2009). This is largely mediated by cytokinin signaling components ARABIDOPSIS RESPONSE REGULATOR 1 (ARR1), ARR10 and ARR12, which together with HD-ZIP III transcription factors like PHABULOSA (PHB), PHAVOLUTA (PHV), and REVOLUTA (REV), directly induce *WUS* expression (Meng et al., 2017; Zhang et al., 2017) (Fig. 1-1). Other important regulators of shoot regeneration are the AP2/ERF transcription factors ENHANCER OF REGENERATION (ESR1) and ESR2, which are upregulated on SIM and directly activate the expression of the shoot meristem regulators *CUP SHAPED COTYLEDON* (*CUC1*) and *CUC2* (Ikeda et al., 2006) (Fig. 1-1). Expression of the homeodomain transcriptional factor *SHOOT MERISTEMLESS* (*STM*), which is dependent on CUCs, is also required for shoot meristem formation and *in vitro* regeneration (Aida et al., 1999; Daimon et al., 2003) (Fig. 1-1). During shoot meristem formation auxin and cytokinin producing domains emerge in mutually exclusive regions. This is achieved partly by type B-ARRs repressing the expression of the auxin biosynthetic enzyme *YUC4* and the auxin-responsive ARF3 repressing expression of

ISOPENTENYLTRANSFERASE 5 (*IPT5*) which codes for a cytokinin biosynthetic enzyme (Cheng et al., 2013; Meng et al., 2017). The auxin-responsive *CUC2* and cytokinin-induced *WUS* expression domains are distinctly established after several days on SIM, suggesting that spatial separation of auxin and cytokinin during meristem formation. Pre-incubation on CIM greatly enhances shoot regeneration by establishing a pluripotent cell population in callus tissue (Valvekens et al., 1988; Che et al., 2007). Interestingly, it is also possible to directly convert lateral root primordia (LRP) to shoot meristem by incubation of on cytokinin (Chatfield et al., 2013; Kareem et al., 2016; Rosspopoff et al., 2017). This is an example of transdifferentiation where a committed cell is reprogramed directly from one cell type to another. Furthermore, converted root to shoot primordia can be reverted back to root meristem after incubation on auxin-containing media, demonstrating that cells are readily reprogrammable given the right conditions (Rosspopoff et al., 2017).

In addition to auxin and cytokinin-induced pathways, accumulating evidence suggests that wounding is required to initiate cellular reprograming during these regenerative processes (Iwase et al., 2015; Ikeuchi et al., 2019; Zhang et al., 2019a). The next section will summarize the possible link between stress and cellular reprograming, with a particular focus on wounding stress.

1.2 Primary signaling cascades induced by wounding

Wounding involves both local and wider systemic signals. Like animals, plants respond rapidly to wounding *via* reactive oxygen species (ROS) production and cellular depolarization by calcium intake and ATP release (Reymond et al., 2000; Davalos et al., 2005; Yin et al., 2007; Tanaka et al., 2014; Niethammer, 2016; Toyota et al., 2018). This results typically in the activation of systemic immunity and the production of secondary metabolites such as ethylene, salicylic acid, jasmonic acid (JA) and camalexin (Rojo et al., 1999; León et al., 2001; Chassot et al., 2008; Ogawa et al., 2010; Sun et al., 2011).

In animals, extracellular ATP may act as a strong wound signal, that acts as a chemical attractant for immune cells and induces production of inflammatory signals such as cytokines to promote inflammation and wound healing (Davalos et al., 2005; Tanaka et al., 2014). Plants also appear to utilize extracellular ATP as an important

signal in response to tissue damage and wounding. ATP, which is usually kept at a low concentration in the apoplast dramatically increases at wounded tissue as a result of leakage from damaged cells. Interestingly, around 60% of the genes induced by exogenous ATP treatment are also induced by wounding (Choi et al., 2014). Overexpression of the ATP receptor DOES NOT RESPOND TO NUCLEOTIDES 1 (DORN1) enhances expression of genes co-regulated by wounding and ATP (Choi et al., 2014). ATP signaling is also thought to activate Ca^{2+} channels in plasma membrane (Tanaka et al., 2014).

The plant cell wall is also thought to be the source of many damage-associated signals. The most well-characterized signal is the pectin derivative oligogalacturonide (OG) (Reymond et al., 1995). The OGs are thought to bind and activate Wall Associated Kinases (WAKs) (Brutus et al., 2010). Exogenous treatment of OG induces extensive phosphorylation of membrane proteins and also activation of MITOGEN ACTIVATED PROTEIN KINASEs (MAPKs) and receptor kinases (Mattei et al., 2016). OG-mediated immunity also requires CALCIUM DEPENDENT PROTEIN KINASEs (CDPKs), suggesting an interaction with calcium signaling (Gravino et al., 2015).

Another primary wound signal is thought to be glutamate, which binds to a family of ligand-gated calcium-channels called GLUTAMATE-RECEPTOR LIKE (GLR) (Qi et al., 2006; Mousavi et al., 2013; Toyota et al., 2018). GLR3.3 and GLR3.6 are required for the propagation of the Ca^{2+} wave from the wound-site to systemic tissue *via* the vasculature where defense response genes are sharply upregulated (Toyota et al., 2018). Like ATP, glutamate is thought to be released from damaged cells to initiate the response although this has not been demonstrated. Exactly how the calcium wave is perceived to induce the defense response is not clear, however recent work in root epidermal cells has demonstrated that Ca^{2+} activates the protease METACASPASE 4 (MC4) in response to wounding within seconds. MC4 cleaves a small elicitor peptide PEP1 to activate the defense response by binding to receptor kinases in neighboring cells (Hander et al., 2019).

Generation and transmission of ROS is another important local and systemic long distance signal in response to wounding (Miller et al., 2009; Gilroy et al., 2014). RESPIRATORY BURST OXIDASE HOMOLOG D (RBOHD), an NADPH oxidase, generates ROS species after wounding (Miller et al., 2009; Evans et al.,

2016). Activation of RBOH occurs *via* several routes including direct binding of Ca^{2+}, phosphorylation by kinases such as CPK5 and botrytis-induced kinase 1 (BIK1) and binding of plant Rho-type (ROP)-GTPase (Kobayashi et al., 2007; Gilroy et al., 2014). ROS signaling is also required for activation of systemic acquired resistance in response to heat and high light (Suzuki et al., 2013; Zandalinas et al., 2019), and may act *via* abscisic acid (ABA) signaling to regulate stomatal opening (Devireddy et al., 2018). Thus, ROS acts as important rapid secondary signaling mechanism in response to various abiotic stresses.

1.3 The role of wounding and other abiotic stress in cellular reprograming

The phenomena of wound healing and regeneration has long been investigated (Bloch, 1941; Sugiyama, 2015), and recent studies have begun to uncover the molecular link between wounding and cellular reprogramming that underlies various modes of regeneration processes. The following sections will summarize the role of wounding and other stresses in several examples of regeneration in plants.

1.3.1 Wound-induced cellular reprograming in animals

Animals often utilize migration of specialized stem cells to repair wounded tissues (Birnbaum and Alvarado, 2008; Cordeiro and Jacinto, 2013). Wounding results in initiation of rapid electrical signaling and an increase in ROS in animals which activate rapid signaling cascades and transcriptional output (Miller et al., 2009). Wounding may activate transcription factors by post-translational modification to initiate cellular reprograming. For example, the phosphorylation of key transcription factors in response to epithelial wounding in Drosophila embryos activate transcription of wound healing and epithelial regeneration genes (Mace et al., 2005; Kim and McGinnis, 2011). Accumulation of ROS in response to wounding was also shown to promote cell division and regeneration of excised Zebrafish tails (Niethammer et al., 2009; Yoo et al., 2012).

1.3.2 Wound-induced root meristem repair

Cutting the root meristem tip from the main root can induce complete regeneration of lost stem cell niche from remaining cells of the proximal meristem (Feldman, 1976; Efroni et al., 2016) (Fig. 1-2B). Lineage tracking and cell type marker analysis showed

cellular origins of regenerated tissue are diverse and that cutting induces reprograming of competent cells within several hours (Efroni et al., 2016). This process is mediated by auxin and cytokinin domain partitioning reminiscent of embryo development (Barlow, 1974; Efroni et al., 2016). A key wounding-inducible regulator of this is ERF115, an AP2-ERF-type transcription factor that together with its interacting partner PHYTOCHROME A SIGNAL TRANSDUCTION 1 (PAT1), promotes reconstruction of the meristem (Heyman et al., 2016). ERF115 induces expression of *PHYTOSULFOKINE 5 (PSK5)* and *WIND1* to subsequently promote cell division and dedifferentiation (Heyman et al., 2013; Heyman et al., 2016). Activation of ERF115-mediated regeneration is thought to be induced by a combination of stress and hormonal cues. The wound-inducible plant hormone JA can induce the expression of *ERF109* and *ERF115* and subsequently promote division of the QC (Zhou et al., 2019). This is carried out by the JA-responsive transcription factor MYC2, which directly binds and activates transcription of *ERF109* and *ERF115* within minutes after wounding and this is dependent on the JA-receptor CORONATINE INSENSITIVE 1 (COI1) (Zhou et al., 2019). ERF109 transcriptionally activates *CYCD6;1* which together with ERF115, suppresses activity of root-stem-cell differentiation-promoting factors, and promotes QC formation and root regeneration. Interestingly both JA and auxin can synergistically activate expression of *ERF115*, indicating a key point of convergence between these pathways during regeneration (Zhou et al., 2019).

In addition to non-targeted wounding of the root meristem, micro-resolution laser ablation has also allowed for cell-type-specific observation of wound-induced regeneration (Hoermayer and Friml, 2019). The QC can regenerate from surrounding cells after being ablated, and this is dependent on SHR-SCR- and PLT-mediated specification of the new QC and restoration of polar-auxin transport (Xu et al., 2006). In addition to QC regeneration, other cell types in the root apical meristem wounded by laser ablation are able to regenerate, following periclinal cell division and cellular reprogramming of inner-adjacent cells (epidermis, cortex, endodermis and pericycle) (Marhava et al., 2019). As with whole root meristem regeneration, the capacity to regenerate wounded cells in the root decreases with distance from the QC, however overexpressing *PLT2* is able to confer competency to more distant cells, suggesting that PLTs are key regulators of pluripotency (Marhava et al., 2019). Wound healing

and regeneration in the RAM of plants provide and exemplary model of the interaction between stress-activated reprograming pathways and hormone-induced networks which typically regulate cellular organization.

1.3.3 Wound-induced shoot meristem repair

Like the root apical meristem, the shoot apical meristem (SAM) is able to repair after wounding (Sussex, 1964; Reinhardt et al., 2003). As in roots, competency to repair damaged stem cells in the SAM relies on the remaining cells to initiate cell division and express shoot stem cell regulators such as *WUS*. A report in tomato (*Solanum lycopersicum*) demonstrated that complete ablation of the SAM central zone can be fully repaird after several days, demonstrating the remarkable regenerative capacity of cells in the SAM (Reinhardt et al., 2003). The authors also tested if application various stress signals such as JA, salicylic acid (SA) and H_2O_2 could promote expression of genes involved in meristem repair. However, as they did not see an effect, they concluded that physical wounding itself is required for initiation of cellular reprograming in this context (Reinhardt et al., 2003).

1.3.4 Wound-induced callus formation

As part of the wound healing process plants often develop callus at the wound site in order to protect against pathogens and repair damaged tissue (Bostock and Stermer, 1989; Ikeuchi et al., 2013). Wound-induced callus sometimes regenerates into new tissues or organs, suggesting that it can be pluripotent like auxin-induced callus (Stobbe et al., 2002). A useful assay to study wound-induced callus utilizes etiolated hypocotyls which readily form callus from the wound site when the apical half is excised (Fig. 1-2C). This is largely driven by up-regulation of cytokinin biosynthesis and cellular proliferation from vasculature cells (Iwase et al., 2011; Ikeuchi et al., 2017). Upregulation of cytokinin biosynthesis genes and consequential activation of cytokinin signaling after wounding are required for callus formation as cytokinin biosynthesis mutant *log123457* and A-type ARR mutants *arr1 arr12* have severely impaired callus formation (Ikeuchi et al., 2017). Transcriptomic analysis by RNA sequencing of wounded hypocotyls interestingly showed rapid upregulation of root

stem cell regulators, such as *ERF115*, *PLT3* and *PLT7*, within one hour, which also contribute to callus formation (Ikeuchi et al., 2017). Although stress hormone JA accumulates in wounded hypocotyls, JA signaling is not required for wound-induced callus formation (Ikeuchi et al., 2017).

It is unclear what role auxin plays in this process as it does not appear to accumulate in wounded hypocotyls as opposed to other wounded tissue such as detached leaves (Chen et al., 2016; Bustillo-Avendaño et al., 2017; Ikeuchi et al., 2017). Despite this difference between tissues, WIND1, ESR1, and ERF115 promote callus induction and growth from both petiole and hypocotyl cut sites, suggesting that they play a more general role in cellular reprograming (Iwase et al., 2011; Ikeuchi et al., 2017). WIND1 likely promotes callus formation from cut petioles by its downstream target *ESR1* as overexpression of *ESR1* can rescue the callus phenotype in *WIND1-SRDX* plants (Iwase et al., 2017). Wound-induced callus formation is thus one example of cellular reprograming governed by wound-induced reprograming genes.

1.3.5 *de novo* root regeneration from leaf explants

After excision from the main plant body, leaf explants in a number of species are able to regenerate roots (Fig. 1-2D). As with other cases of regeneration, auxin plays an important role in this process by accumulating within hours after detachment in vascular tissue near the cut site and initiating cell division (Sukumar et al., 2013; Liu et al., 2014; Chen et al., 2016). Auxin acts by activating the ARFs, which transcriptionally activate homeobox transcription factor *WOX11* which in turn promotes fate transition of cells in the vasculature near the wound site to root founder cells (Liu et al., 2014). Importantly, this is dependent on wound-inducible auxin biosynthesis genes including *YUCCA1* (*YUC1*) and *YUC4* (Chen et al., 2016), as well as *ANTHRANILATE SYNTHASE α1* (*ASA1*), which encodes an enzyme in tryptophan biosynthesis, a precursor to auxin (Zhang et al., 2019a). Jasmonic acid (JA) is an important wound signal, which activates expression of JA-responsive genes within 10 minutes after detachment. These include *ERF109*, a transcription factor involved in wound healing that directly binds *ASA1* to promote auxin biosynthesis (Zhang et al., 2019a). Wounding therefore directly activates cellular reprogramming *via* the phytohormones JA and auxin in the context of *de novo* root regeneration.

1.3.6 Role of wounding during *in vitro* shoot regeneration

Exogenous hormone application itself is usually insufficient to induce shoot regeneration on tissue culture from roots of intact seedlings. Wounding and excision of root explants is required to regenerate shoots from roots, suggesting wounding provides a key trigger to initiate cellular reprograming (Iwase et al., 2015). Wound-inducible transcription factor *WIND1*, and its homologs, *WIND2-4*, promote callus formation and acquisition of regeneration competency (Iwase et al., 2011; Iwase et al., 2015; Iwase et al., 2017). As overexpression of *WIND1* is sufficient to promote shoot regeneration in uncut seedlings and *WIND1-SRDX* explants are severely defective in shoot regeneration on SIM, it is considered to be a key component of wound-inducible signals to confer cellular reprograming (Iwase et al., 2015). WIND1 promotes shoot regeneration by directly upregulating *ESR1* expression near the cut sites (Iwase et al., 2017). Hormone application further promotes expression of *ESR1*, thus providing an example of molecular convergence of stress and hormone signaling during regeneration. ESR1 is thought to directly activate its homologue *ESR2* and subsequently promote expression of other shoot meristem regulators (Banno, 2001; Ikeda et al., 2006; Matsuo et al., 2011; Iwase et al., 2017). It is not clear whether the WIND1-ESR1 pathway is required immediately after wounding or later after incubation on SIM. How wounding and stress signals initiate expression of reprograming genes such as *WIND1* and interact with hormonal cues during *in vitro* shoot regeneration is also not known.

The contribution of wound and stress-inducible signals such as JA to organ regeneration seems to be context-dependent. JA treatment improves shoot and root regeneration of Pistachio (*Pistacia Vera L.*, Dolcet-Sanjuan and Claveria, 1995) but inhibits shoot regeneration from pine (*Pinus radiata,* Tampe et al., 2001). As JA is transiently induced upon wounding (Koo et al., 2009) it is possible that this is only required for the initial hours after cutting and not during incubation on hormone-supplemented media. This is supported by a recent report that shows pretreatment of JA before cutting and incubating explants on hormone-supplemented media promotes shoot regeneration (Park et al., 2019). Additionally, JA-receptor *coi1* mutants show reduced regeneration efficiency, suggesting JA is required for *in vitro* shoot

regeneration (Park et al., 2019). Although largely governed by hormones auxin and cytokinin, evidence described here suggests stress stimuli and downstream reprograming transcriptional regulators also contribute to *in vitro* shoot regeneration. Given the complexity of the plant stress response, other novel wounding- or other stress-induced transcriptional regulators are likely involved in shoot regeneration.

1.3.7 Role of abiotic stress during somatic embryogenesis

Somatic embryogenesis is the process where embryos form from somatic cells and this can be induced by application of the synthetic auxin 2,4-dichlorophenoxyacetic acid (2,4-D) (Su et al., 2009). In addition to auxin, abiotic stress is also thought to play a key role. Shoot meristem explants from carrot induce somatic embryogenesis when incubated on hormone-free media containing high concentration of NaCl and then transferred to media with low salt concentration (Kiyosue et al., 1989). Other treatments with sodium hypochlorite, cadmium, and sucrose similarly induces somatic embryogenesis (Kamada et al., 1989). Extended incubation at high temperature can also induce somatic embryogenesis from carrot seedlings (Kamada et al., 1994) and from immature microspores of brassica species (Keller and Armstrong, 1979; Ahmadi et al., 2014). The stress-induced hormone ABA accumulates during the initial few days of incubation of carrot seedling explant on phytohormone-free hyperosmotic media and this is required for stress-induced embryogenesis (Kikuchi et al., 2006). JA has also been shown to partially rescue the requirement for wounding in somatic embryos formed from Arabidopsis seedlings (Mozgová et al., 2017) and enhance efficiency of somatic embryogenesis from microspores in *Brassica napus* (Ahmadi et al., 2014). Other reports have shown that H_2O_2 treatment can improve embryogenesis from immature wheat embryos (Szechyńska-Hebda et al., 2012; Becker et al., 2014; Schmidt and Schippers, 2015). It appears that during somatic embryogenesis, cellular reprograming pathways are activated by extreme external stimuli such as severe heat and osmotic stresses in addition to wound stress.

1.4 Activation of heat response pathway by wounding

It is clear that the wound response in plants is complex and wound-inducible factors influence cellular reprograming differently depending on the context. One approach taken in our laboratory to better understand the transcriptional response to wounding in plants, was to perform time-series RNA-sequencing (RNA-seq) analysis of wounded plants (Ikeuchi et al., 2017; Rymen et al., 2019). These studies suggested that some components of the heat stress response (HSR) are upregulated after wounding in both hypocotyl and root tissues (Ikeuchi et al., 2017; Rymen et al., 2019). The HSR involves expression of ROS scavenging enzymes, and chaperone *HEAT SHOCK PROTEINs* (*HSPs*) which protects the cell from proteotoxic stress (Kotak et al., 2007; Ohama et al., 2016b). Plants have evolved an extensive transcriptional network that governs rapid response to heat stress as a means to withstand extreme temperature changes experienced in the natural environment. The master regulators of HSR are the HEAT SHOCK FACTOR A1 (HSFA1) family of transcription factors. HSFA1s act as transcriptional activators, upregulating other important transcription factors involved in the HSR such as *DEHYDRATION-RESPONSIVE ELEMENT BINDING PROTEIN 2A* (*DREB2A*), *HSFA2* and *HSFBs*. *HSFA2* expression is required for thermotolerance (Charng et al., 2006). The transcriptional repressors *HSFB*s are also induced by HSFA1 and act in a negative feedback mechanism to repress other HSFs including HSFA1 (Ikeda et al., 2011). Gene expression profiling of these *HSF*s revealed that they are upregulated in response to a number of other stresses including high light, salt, drought and pathogen infection (Miller and Mittler, 2006; Liu et al., 2011). Thus, the HSFs are thought to play a wider role in stress responses in plants, however, little is known in regard to their role in response to wounding.

1.5 HSFs are a potential regulator of cellular reprograming

HSFs function as important regulators of stress response to maintain cellular integrity during severe stress such as heat stress. Additionally, they may play a role in plant growth and development during benign stress since HSFA1b binds to and regulates a number of developmental genes (Albihlal et al., 2018). Several lines of evidence suggest that HSFs function in cellular reprograming. For example, overexpression of

HSFA2 can promote CIM-induced callus growth from root explants (Ogawa et al., 2007). Overexpression of *HSFA2* in the *hsfa1abde* background also promotes callus formation from the SAM after addition of heat stress (Liu and Charng, 2013). In addition, many components of HSR including *HSF*s and *DREB*s are highly expressed during CIM-induced callus formation (Che et al., 2006), which might be induced by wounding and/or highly active cell proliferation and metabolism in callus. Furthermore, gene regulatory network analysis by a yeast-one-hybrid assay revealed that HSFs can bind to the promoter of many known reprograming genes including *PLT3*, *ESR1* and *ARR*s (Ikeuchi et al., 2018). It is also shown that HSFB1 and HSFA2 can directly activate expression of *HSFB4/ SCHIZORIZA (SCZ)* which codes for an important cell fate regulator in the root meristem (Pernas et al., 2010). These previous studies together suggest that HSFs are potential regulators of stress-induced cellular reprograming.

1.6 Mechanism of stress-induced HSFA1 activation

Increasing evidence suggests that the activity of HSFA1s is strictly regulated by multiple mechanisms including post-translational modification and protein-protein interaction (Ohama et al., 2016b). While it is not clear exactly how plants sense heat stress, it is generally accepted that ROS and calcium signaling are involved (Volkov et al., 2006; Kotak et al., 2007; Driedonks et al., 2015; Vu et al., 2018). Stress-induced ROS is shown to be required for full HSR activation (Volkov et al., 2006), and the product of ROS results in nitrogen oxide accumulation that may activate HSFA1s *via* the secondary signaling component calmodulin 3 (CaM3) (Xuan et al., 2010). Calcium-permeable channels which open in response to heat have also been proposed to activate HSFA1s (Ohama et al., 2016b). Accordingly, the regulation of HSFA1s occurs almost exclusively at the protein level. This is demonstrated by the relatively limited impact that *HSFA1* overexpression has on heat-stress-inducible genes compared to overexpression of other *HSFA*s such as *HSFA2* or *HSFA3* (Nishizawa et al., 2006; Yoshida et al., 2008; Yoshida et al., 2011; Ohama et al., 2016a). A key regulatory mechanism of HSFA1s is the inhibitory interaction with HSP70 and HSP90 (HSP70/90). Under non-stressed conditions HSP70/90 binds HSFA1 at a conserved HSFA1-specific domain designated the temperature-dependent repression (TDR)

domain. HSP70/90 binding appears to partially inhibit HSFA1 by sequestering the protein in the cytoplasm, as HSFA1d mutant protein with a deleted TDR domain (HSFA1dΔ1) is localized almost exclusively in the nucleus, while the wild type protein is localized in the cytoplasm and nucleus (Ohama et al., 2016a). Upon heat stress HSFA1 protein is liberated from HSP70/90 and becomes nuclear localized where it activates transcription of downstream genes. The mechanism of how HSP70/90 dissociates is unclear but it is proposed that accumulation of unfolded protein in the cytoplasm during heat stress draws the HSP70/90 away from HSF, allowing it to become activated (Richter et al., 2010).

Additionally, post-translational modification and oligomerization are thought to provide the necessary precise control of HSFA1 activation (Åkerfelt et al., 2010; Ohama et al., 2016b). Phosphorylation of HSFA1 orthologue in *Chlamydomonas reinhardtii.*upon heat stress has been observed (Schmollinger et al., 2013). In Arabidopsis CYCLIN-DEPENDENT KINASE A1 (CDKA1) and CALMODULIN-BINDING PROTEIN KINASE 3 (CBK3) phosphorylate and regulate DNA-binding activity of HSFA1, while PROTEIN PHOSPHATASE (PP7) can interact with HSFA1 potentially to dephosphorylate it (Reindl et al., 1997; Liu et al., 2008). While it is not clear which phosphorylated residues contribute to HSFA1 activity, mutation of a putatively phosphorylated tyrosine residue located in its TDR domain leads to its activation, indicating that this phosphorylation may be an important point of regulation (Ohama et al., 2016a). As phosphorylation-mediated activation of human HSFA1 is important, it is expected that plants employ a similar mode of activation (Holmberg et al., 2001; Åkerfelt et al., 2010). HSFA1-mediated promotion of target gene expression is thought to involve the eviction of the repressive histone variant H2A.Z, thus providing another layer of regulation to this response in order to prevent leaky expression (Cortijo et al., 2017). Regulation of HSFA1 protein activity is mediated by post-translational modifications and protein-protein interactions that allow rapid and precise control of its activity and the HSR.

1.7 Roles of SUMOylation in stress response and development

Abiotic stresses such as heat, drought, and wounding have been shown to induce transcriptional-independent signals that act as important primary trigger to alter gene

expression of stress-responsive genes (Cheong et al., 2002; Rymen et al., 2019). Post-translational modification of protein represents an important layer of regulation that enables intricate control of protein function in many signaling pathways which regulate environmental responses and developmental processes. Advantages of post-translational modification include enabling rapid activation of protein function in response to acute stress, as well as energy-efficient fine-tuning of transcriptional responses appropriate for the perceived stress (Mazzucotelli et al., 2008). Despite the rapid progress in the elucidation of transcriptional mechanisms underlying organ regeneration, little is known about the contribution of post-translational regulation in this process.

Plants utilize a combination of protein modifications to regulate protein activity, including the extensively characterized phosphorylation and ubiquitination (Bachmair et al., 2001; Mazzucotelli et al., 2008; Guerra et al., 2015). Additionally, conjugation of the SMALL UBIQUITIN-LIKE MODIFIER (SUMO) peptide has been implicated in regulating a number of important transcriptional regulators (Castro et al., 2012; Augustine and Vierstra, 2018). SUMOylation is a multi-step process and involves, sequentially, SUMO-activation by E1 enzymes, SUMO-conjugation by E2 enzymes and the final step of ligation catalyzed by E3 enzymes (Augustine and Vierstra, 2018). Unlike ubiquitination for which over 1400 putative E3 ligases have been found in Arabidopsis (Kraft et al., 2016), SUMOylation is catalyzed by only two E3 ligases, the SAP-MIZ domain-containing (SIZ1) and METHYL METHANESULFONATE-SENSITIVE 21 / HIGH PLOIDY2 (MMS2/HPY2) (Ishida et al., 2009; Ishida et al., 2012; Kwak et al., 2016; Liu et al., 2016). Recent advances in proteomic approaches have identified around 1000 SUMOylated proteins, of which a large number (80%) are predicted to be nuclear localized, such as transcription factors, chromatin remodeling enzymes and histones (Shiio and Eisenman, 2003; Miller et al., 2010; Rytz et al., 2018). Transcriptomic profiling of *siz1* mutants showed that around 7% of all genes (~1600) are differentially expressed under control conditions, suggesting basal SUMO-mediated gene expression is broad and involved in a range of transcriptional networks (Catala et al., 2007).

SUMOylation of proteins in plants is increased in response to stresses such as severe heat, ROS, cold, and drought stress (Kurepa et al., 2003; Catala et al., 2007;

Castro et al., 2012; Miller et al., 2013). SUMO is thought to play a protective role against proteotoxic stress (protein unfolding) as well as regulating protein activity. Heat stress induces destabilization of proteins and induction of the HSR. In animals SUMO-mediated regulation of HSFs is much more established in the literature than in relation to plants (Hietakangas et al., 2003; Hietakangas et al., 2005; Åkerfelt et al., 2010). In plants, HSR components are particularly over-represented among SUMOylated proteins identified by proteomics including HSFA1D, HSFA2, HSFB2B, HSFC1, HSP70-1, suggesting that this response is directly regulated by SUMOylation (Miller et al., 2010; Rytz et al., 2018). The role of SUMOylation in the HSR appears to be complex, as different pathways of the response are antagonistically regulated by SUMOylation. Homeostasis of SUMOylated protein levels in the plant is required for thermotolerance as either increasing SUMOylation by overexpressing *SUMO1 (SUM1)* or *SIZ1*, or conversely, mutating *SIZ1*, which reduces SUMOylation, both result in reduced thermotolerance and misexpression of HSR genes (Yoo et al., 2006; Catala et al., 2007; Saracco et al., 2007; Cohen-Peer et al., 2010; Zhang et al., 2018). SIZ1 modifies several HSFs including the seed-specific HSFA9 and HSFA4a (Carranco et al., 2017), HSFA2 (Cohen-Peer et al., 2010), as well as SlHSFA1 in tomato (Zhang et al., 2018). It is therefore possible that SIZ1 promotes thermotolerance by moderating and fine-tuning the expression of their target genes in response to severe stresses.

The loss-of-function *siz1* mutant in Arabidopsis displays a pleiotropic phenotype, due to the many roles that SUMO plays in regulating stress and developmental pathways (Lomelí and Vázquez, 2011). Several well characterized targets of SIZ1 in addition to HSFs include TOPLESS-RELATED 1 (TPR1), a negative regulator of SA-mediated immunity, that when SUMOylated, suppresses plant immunity (Lee et al., 2007; Niu et al., 2019). Mutants of *SIZ1* therefore display stunted growth and an autoimmune response partially due to accumulation of SA, and this can be rescued by expressing the bacterial SA-degrading enzyme *NahG* or introducing a mutation in SA signaling into the *siz1* mutant (Lee et al., 2007; Hammoudi et al., 2018). SIZ1 also suppresses ABA signaling by SUMOylation of the key regulator of the ABA response ABA-INSENSITIVE 5 (ABI5) (Miura et al., 2009). Additionally, SUMO negatively regulates JA signaling by enhancing the inhibitor of COI1, JASMONATE

ZIM 6 (JAZ6) (Srivastava et al., 2018). Growth and developmental pathways regulated by SUMO include FLOWERING LOCUS C (FLC)-mediated flowering (Kong et al., 2017), secondary cell wall formation (Liu et al., 2019), DELLA-mediated growth (Achard et al., 2009; Conti et al., 2014), and photomorphogenesis by negatively regulating the ubiquitin E3 ligase COP1 and phytochrome-B (Sadanandom et al., 2015; Lin et al., 2016; Kim et al., 2017; Hammoudi et al., 2018). SUMO also regulates key players of auxin signaling, described in a recent study which demonstrated ARF7 SUMOylation promotes interaction with its negative regulator INDOLEACETIC ACID-INDUCED PROTEIN 3 (IAA3), consequently contributing to root branching toward water (Orosa-Puente et al., 2018). Together these examples demonstrate that SUMO-mediated regulation spans a range of processes in plants.

1.8 Purpose of thesis

The purpose of this thesis is to uncover new regulators of stress-induced cellular reprograming in the context of *in vitro* shoot regeneration. Previous work in our

•

Chapter 3 will be submitted for publication mid 2020 to an appropriate journal

•

Chapter 4 is under submission for publication with Plant Physiology

chapter, will describe the role of the SUMO E3 ligase SIZ1 as a negative regulator of *in vitro* shoot regeneration. In the loss-of-function *siz1* mutants, I show the wound response is hyperactivated, and that this partially contributes to enhanced shoot regeneration *via* regulators such as *WIND1*. [redacted]

[redacted]

[redacted] Altogether, this thesis aims to provide important insights into stress-induced cellular reprogramming and uncover a novel ppathways regulating *de novo* organogenesis.

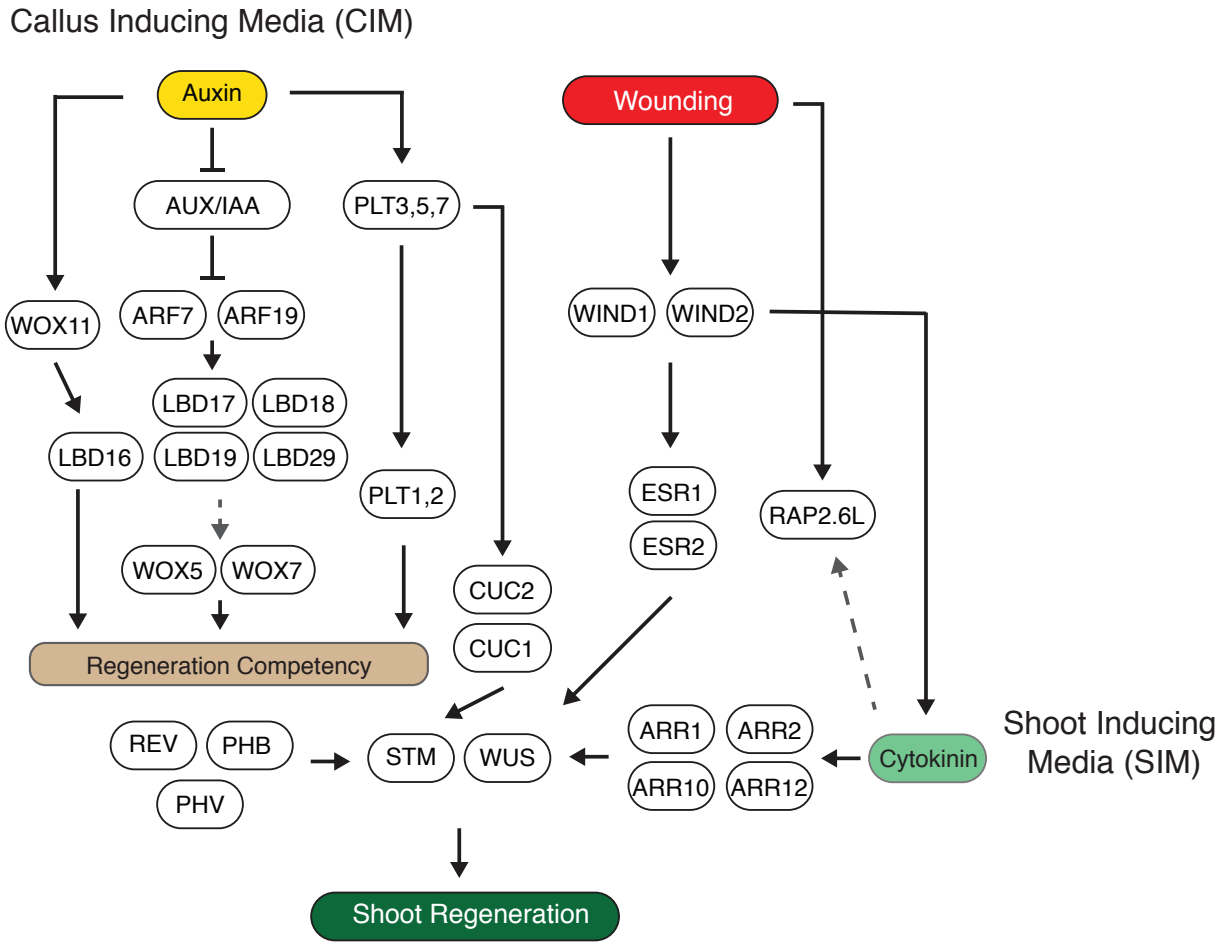

Figure 1-1. **Molecular mechanism of in vitro shoot regeneration.**
Auxin activates ARF7 and ARF19 to promote expression of the *LBD*s. This leads to cell proliferation and expression of root meristem regulators *WOX5* and *WOX7*. Auxin also induces expression of *PLT*s which are required for regeneration competency. Wounding promotes expression of *WIND1* and *WIND2* which upregulate *ESR1* and *ESR2* to promote expression of shoot meristem genes. Cytokinin induces expression of shoot meristem regulators *WUS* and *STM* by the A-type ARRs which also require HD-ZipIII transcription factors REV, PHB, PHV as binding partners.

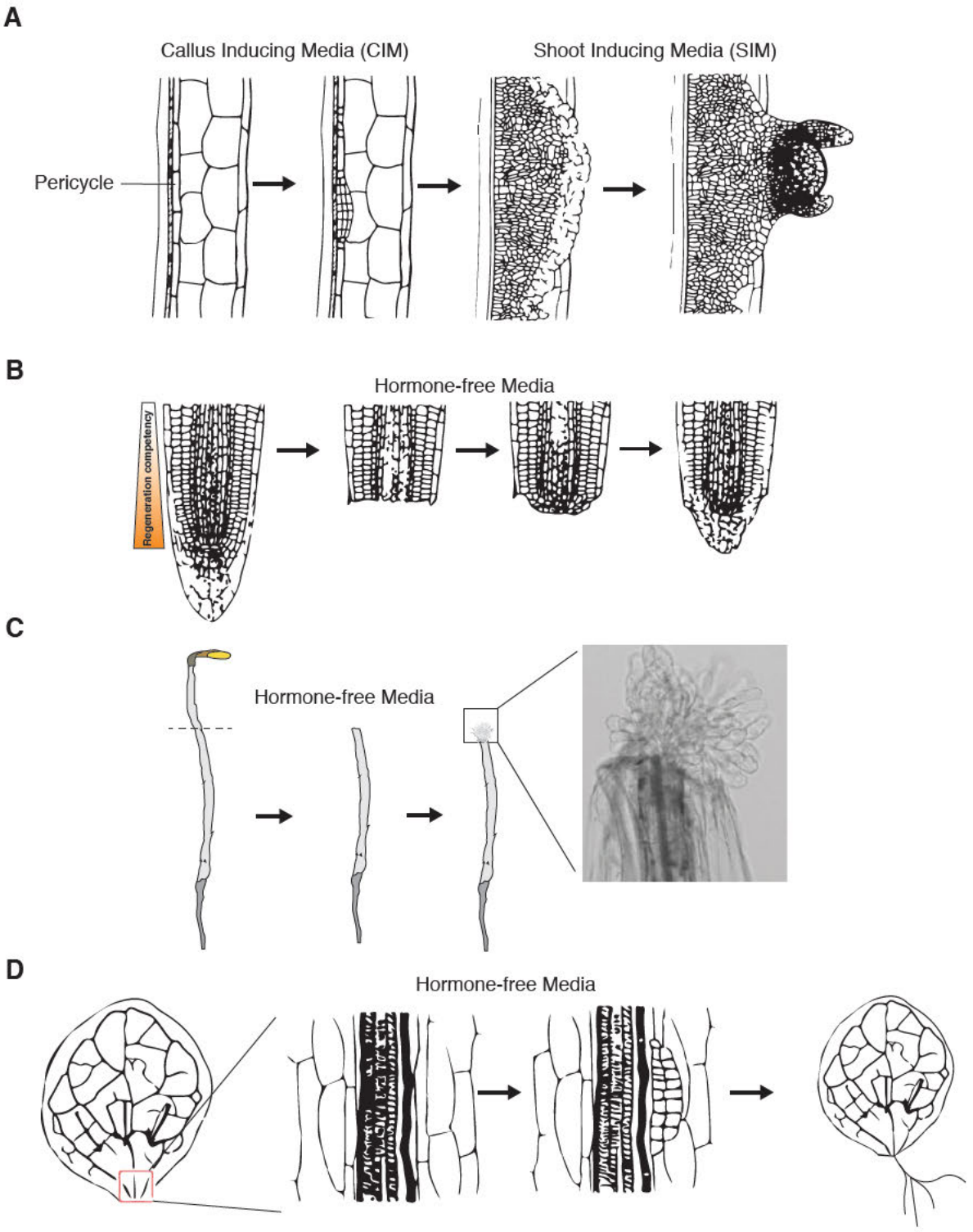

Figure 1-2. **Examples of cellular reprograming**.
(A) *in vitro* shoot regeneration from root explants or hypocotyl explants. auxin-rich callus inducing media (CIM) induces callus from pericycle cells which gain pluripotency and regenerate shoot meristem after incubation on cyotokinin rich shoot inducing media (SIM).**(B)** Root meristem repair after exision of the root tip occurs after incubation on hormone free media. The ability to repair diminishes with distance from the quiescent center (QC). **(C)** Wound-induced callus formation from cut hypocotyl of dark-grown seedlings. **(D)** *de novo* root regeneration from detached leaf explants occurs as cells near the cut site in the vasculature reprogram and divide to form root meristem. Images **(A , B and D)** were modified from Ikeuchi et al., (2019) and **(C)** was modified from Ikeuchi et al., (2017).

Chapter 2 Materials and Methods

2.1 Plant materials and growth conditions

All *Arabidopsis thaliana* (Arabidopsis) genotypes used in this study are listed in Table 2-1. Double mutants were generated by cross pollinating respective genotypes and heterozygous F1 seedlings were selected either by PCR or presence of fluorescent protein using a fluorescent dissection microscope (Leica M165FC). Homozygous F2 plants were selected by PCR (for tDNA mutants) or at F3 for other transgenic lines. Genotypes of *arf7-2 arf19-5* (Goh et al., 2012) was confirmed by CAPS/dCAPs using the primers listed in Table 2-2 , and PCR products were digested using *Hpy*99I for *arf7-2* and *Alu*I for *arf19-5*. Multiple mutants and transgenic lines previously published are listed (Table 2-1). Seeds were stratified for 3 days at 4°C and then sown onto Murashige and Skoog (MS) media containing 1% Sucrose and 0.6% (w/v) Gelzan™ (Sigma-Aldrich). Seedlings were incubated under constant fluorescent white light (approximately 50 μmol m^{-2} s^{-1}) at 22°C.

2.2 *in vitro* shoot regeneration

Seedlings were grown in the dark for 7 days to induce etiolation. Hypocotyl explants (around 10 mm long) were excised using a razor blade (Feather) and incubated on CIM (Gamborg B5 medium with 0.25% Gelzan, 0.5 μg/ml 2,4-dichlorophenoxyacetic acid [2,4-D] and 0.05 μg/ml kinetin) for 4 days under constant light. Hypocotyl explants were then transferred to SIM (Gamborg B5 medium with 0.25% Gelzan, 0.15 μg/ml IAA and 0.5 μg/ml 2-IP) and incubated for several days to induce shoot regeneration. To quantify callus growth on CIM, individual calli ($n > 30$) were first dabbed on a Kimwipe to remove media and then weighed using an XS104 balance (Mettler Toledo). Projection of callus area from callus after 4 days on CIM was quantified from DIC images taken with an OLYMPUS BX51 microscope and the area of visible callus was quantified using ImageJ software. To quantify shoot regeneration on SIM, the number of shoots visible per explant was counted. Shoots were defined as regions with viable leaves with trichomes and appearing to arise from a single meristem as visualized from the top with an OLYMPUS SZX7 microscope.

2.3 Wound-induced callus assay

Wound-induced callus assay was performed by cutting the hypocotyl of 7-day-old dark-grown seedlings about 3 mm below the shoot apical meristem and incubating them on MS in constant light at 22°C for 4 days. Presence of callus was assessed by formation of more than 3 callus cells protruding from the cut-site when visualized with an Olympus SZX7 microscope. Images of growing callus was measured after 10 days on MS and the projected area of each callus was measured using ImageJ software.

2.4 Confocal microscopy analysis and imaging

For all fluorescent marker lines explants were mounted in either water or propidium iodide (PI) before imaging with a Leica SP5 confocal microscope with an HCXPLAPO CS 20x0.70 DRY UV lens. GFP was excited at 488nm. A z-stack was taken through the sample and projected images were generated using ImageJ Bio-Formats plugin with sum of slices.

2.5 Cloning of *HSFA1dΔ1* and transformation of *XVE-HSFA1dΔ1*

DNA was extracted from plants with the *35S::HSFA1dΔ1* transgene (Ohama et al., 2016a) and the coding region of *HSFA1dΔ1* was amplified with PRIMESTAR MAX polymerase (Takara) and the forward primer (5'-CACCATGGATGTGAGCAAAGTAAC-3') and reverse primer (5'-TCAAGGATTTTGCCTTGAGAGATC-3'). The amplified PCR product was cleaned up with Wizard® SV Gel and PCR Clean-Up System (Promega) and ligated into the entry vector pENTR/D-TOPO Cloning Kit (Invirogen). After confirmation by sequencing, the construct was then cloned into the gateway-compatible binary vector pER8GW (Papdi et al., 2008) using the Gateway LR Clonas II Enzyme (Invitrogen). The binary vector was transformed into wild type Col-0 plants using the floral-dip method (Clough and Bent, 1998). Seedlings containing the transgene were selected on media containing spectinomycin and hygromycin antibiotics. T2 lines segregating in a 3:1 ratio were selected followed by selection of non-segregating homozygous T3 lines again on antibiotic containing media.

2.6 Analysis of gene expression by RT-qPCR

RT-qPCR was performed as previously described (Shibata et al., 2018). Total RNA was extracted from 7-day-old whole seedlings using an RNeasy Plant Mini Kit (Qiagen). Extracted RNA was reverse transcribed using a PrimeScript RT-PCR kit with DNase I (Perfect Real Time) (Takara) in accordance with the accompanying protocol. Transcript levels were determined by RT-qPCR using a THUNDERBIRD SYBR qPCR Mix kit (Toyobo) and an Mx399P QPCR system (Agilent). The primers used are listed in Table 2-3.

2.7 Transcriptomic analysis by RNA-seq

Total RNA was extracted from ~50 hypocotyl explants either immediately after cutting, following 4 days of incubation on CIM or following either 4 or 6 days of incubation on SIM. Samples for different genotypes within the same biological replicate set were incubated on the same plate, and three biological replicates were used. WT and *siz1-2* explants were harvested simultaneously, one replicate at a time. Total RNA was isolated using the RNeasy plant mini kit (Qiagen) following the manufacturer instructions. Isolated RNA was subject to library preparation with the Kapa stranded mRNA sequencing kit (KK8420, Kapa Biosystems) and Illumina-compatible FastGene adapters (NGSAD24, Nippon Genetics). Single-end sequencing was performed on an Illumina NextSeq500 platform, and mapping was carried out using Bowtie (Langmead and Salzberg, 2012), and over 85% of reads were uniquely mapped on the TAIR10 Arabidopsis genome, resulting in 8 to 15.5 million mapped reads per sample.

Differences in expression between wild type and mutants was calculated with the edgeR package (Robinson et al., 2009) in R using the weighted-trimmed-mean method to calculate normalization values, and the HTSFilter package (Rau et al., 2013) was used to filter lowly-expressed genes. Volcano plots were made using the ggplot2 package (Wickham, 2016), clusterProfiler (Yu et al., 2012) was used for GO analysis, and the heatmaps.2 function in the gplots package was used to generate heatmaps. Venn diagrams were generated using an online tool available at http://bioinformatics.psb.ugent.be/webtools/Venn/.

2.8 Immunoprecipitation of HSFA1-GFP

Approximately 60 2-week-old seedlings grown at 22°C were subject to heat stress (37°C 1 hour), frozen in liquid Nitrogen and ground using a bead shocker (Yasui Kikai) in 50 ml tubes. Next, 4-5 ml of extraction buffer (100mM Tris-HCl (pH 8.0), 0.1% (w/v) SDS, 0.5% (v/v) Sodium Deoxycholate, 1% (v/v) Glycerol, 50mM Sodium Metabisulfite, 20mM N-Ethylmaleimide (NEM), cOmplete™ Protease Inhibitor Cocktail (Sigma-Aldrich), Pefabloc SC (Sigma-Aldrich) was added and mixed. Samples were then cleared by centrifugation at 2500 rpm 15 minutes and supernatant was kept and protein concentration was measured by Bradford assay (Bio-Rad) as follows. Sample was diluted (1/10) in water and 10 μl was mixed with Bradford reagent in a 96 well plate and incubated at room temperature for 15 minutes. Absorbance was read using a plate reader (Infinite 200 Pro, TECAN) at 595 nm. Protein (2 ml diluted to 4-5μg/ul in extraction buffer) was used for immunoprecipitation. 25 μl per sample of GFP-Trap (Chromotek) beads were equilibrated by washing 3 times with 1 ml of extraction buffer and then added to the protein sample. The sample was incubated for 1 hour at 4°C and then the beads were pulled down with a magnetic rack and supernatant was discarded. Beads were washed 3 times with extraction buffer and protein was eluted with 70 μl of 1xSDS-sample buffer pre-heated to 96°C, and then further incubated at 96°C for 5 minutes. Beads were removed and the sample was loaded onto SDS-PAGE and subject to western blot (described in detail below).

2.9 Western blot analysis with antibody against SUMO1

Around five 7-day-old light-grown seedlings were frozen in liquid nitrogen and ground with a bead shaker (Yasui Kikai) in 2 ml tubes. After thawing on ice, 200 μl of extraction buffer (10 mM TrisHCl pH 9.0, 6 M Urea, cOmplete™ Protease Inhibitor Cocktail (Sigma-Aldrich), and 0.05% Triton-X) was added to the sample and briefly vortexed. Protein concentration was measured by Bradford assay (as described above), denatured by addition of Laemmli buffer (Bio-Rad), 50 μg was run on SDS-PAGE (AnyKB, Bio-Rad) and transferred to PVDF membrane with Trans-Blot Turbo (Bio-Rad) semi-dry transfer system. The membrane was blocked with either 5% skim milk for 3 hours or with Can-Get-Signal enhancer kit (Toyobo) according to manufactures

instructions and propped with Anti-GFP-HRP antibody (sc-8334) or custom-made anti-SUMO1 (Ishida et al., 2009) and donkey-anti-rabbit-HRP (Sigma-Alrich).

2.10 Accession numbers

RNA-sequencing data have been deposited to Gene Expression Omnibus (https://www.ncbi.nlm.nih.gov/geo/) under accession number GSE141188 (The review token to access the private GEO record is: ijazegecjliftgp).

Table 2-1. List of plant materials

AGI	gene name	allele	code	Accession	Reference
AT5G60410	*SIZ1*	*siz1-2*	SALK_065397	Columbia	
AT5G60410	*SIZ1*	*siz1-3*	SALK_034008	Columbia	
AT5G60410	*SIZ1*	*siz1-2 pSIZ1::SIZ1*		Columbia	Jin et al., 2008
	NahG	*NahG*		Columbia	Delaney et al., 1994
		siz1-2 NahG		Columbia	Lee et al., 2007
AT2G17950	*WUS*	*gWUS-GFP$_3$ (WUS-GFP)*		Columbia	Tucker et al., 2008
AT3G11260	*WOX5*	*pWOX5::ER-GFP (WOX5-GFP)*		Columbia	Billou et al., 2005
	WIND1	*pWIND1::WIND1-SRDX (WIND1-SRDX)*		Columbia	Iwase et al., 2011
		DR5rev::GFP (DR5-GFP)		Columbia	Benková et al., 2003
		TCSn::GFP (TCS-GFP)		Columbia	Zürcher et al., 2013
AT5G20730, AT1G19220	*ARF7 ARF19*	*arf7-2 arf19-5*		Columbia	Goh et al., 2012
AT4G14550	*IAA4/SLR1*	*slr1-1*		Columbia	Fukaki et al., 2002
		siz1-3 slr1-1		Columbia	
		siz1-3 arf7-2 arf19-5		Columbia	
		siz1-3 WIND1-SRDX		Columbia	
		siz1-3 WUS-GFP		Columbia	
		siz1-3 WOX5-GFP		Columbia	
		siz1-3 DR5-GFP		Columbia	
		siz1-3 TCS-GFP		Columbia	
AT4G17750, AT1G32330, AT5G16820	*HSFA1a HSFA1b HSFA1d*	*hsfa1abd*	SAIL_410_E01	Columbia/ Wassilewskija	Lohmann et al., 2003; Yoshida et al., 2011
		hsfa1abd pHSFA1d::HSFA1d		Columbia/ Wassilewskija	Ohama et al. 2016
AT1G32330	*HSFA1d*	*hsfa1d*	SALK_022404	Columbia	
AT2G26150	*HSFA2*	*hsfa2*	SALK_008978	Columbia	
AT1G32330	*HSFA1d*	*35S::HSFA1d*		Columbia	Ohama et al. 2016
AT1G32330	*HSFA1d*	*35S::HSFA1dΔ1*		Columbia	Ohama et al. 2016
AT1G32330	*HSFA1d*	*XVE-HSFA1dΔ1*		Columbia	

Table 2-2. List of primers used for genotyping

Gene	Allele	WT forward	WT reverse	Left border (LB)
SIZ1	*siz1-2*	GAGCTGAAGCATC TGGTTTTG	CACGACAGATGAA GCATTGTG	TGGTTCACGTAGTGG GCCATCG
SIZ1	*siz1-3*	TCCCTCGTAGACA TCTGATGG	AAAGAGAGAGTGAG CGAAGGG	TGGTTCACGTAGTGG GCCATCG
NahG	*NahG*	GCCTTAGCACTGG AACTCTG	TCGGTGAACAGCAC TTGCAC	TGGTTCACGTAGTGG GCCATCG
WUS	*WUS-GFP*	CCCTTGCGCTTTC TCTTGAGC	TTGAAGTCGATGCCCT	TGGTTCACGTAGTGG GCCATCG
WIND1	*WIND1-SRDX*	CAGTGGAACGAGA CGTTCTCG	AGCGAAACCCAAACCG AGTTCGAG	TGGTTCACGTAGTGG GCCATCG
HSFA2	*hsfa2*	AAGGTTCCGAACC AAGAAAAC	TCCTTCCACGTTACTT CAAGC	TGGTTCACGTAGTGG GCCATCG
ARF7	*arf7-2*	GCAGATGACTCTT CAGCCAGT	AGCTCCTGACAAGGT GGTTG	
ARF19	*arf19-5*	TGAAACATAAATG CCGCTCA	AAATAGTTTGAAACGC AATGAACTTACTA	

Table 2-3. List of primers used for RT-qPCR

Gene	AGI	Forward (5'-3')	Reverse (5'-3')
PP2A	AT1G69960	TAACGTGGCCAAAATG	GTTCTCCACAACCGCTTGGT
HSFA1d	AT1G32330	TCGTTTGGAAACCACCGGAGT	CTGGGTCAACCTTCCTGAAACCAT
PP2A	AT1G69960	TAACGTGGCCAAAATG	GTTCTCCACAACCGCTTGGT
OBP4	AT5G60850	TGGAGATCGAACGGCTCAGGTTGA	CCACTTCCCCAATCCAACGGTTCA
WIND1	AT1G78080	GATCTCACATCGGAGGCGATT	CCACCGATCGAAACCGAATTC
WIND2	AT1G22190	GAGCTGACGTTTGGTGATACG	TTACAAGACTCGAACACTGAAG
RAP2.6	AT1G43160	CCATTGATTACCGGTTCAGCTGTG	ATACACGTGTCGCTTGTGTGG
WOX2	AT5G59340	TTGAATGCAAGTAATGCTGATGG	TCAATAAACGGCTGCTCTCGGC

•

Chapter 3 will be submitted for publication mid 2020 to an appropriate journal

•

Chapter 4 is under submission for publication with Plant Physiology

Chapter 3 will be submitted for publication mid 2020 to an appropriate journal

Chapter 3 will be submitted for publication mid 2020 to an appropriate journal

Chapter 3 will be submitted for publication mid 2020 to an appropriate journal

Chapter 3 will be submitted for publication mid 2020 to an appropriate journal

Chapter 3 will be submitted for publication mid 2020 to an appropriate journal

Chapter 3 will be submitted for publication mid 2020 to an appropriate journal

Chapter 3 will be submitted for publication mid 2020 to an appropriate journal

Chapter 3 will be submitted for publication mid 2020 to an appropriate journal

Chapter 3 will be submitted for publication mid 2020 to an appropriate journal

Chapter 3 will be submitted for publication mid 2020 to an appropriate journal

Chapter 3 will be submitted for publication mid 2020 to an appropriate journal

Chapter 3 will be submitted for publication mid 2020 to an appropriate journal

Chapter 3 will be submitted for publication mid 2020 to an appropriate journal

Chapter 3 will be submitted for publication mid 2020 to an appropriate journal

Chapter 3 will be submitted for publication mid 2020 to an appropriate journal

Chapter 4 SIZ1 negatively regulates shoot regeneration

4.1 SIZ1 negatively regulates *in vitro* shoot regeneration

Post-translational regulation of transcriptional regulators is an important mechanism to efficiently and rapidly modulate their activity in response to external stimuli and during development (Mazzucotelli et al., 2008). The attachment of the SMALL UBIQUITIN-LIKE MODIFIER (SUMO), catalyzed by the E3 ligase SIZ1, to protein regulates several important stress and developmental pathways (Castro et al., 2012; Augustine and Vierstra, 2018). In order to investigate the role of SIZ1 in the control of *de novo* organogenesis, I tested whether mutants for *SIZ1* display altered shoot regeneration using a two-step tissue culture procedure. Two *siz1* loss-of-function alleles, *siz1-2* and *siz1-3* produce truncated proteins, however still retain all DNA binding domains and an E3 ligase catalytic domain (Fig. 4-1). Both of these mutations result in impaired SUMOylation and consequently pleiotropic phenotypes (Catala et al., 2007; Miura et al., 2010; Rytz et al., 2018). I sought to characterize these mutants during organ regeneration on tissue culture media. As previously described (Valvekens et al., 1988), I cut hypocotyl segments and incubated them on CIM for 4 days, before transferring them to SIM. Wild type Col-0 (WT) explants start to regenerate shoots around 9 days after transfer to SIM, leading to the formation of on average 5 visible shoot per explant at 14 days (Fig. 4-2A, B). However, in two loss-of-function mutant alleles for *SIZ1*, *siz1-2* and *siz1-3*, shoot regeneration is dramatically enhanced, with regenerated shoots appearing by 8 days on SIM and more than 12 shoots regenerating after 14 days (Fig. 4-2A, B). Explants of *siz1* mutants also appeared greener than WT by 7 days on SIM (Fig. 4-2C), supporting that the initiation of shoot developmental program is advanced by the *siz1* mutation. These enhanced shoot regeneration phenotypes in *siz1-2* are rescued in *siz1-2 pSIZ1::SIZ1*, expressing *SIZ1* under the control of its native promoter which was previously shown to complement the thermotolerance phenotype in *siz1-2* (Jin et al., 2008) (Fig. 4-2A, B). These results thus clearly demonstrate that SIZ1 negatively regulates shoot regeneration. Next, to test whether *siz1* mutation could enhance shoot regeneration in other tissues I performed the same shoot regeneration procedure using root explants from light-grown seedlings. As with hypocotyl explants, *siz1* mutants regenerated 2 to 3 times more shoots from root explants after incubation on SIM for 17 days than WT and this phenotype was also rescued in *siz1-2 pSIZ1::SIZ1* (Fig. 4-

2D, E). These data thus demonstrate that SIZ1 suppresses shoot regeneration in multiple tissue types.

Since pre-incubation of explants on CIM is a prerequisite for shoot regeneration on SIM (Che et al., 2007), I next tested if the *siz1-3* mutation causes enhanced callus formation on CIM which could be responsible for the observed subsequent promotion of shoot regeneration on SIM. As shown in Fig. 4-3A, B, however, both callus size and morphology are indistinguishable between WT and *siz1-3* after 4 days on CIM, the time point at which the explants are transferred to SIM. It is therefore unlikely that enhanced shoot regeneration on SIM is a secondary consequence of enhanced callus formation during CIM incubation. However, I did observe that after prolonged incubation on CIM, the *siz1* mutants eventually develop substantially larger callus (Fig. 4-3C, D), indicating that SIZ1 also negatively regulates callus formation on CIM in the long term culture.

4.2 The *siz1* mutation causes a hyperactivation of the wound response

In order to explore the molecular basis underlying enhanced shoot regeneration in *siz1* mutant, I performed genome-wide transcriptomic analysis using RNA-sequencing (RNA-seq). Similar to analysis described in chapter 3, I compared gene expression in WT and *siz1-2* at 4 time points; immediately after excising the hypocotyls (after cut), after 4 days on CIM and after both 4 and 6 days on SIM (Fig. 4-4A). Among these time points, I observed the most drastic differences in the global gene expression pattern immediately after cutting, when 1375 genes are upregulated and 912 genes are downregulated in *siz1-2* (edge-R; FDR < 0.05) (Fig. 4-4B). The differences in the gene expression profile are far less prominent at 4 days on CIM where only 187 genes are upregulated and 66 genes are downregulated (Fig. 4-4B). After transfer to SIM however, the gene expression pattern is again profoundly affected by the *siz1* mutation. After 4 days on SIM, I detected 593 genes upregulated and 640 genes downregulated, and by 6 days on SIM the number of mis-expressed genes further increased (Fig. 4-4B). It is worth noting that this expression pattern is similar to the *35S::HSFA1dΔ1* line described in Fig. 3-6. Interestingly, I found that mis-expressed genes in *siz1-2* are largely distinct to after cut, on CIM and on SIM (Fig. 4-4C). For instance, I detected that only 15% of the genes upregulated after cutting are also up on SIM (211 genes

out of 1375 genes), and I observed a similar trend for downregulated genes in *siz1-2*, as the overlap between downregulated genes after cutting, on CIM and on SIM is small (Fig. 4-4C). Consistently, Gene Ontology (GO) enrichment analysis demonstrated that genes associated with unique biological processes are upregulated in *siz1-2* at each of these time points (Fig. 4-5A). In contrast, I observed less distinct GO enrichment among downregulated genes (Fig. 4-5B). Using these datasets I additionally found that while some genes of the SUMOylation pathway are differentially expressed in WT across the different time points, expression of *SIZ1* is fairly stable (Fig. 4-6), implying that the activity of SIZ1 is not regulated at the transcriptional level.

Among genes upregulated in *siz1-2* immediately after cutting, I found that those associated with stress response are strongly represented. GO categories such as "response to water" (p = 2.5e-31), "response to oxidative stress" (p = 6.7e-25), and "response to wounding" (p = 1.1e-14) are highly represented (Fig. 4-5A), implying that the stress response is hyperactivated in *siz1-2,* again similar to *35S::HSFA1dΔ1* (Fig. 3-7). To test whether this apparent hyper response is caused by cutting or constitutively present in *siz1* even in non-stress conditions, I examined the overlap between the genes highly expressed upon cutting in my dataset and those upregulated in intact *siz1-2* and *siz1-3* plants as reported in other studies (Catala et al., 2007; Rytz et al., 2018). As shown in Fig. 4-7A, more than 80% of the genes present in my dataset (1112 genes out of 1375 genes) are unique to it, supporting that a substantial portion of the transcriptional upregulation we detect in *siz1* is caused by cutting. I did still see the overlap of our dataset with either of the previously published ones is still significant (p = 1.0e-58 and p = 3.7e-16; hypergeometric test), suggesting that my dataset includes some genes constitutively activated in *siz1*. To further examine how much of the genes in my dataset are induced by wounding, I compared my dataset with previously published transcriptomic data for wounded hypocotyls (Ikeuchi et al., 2017). As shown in Fig. 4-7B, more than 40% of genes (561 genes out of 1375 genes, p = 4.8e-28; hypergeometric test, representation factor = 1.5) upregulated in *siz1* are induced within 3 hours following cutting of hypocotyls in WT. Importantly, 404 genes out of these 561 genes are upregulated only after cutting and not in intact *siz1* plants

(Fig. 4-7B), indicating that *siz1* mutants display a hypersensitive response to wounding stimuli.

Phytohormones including SA, JA, ABA and ethylene are known to play complex inter-dependent roles in regulating the response to wounding (Mcconn et al., 1997; Birkenmeier and Ryan, 1998; Wang et al., 2002; Yamada et al., 2004). Accordingly, GO categories such as response to JA (p = 3.89e-14) and response to SA (p = 4.24e-9) are enriched among genes upregulated in *siz1-2* (Fig. 4-5A). I indeed found that around 380 genes implicated in SA and/or JA-mediated signaling are transiently induced by wounding in WT hypocotyls and their induction is much more pronounced in *siz1-2* (Fig. 4-7C). These include SA-induced *UBIQUITIN 10* (*UBQ10*) (Blanco et al., 2005) and *MYB DOMAIN PROTEIN 51* (*MYB51*), the latter of which encodes a transcription factor acting as a major regulator of stress-induced glucosinolate biosynthesis (Frerigmann and Gigolashvili, 2014). JA-induced *VEGETATIVE STORAGE PROTEIN 1* (*VSP1*) (Ellis and Turner, 2002; Nemhauser et al., 2006) is also among genes highly expressed in *siz1-2* after wounding (Fig. 4-7 C, D).

Previous studies have shown that *siz1* mutants exhibit an auto-immune response due to the accumulation of SUPPRESSOR OF NPR1-1, CONSTITUTIVE 1 (SNC1) protein and consequential increase in SA levels (Gou et al., 2017; Hammoudi et al., 2018; Niu et al., 2019). My RNA-seq data, however, showed that the expression of *SNC1* and several SA-induced genes is mostly comparable after cut between WT and *siz1-2* explants (Fig. 4-8A). I did observe upregulation of *SNC1* and SA-induced genes such as *PATHOGENESIS RELATED 2* (*PR2*) and *PR5* in *siz1-2* explants on SIM (Fig. 4-8), implying that SA signaling is enhanced on SIM. The dwarf phenotype caused by SA accumulation in *siz1* mutants can be suppressed by introduction of a bacterial salicylate hydroxylase, *NahG*, which degrades this phytohormone (Lee et al., 2007; Miura et al., 2010). In order to investigate if hyper-accumulation of SA could be responsible for the enhanced shoot regeneration phenotype observed in *siz1* mutants, I compared *siz1-2* mutant expressing *NahG* (*siz1-2 NahG)* (Lee et al., 2007) with the *siz1-2* single mutant. As shown in Fig. 4-8B,C, the introgression of *NahG* does not affect the enhanced shoot regeneration phenotype in *siz1-2*, indicating that this phenotype is independent of SA signaling. Consistently, I found that the enhanced

callus phenotype of *siz1* is not rescued by expressing *NahG*, indicating that it is also independent of SA accumulation in the mutant (Fig. 4-8 D, E).

Further investigation of differentially expressed genes after cutting revealed that 39 genes associated with the GO category “cellular response to abscisic acid stimulus” are hyper-induced in *siz1-2* after cut (p = 3.49e-9). SIZ1 is known to negatively regulate ABA signaling by SUMOylating the transcription factor ABI5, leading to the downregulation of its direct target gene *RESPONSE TO ABA 18* (*RAB18*) (Miura et al., 2009). In my dataset I found that the expression of *RAB18* is upregulated in *siz1-2* (Fig. 4-7C, D), implying that ABI5-mediated ABA signaling is hyperactivated in *siz1-2* after wounding. Similarly, I found that 51 genes associated with GO categories “response to ethylene” or “cellular response to ethylene stimulus” are strongly expressed in *siz1-2* after cut (p = 3.9e-11 and p = 8.8e-3 respectively, Fig. 4-7C, D). These include the ethylene-induced ethylene receptor *ETHYLENE RESPONSE SENSOR 2* (*ERS2*) (Wang et al., 2002; Nemhauser et al., 2006), suggesting that ethylene signaling is also affected in *siz1-2.*

When Arabidopsis hypocotyls are subjected to wounding without any external hormone application, they develop callus from wound sites (Iwase et al., 2011). Given that the *siz1* mutants display enhanced transcriptional responses to wounding, I next tested if this could affect callus formation at wound sites. As previously reported (Iwase et al., 2011), I cut the top end of hypocotyls and incubated the explants on hormone-free media. I found that callus induction is clearly more pronounced in both *siz1-2* and *siz1-3* mutants, with nearly 75% of their hypocotyl explants producing callus within 4 days after cutting, as opposed to 56% for the WT (Fig. 4-9A). Importantly, this enhanced callus formation is also not caused by SA accumulation, as introduction of *NahG* does not abolish this phenotype (Fig. 4-9A). To test whether SIZ1 regulates callus growth after wounding I measured the area of callus which formed at the wound site of hypocotyls. I found that there was no significant difference between the area of callus formed from the wound site (Fig. 4-9B), indicating that SIZ1 negatively regulates the induction of wound-induced callus but not its growth.

4.3 SIZ1 negatively regulates expression of HSR genes

SIZ1 is known to regulate the HSR by SUMOylating several Heat Shock Factors (HSFs) including HSFA2 (Cohen-Peer et al., 2010). Since several components of the HSR are upregulated after wounding (Fig. 3-1) (Ikeuchi et al., 2017; Rymen et al., 2019) I wanted to test if the *siz1* mutation would result in hyper induction of these genes, as observed with other wound-inducible genes (Fig. 4-7). As *35S:HSFA1dΔ1-GFP* expressing plants have constitutively active HSR, I first compared the list of genes upregulated in *35::HSFA1dΔ1-GFP* explants (Fig. 4-10A) with genes upregulated in *siz1-2* . As shown in Fig. 4-10A, the overlap between the sets of genes was significant (p = 4.1e-143, hypergeometric test) with 857 from 3077 genes upregulated in *35:HSFA1dΔ1-GFP* being also upregulated in *siz1-2.* This suggested that *siz1-2* mutation and *HSFA1dΔ1* overexpression can influence expression of a common set of genes. Closer inspection of known components in the HSR revealed that many are highly expressed in *siz1-2*, particular after cutting (Fig. 4-10), suggesting that SIZ1 negatively regulates wound-induced expression of the HSR. As HSFA2 activity is partially regulated by SUMOylation and is known to be required for full activation of the HSR (Cohen-Peer et al., 2010) I tested if HSFA2 is involved in shoot regeneration. Compared to WT, the loss-of-function *hsfa2* mutant did not display altered callus formation or shoot regeneration (Fig. 4-10C, D). Furthermore, introgression of *hsfa2* into *siz1-3* did not appear to suppress either the enhanced callus formation phenotypes or shoot regeneration phenotype in *siz1-3* (Fig. 4-10C, D). Together these data demonstrate that SIZ1 does not suppress shoot regeneration and callus formation in an HSFA2-dependent pathway. This result does, however, support the possibility that SIZ1 represses regeneration by negatively regulating the HSFA1s.

4.4 HSFA1d is a SUMOylation target *in vivo*

The activity of HSFA1s is regulated primarily at the protein level by protein-protein interaction with HSP70/90, phosphorylation and potentially by SUMOylation (Ohama et al., 2016b). While previous work showed that HSFA1s are extensively phosphorylated (Ohama et al., 2016a), there is no direct evidence that HSFA1s can be SUMOylated in Arabidopsis. Given that several HSFA1 downstream genes are

upregulated in *siz1-2* (Fig.4-10A) and HSFA1s are involved in shoot regeneration (Chapter 3), I wanted to test if HSFA1 could be modified by SUMOylation. To address this question, I performed an immunoprecipitation on whole-protein extracted from *35::HSFA1d-GFP* and *35S::HSFA1dΔ1-GFP* seedlings. As heat strongly induces protein SUMOylation in plants, these seedlings were subjected to heat stress by incubating at 37°C for 1 hour before pulling down the GFP protein conjugated to HSFA1d and HSFA1dΔ1. Probing the whole-protein extract with an anti-SUMO1 antibody revealed that SUMOylated proteins dramatically accumulate in these plants following heat stress (Fig. 4-11A). After pulling down and probing the HSFA1-GFP proteins with the anti-SUMO1 antibody, I observed that the full-length protein is highly SUMOylated after heat stress treatment (Fig. 4-11B), while SUMOylation of HSFA1dΔ1-GFP was dramatically reduced to around 16% of the levels observed in full-length protein (Fig. 4-11B). These data demonstrate that HSFA1d is modified by SUMOylation *in vivo*, and that this process requires the region truncated in the HSFA1dΔ1 protein.

4.5 Elevated *WIND1* expression contributes to the enhanced shoot regeneration phenotype in *siz1* mutants

Wounding induces transcriptional activation of many key regulators that mediate cellular reprograming and organ regeneration (Iwase et al., 2011; Ikeuchi et al., 2017; Rymen et al., 2019). According to my RNA-seq dataset, some of these wound-induced reprogramming regulators are upregulated in *siz1-2* (Fig. 4-12A). Consistent with previous reports (Iwase et al., 2011; Ikeuchi et al., 2017; Rymen et al., 2019), the expression of both *WIND1* and *WIND2* is transiently elevated upon wounding in our dataset, and these genes are hyperactivated after cut in *siz1-2* (Fig. 4-12B). My qRT-PCR analysis further showed that the expression of these and several other wound-induced genes is also enhanced in *siz1-2 NahG* (Fig. 4-12C), strongly suggesting that this transcriptional activation is not due to the SA-dependent auto-immunity. To test if enhanced expression of *WIND1 or WIND2* may be responsible for the enhanced shoot regeneration phenotype observed in *siz1* mutants, I crossed *pWIND1:WIND1-SRDX* (*WIND1-SRDX*), which expresses a dominant-negative version of WIND1 proteins, into *siz1-3*. As shown in Fig. 4-12D, the *siz1-3 WIND1-SRDX* explants regenerate a

significantly reduced number of shoots compared to *siz1-3*, and additionally, regenerate shoots at levels greater than WT. This suggests that enhanced shoot regeneration in *siz1* mutants is partially dependent on WIND1 but may also act on pathways downstream of WIND1 to repress shoot regeneration. To further explore whether SIZ1 acts in the same pathway with WIND1, I compared genes upregulated in *35S:WIND1* plants (Iwase et al., 2011) with our dataset. Around 12% of genes upregulated in *siz1-2* after cut (163 of 1375 genes) and 23% of genes upregulated in *siz1-2* at 4 days on CIM (43 of 187 genes) are also overexpressed in *35S:WIND1* seedlings (Fig. 4-12E). Genes upregulated in *siz1-2* on SIM also included a significant but relatively smaller number of WIND1-mediated genes (Fig. 4-12E). This indicates that SIZ1- and WIND1-mediated pathways regulate a significantly overlapping set of genes. Taken together, these results show that the hyperactive wound response in *siz1* mutants contributes to their enhanced ability to regenerate shoots.

4.6 The auxin response is minimally affected in the *siz1* mutant

When performing GO analysis on the 187 genes up-regulated in *siz1-2* explants compared to WT after a 4-day incubation on CIM, I observed a lower degree of functional enrichment compared to other time points, suggesting that SIZ1 plays a minimal role during CIM incubation (Fig. 4-5). Given that auxin is primarily responsible for cell cycle re-entry and acquisition of regeneration competency during CIM incubation (Fan et al., 2012; Ikeuchi et al., 2013), I further examined whether a transcriptional response to auxin is altered in *siz1-2*. Among the 6935 genes in my RNA-seq dataset that are significantly induced in WT explants after 4 days of CIM incubation compared to after cut, 716 genes are induced by auxin according to previously published transcriptome datasets (Nemhauser et al., 2006; Goda et al., 2008; Omelyanchuk et al., 2017) (Fig. 4-13A). As shown in Fig. 4-13B, more than 50% of these auxin-induced genes are specifically expressed on CIM according to my dataset, although a substantial proportion of genes also continue to be expressed after transfer to SIM. Importantly, only 10 of these genes are differentially expressed in *siz1-2* (Fig. 4-13B), suggesting that the overall transcriptional response to auxin is not altered in the *siz1* mutants on CIM. Most of these differentially expressed genes

appeared specifically induced upon CIM incubation and are clustered in the heat map (Fig. 4-13B).

In addition to the RNA-seq data, which does not account for spatial and explant to explant variation, I also investigated the auxin response during regeneration by observing a line expressing a synthetic auxin-responsive fluorescent reporter *DR5rev::GFP* (*DR5-GFP*). After introgression of the *DR5-GFP* into the *siz1-3* mutant I observed the DR5-GFP signal by confocal microscopy. After 4 days of CIM incubation, *DR5-GFP* was expressed in the vasculature in both WT and *siz1-3*, and the signal generally appeared stronger in *siz1-3* mutant (Fig. 4-14). After transfer to SIM and further incubation for 4 days, the DR5-GFP signal became stronger than in explants on CIM. Interestingly, however, WT and *siz1-3* were visibly indistinguishable at this stage (Fig. 4-14). The *siz1-3* mutant produced bigger callus after 9 days on CIM and as expected, produced a larger surface area of *DR5-GFP* expressing cells although the intensity of the signal was visibly indistinguishable (Fig. 4-14). DR5-GFP analysis thus revealed no clear difference between WT and *siz1* during shoot regeneration, however, further analysis at the CIM 4-day time point may help clarify whether *siz1* mutants display locally enhanced auxin response. Based on both fluorescent marker observation and RNA-seq analysis, mutation of *SIZ1* does not alter the spatial pattern on auxin response or the overall expression levels of auxin responsive genes.

Shoot regeneration is thought to require auxin-induced root meristem regulators whose expression is largely dependent on AUX/IAA-ARF signaling pathway (Fan et al., 2012; Liu et al., 2018a). To test if *siz1* mutation promotes shoot regeneration by an ARF-dependent pathway, I observed the shoot regeneration phenotype of *siz1-3* with impaired function of ARF7 and ARF19 either by introducing the dominant negative *slr-1*, which constitutively represses ARF activity, or the loss-of-function *arf7-2 arf19-5* mutant into *siz1-3*. I found that both of these mutations completely abolish the ability to regenerate shoots (Fig. 4-15). Among ARF and auxin-induced genes are several key regulators of callus formation, such as *LBD16*, *LBD18* and *LBD29* (Fan et al., 2012; Liu et al., 2014; Liu et al., 2018b), as well as regulators of pluripotency acquisition, like *PLT1*, *PLT2* and *WOX5* (Kareem et al., 2015; Kim et

al., 2018). RNA-seq analysis revealed that all of these genes were highly induced on CIM but none of these are mis-expressed in *siz1-2* explants on CIM (Fig. 4-16).

In order to further check the expression pattern of *WOX5* gene in *siz1*, I crossed the *WOX5* marker (*pWOX5::ER-GFP*) (Billou et al., 2005) into *siz1-3* and examined its expression in CIM-induced callus. The pattern of the GFP expression in developing callus is comparable between WT and *siz1-3* explants after 4 days on CIM (Fig. 4-17), though I did observe an increased number of *WOX5*-expressing cells in *siz1-3* by 9 days on CIM (Fig. 4-17). These results suggest that after 4 days of incubation loss of SIZ1 function does not impact the expression of pluripotency and callus genes, thus this likely does not explain the enhanced shoot regeneration phenotype of *siz1* mutants. However, after prolonged incubation on CIM, *WOX5* expressing domain increases in proportion to increased callus observed in the *siz1* mutant.

4.7 Expression of SIM-induced shoot meristem genes is more pronounced in *siz1*

WT and *siz1-2* explants do not show visible greening at 4 days after transfer to SIM and similarly microscopic observation revealed that callus is morphologically comparable at this time point. However, a clear enrichment of GO categories such as shoot system morphogenesis (p = 1.58e-7) and stomatal complex development (p = 3.74e-6) is already observed among the 593 genes upregulated in *siz1-2* at 4 days of SIM incubation. These two GO categories become even more strongly over-represented among the 982 genes upregulated at 6 days (Fig. 4-5A), the timing at which *siz1* explants appear visibly greener than WT around this time WT (Fig. 4-2C). As expected, genes which are upregulated in *siz1-2* compared to WT on SIM include key regulators of shoot meristem development such as *REV*, *ESR2, STM* and *WUS* (Fig. 4-18). In order to further characterize these early transcriptional changes on SIM, I crossed the *gWUS-GFP*$_3$ marker (Tucker et al., 2008) into *siz1-3* and examined its expression in explants following SIM incubation. It was previously described that *WUS* expression is broadly distributed in callus cells at 4 days on SIM and it becomes spatially confined to form foci by 6 days (Zhang et al., 2017). While *WUS*-expressing foci was observed in hypocotyl explants in both WT and *siz1-3* after a 6-day-SIM incubation, the number of these foci is greatly increased in *siz1-3* explants compared to WT (Fig. 4-19). This suggests that the higher level of *WUS* expression detected in

my RNA-seq dataset is due to the higher abundance of *WUS*-expressing cells rather than its elevated expression in individual cells.

Given that cytokinin induces *WUS* expression during shoot regeneration on SIM, I next investigated whether transcriptional responses to cytokinin are altered in *siz1-2*. Among the 7234 genes that are induced in WT explants at 4 or 6 days on SIM compared to after cut, I found 342 genes that are cytokinin-inducible in previously published transcriptomic datasets (Nemhauser et al., 2006; Goda et al., 2008; Bhargava et al., 2013) (Fig. 4-20A). A subset of these cytokinin-induced genes (22 genes) are over-induced in *siz1-2* explants on SIM (Fig. 4-20B, Table 2-1). In addition, I detected 110 genes that are down-regulated in *siz1-2* (Fig. 4-20B, Table 2-1). Most of these differentially expressed genes are clustered together in my heat map and are induced specifically on SIM (Fig. 4-20B).

An alternative method of observing the transcriptional output of cytokinin signaling is with the synthetic reporter *TCSn::GFP* (*TCS-GFP*) (Zürcher et al., 2013). I crossed this reporter into the *siz1-3* mutant and observed the GFP fluorescence by confocal microscopy after incubation on CIM for 4 days and then incubation on SIM. After 4 days of incubation on SIM the domain of *TCS-GFP* expression appeared enlarged in *siz1-3* compared to WT. The *TCS-GFP* signal became less uniformly distributed in *siz1-3* after 6 days on SIM (Fig. 4-21). As *siz1-3* forms promeristem earlier than WT (Fig. 4-19), it is possible that these changes in the *TCS-GFP* expression are correlated with the altered spatial distribution of cytokinin-responding cells. To further examine the level of cytokinin response in WT and *siz1* mutants, I incubated hypocotyl explants on Gamborg B5 media that contain 0 to 500 ng/ml 6-benzylaminopurine (BA). As shown in Fig. 4-22, *siz1* hypocotyl explants, but not WT, display increased callus growth in response to BA. These data together suggest that cytokinin response is altered in *siz1*, which may contribute to the enhanced expression of shoot meristem regulators.

4.8 Global SUMOylation is decreased in *siz1-3*

As SIZ1 catalyzes the conjugation of SUMO to target proteins, I wanted to investigate how SUMOylation was affected in the mutant after wounding and during incubation on hormone-containing media. Using an antibody that targets SUMO1 protein (Ishida et al., 2009), I performed western blot analysis with whole protein extracted from

seedlings incubated at 37°C as heat stress induces dramatic accumulation of SUMOylated proteins (Kurepa et al., 2003). As expected, SUMOylated protein accumulates after 1 hour and is sustained at 3 hours of heat stress (Fig. 4-23A). The *siz1-3* mutant displayed a dampened response to heat stress. This confirmed previous reports (Kurepa et al., 2003) and verified that the antibody indeed reacts with proteins SUMOylated by SIZ1. To investigate if wounding induces sustained changes in SUMOylation, protein from whole seedlings cut multiple times with a razor and incubated on MS was probed with the anti-SUMO1 antibody. In both WT and *siz1-3* I did not detect a substantial change in SUMOylated protein levels from 2.5 to 25 hours after cutting. However, the *siz1-3* mutant had consistently lower levels of SUMOylated proteins compared to WT (Fig. 4-23B). Similarly, SUMOylation was impaired in *siz1-3* hypocotyl explants incubated on CIM or SIM and interestingly, hypocotyl explants incubated on only CIM displayed higher levels of SUMOylation than those incubated on CIM followed by SIM (Fig. 4-23C). Together these results demonstrate that the *siz1* mutant accumulates less SUMOylated protein than WT, however, more analysis is required to demonstrate if wounding or application of hormones can induce an accumulation of SUMOylated proteins in WT.

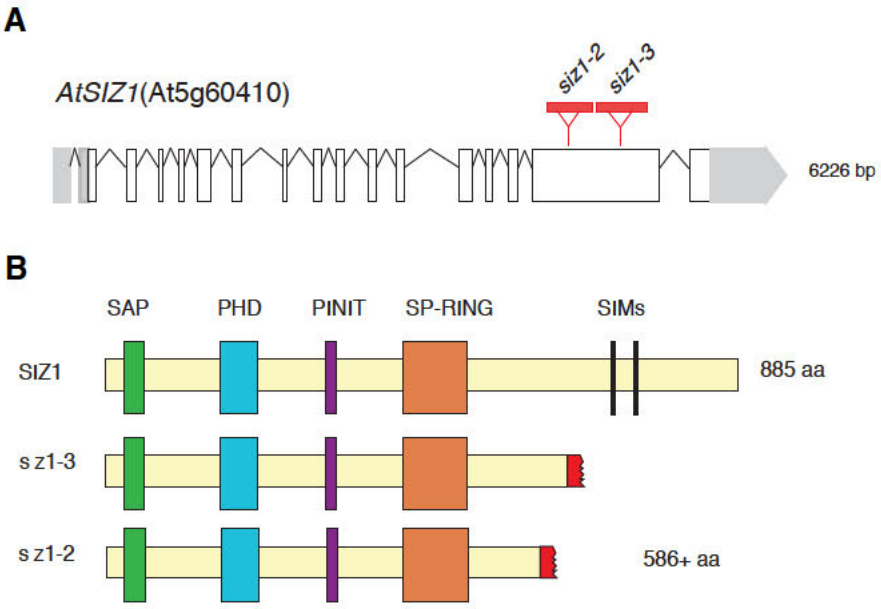

Figure 4-1. SIZ1 contains multiple conserved domains.
(A) Map of the *SIZ1* gene showing the position of T-DNA insertions in the two alleles used in this study. **(B)** Canonical protein product from the *SIZ1* gene in WT, *siz1-2* and *siz1-3*. SIZ1 has a SAP-domain with DNA binding activity, plant homeodomain-finger (PHD) domain with histone binding activity, a PINIT motif (nuclear retention), an SP-RING domain that has SUMO E3 ligase activity and two putitive SUMO interacting domains (SIMs). Figure was modified from Miura et al., 2005 and Miller et al., 2010.

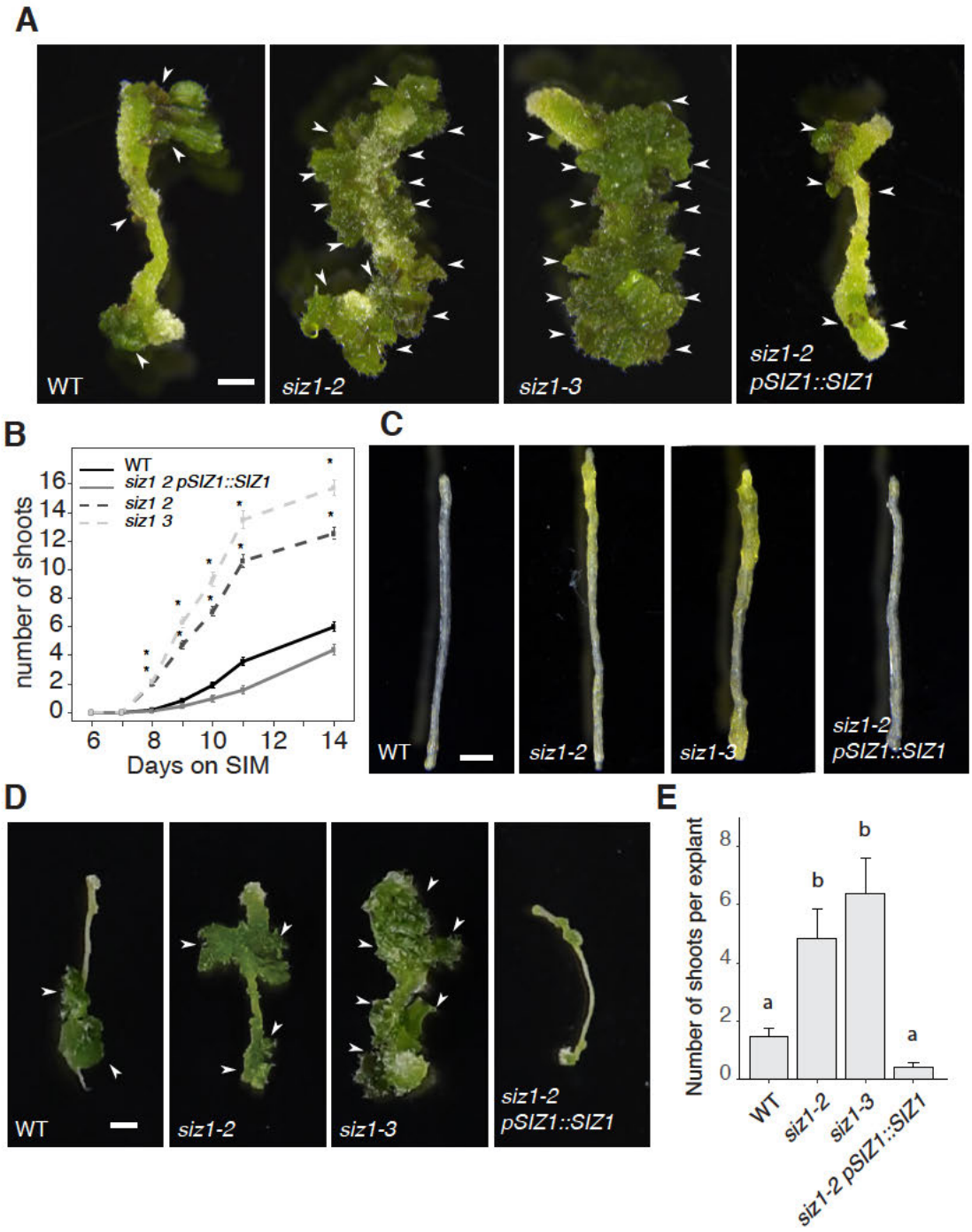
A
WT
siz1-2
siz1-3
siz1-2
pSIZ1::SIZ1
B
WT
siz1 2 pSIZ1::SIZ1
siz1 2
siz1 3
number of shoots
Days on SIM
C
WT
siz1-2
siz1-3
siz1-2
pSIZ1::SIZ1
D
WT
siz1-2
siz1-3
siz1-2
pSIZ1::SIZ1
E
Number of shoots per explant
WT
siz1-2
siz1-3
siz1-2 pSIZ1::SIZ1

Figure 4-2. SIZ1 negatively regulates shoot regeneration *in vitro.*
(A) Representative images showing shoot regeneration phenotypes in hypocotyl explants of *siz1-2*, *siz1-3* and *siz1-2 pSIZ1::SIZ1* compared to Col-0 wild type. Explants were incubated on CIM for 4 days then on SIM for 14 days. Scale bar = 1 mm. **(B)** Time series quantification of shoot regeneration in hypocotyl explants of *siz1-2*, *siz1-3,* and *siz1-2 pSIZ1::SIZ1* compared to wild type. Explants were incubated on CIM for 4 days followed by SIM for the indicated number of days. Sample sizes are WT (n = 68), *siz1-2* (n = 103), *siz1-3* (n = 99), *siz1-2 pSIZ1::SIZ1* (n = 47). **(C)** Representative images showing greening of hypocotyl explants is accelerated in siz1-2 and siz1-3 compared to wild type and *siz1-2 pSIZ1::SIZ1*. Explants were incubated on CIM for 4 days followed by SIM for 7 days. Scale bar = 1 mm. **(D)** Representative images showing shoot regeneration phenotypes in root explants of *siz1-2*, *siz1-3* and *siz1-2 pSIZ1::SIZ1* compared to Col-0 wild type. Explants were incubated on CIM for 4 days then on SIM for 17 days. Scale bar = 1 mm. **(E)** Barplot of number of shoots regenerated in **(D)**. Explants were incubated on CIM for 4 days followed by SIM for 17 days. Sample sizes are WT (n = 13), *siz1-2* (n = 13), *siz1-3* (n = 11), *siz1-2 pSIZ1::SIZ1* (n = 19). Error bars in **(B, E)** represent +/- standard error (SE) of the mean. *, $P < 0.05$ (one-way ANOVA and post-hoc Tukey's HSD). Arrowheads in **(A, D)** indicate regenerated shoots.

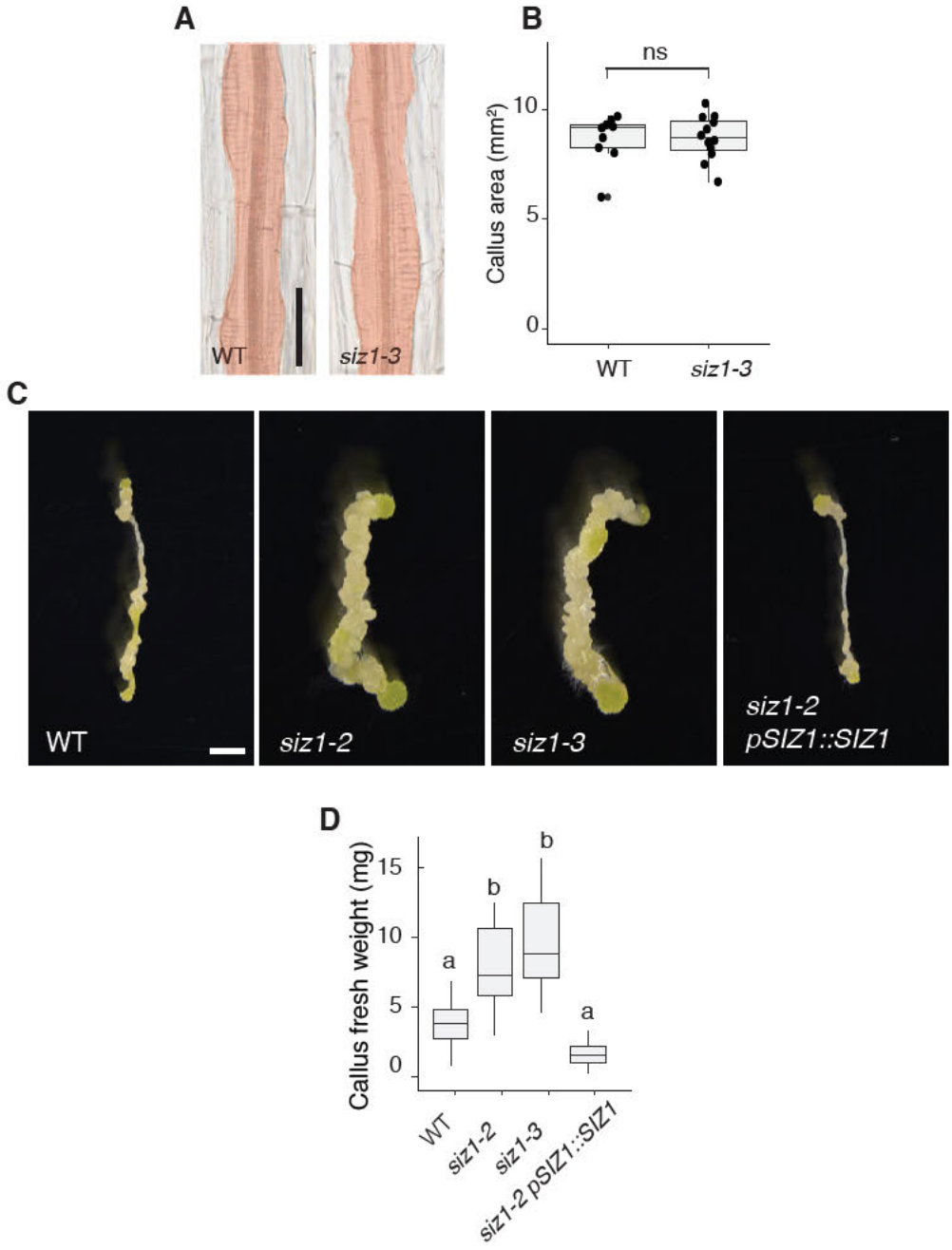

Figure 4-3. SIZ1 suppresses callus formation on CIM.

(A) Representative DIC images showing similar callus production in WT and siz1-3 following 4 days of CIM incubation. Area marked in red highlights the callus-containing region. Scale bar = 50 µm. **(B)** Quantification of projected callus area from **(A)**. Sample sizes are WT (n = 9), *siz1-3* (n = 12). "ns" indicates not significant as evaluated by Wilcoxon rank-sum test ($P = 0.917$). **(C)** Representative images showing enhanced callus formation in *siz1* explants compared to WT and a *SIZ1* complementing line following prolonged incubation on CIM. Explants were incubated on callus inducing media (CIM) for 17 days. Scale bar = 1mm. **(D)** Fresh weight of calli generated from hypocotyl explants as described in **(C)**. Different letters indicate significant differences based on one-way ANOVA and post-hoc Tukey test ($p < 0.05$). Sample sizes are; WT (n = 25), *siz1-2* (n = 26), *siz1-3* (n = 27), *siz1-2 pSIZ1::SIZ1* (n = 19).

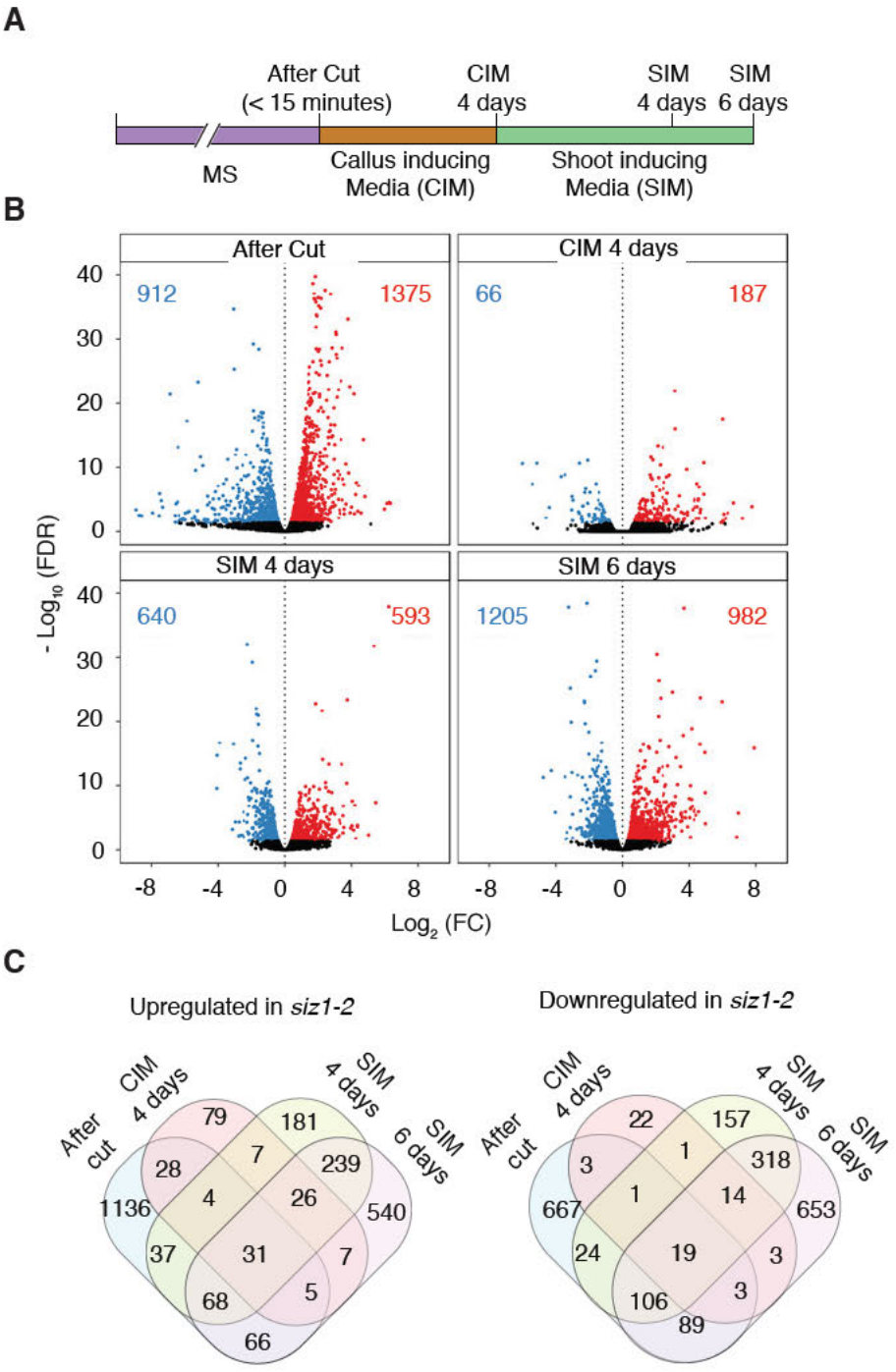

Figure 4-4. SIZ1 mutation alters transcription at multiple time points during *in vitro* shoot regeneration.

(A) Graphical depiction of the RNA-seq analysis experimental set-up. **(B)** Volcano plots showing differentially expressed genes (edgeR, FDR < 0.05) between *siz1-2* and WT. Significantly upregulated or downregulated genes in *siz1-2* are depicted as red or blue dots, respectively. Red or blue numbers indicate the total number of upregulated or downregulated genes. **(C)** Venn diagram showing the overlap between genes upregulated and downregulated in *siz1-2* at different time points.

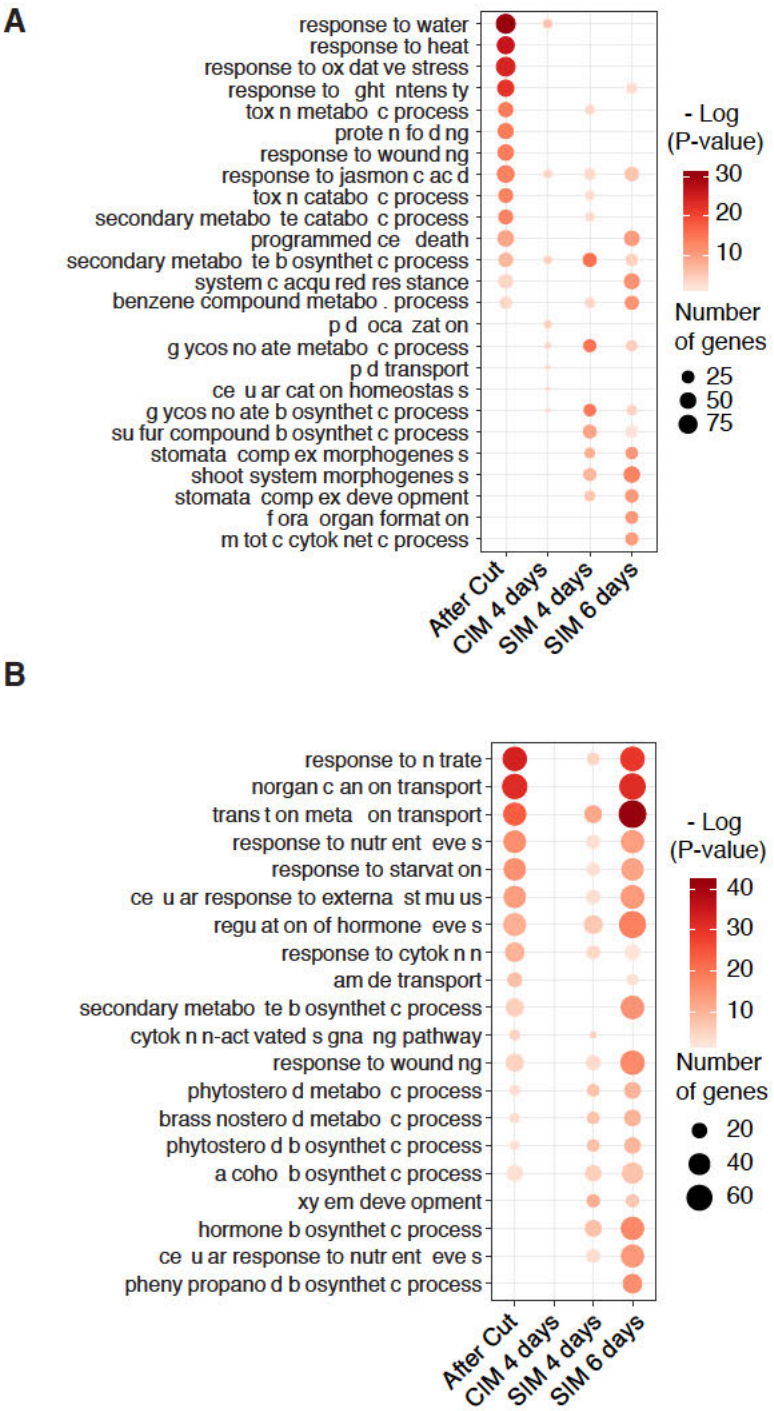

Figure 4-5. Gene ontology (GO) enrichment analysis for differentially expressed genes in *siz1-2* reveals diverse stress and developmental pathways are missexpressed.

(A) GO enrichment analysis of genes upregulated in *siz1-2* at each time point **(B)** GO enrichement analysis of genes downregulated in *siz1-2* at each time point. Differentially expressed genes were identified from RNA-seq analysis. Displayed are all GO categories which are among the top 15 most enriched terms among differentially expressed genes at any given time point. Redundant categories were manually removed.

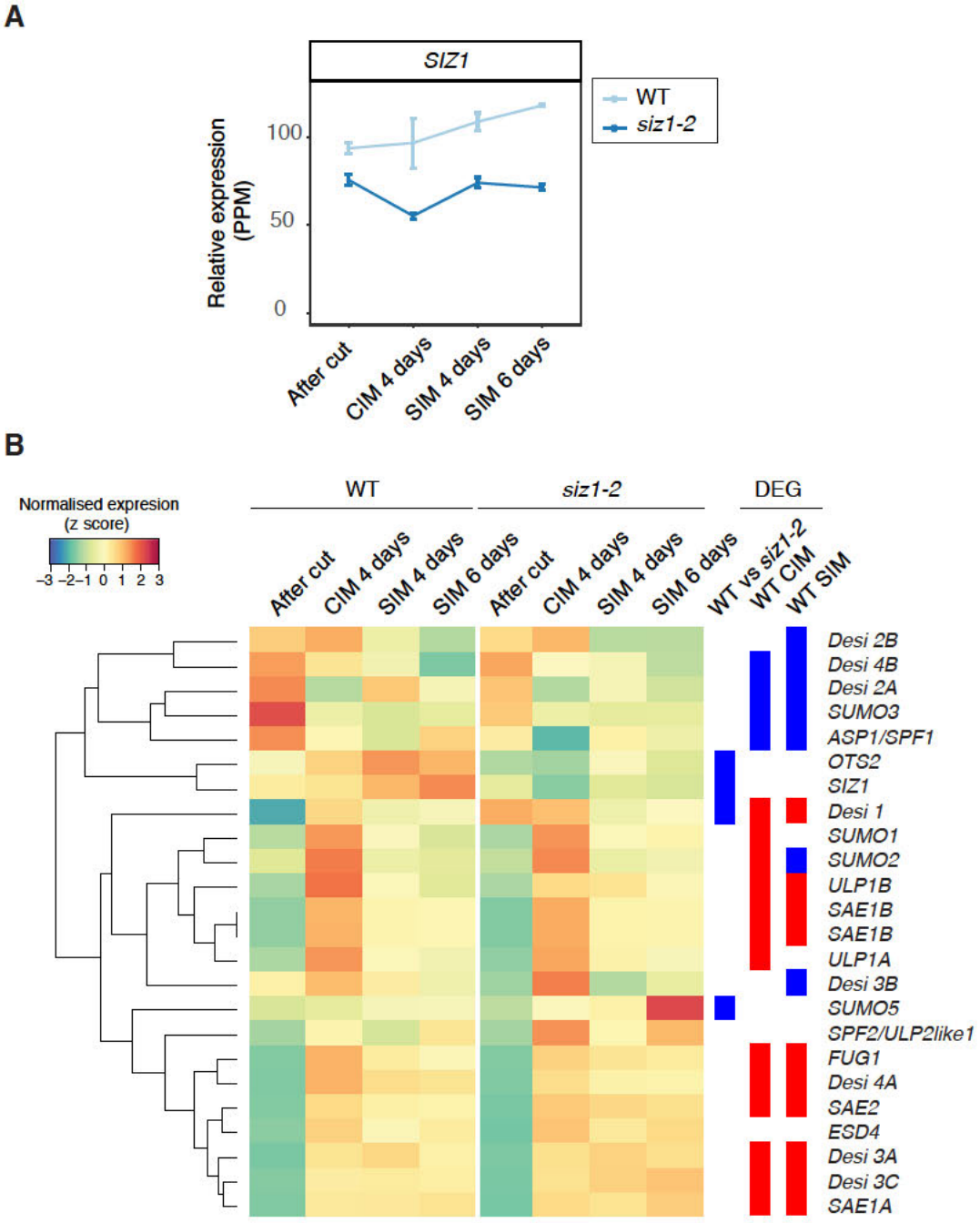

Figure 4-6. Expression of *SIZ1* and other genes implicated in SUMOylation during shoot regeneration.

A) Expression of *SIZ1* is stable during the shoot regeneration procedure. Line graph shows the relative levels of *SIZ1* transcript from our RNA-seq data.

B) Heatmap showing relative expression of major SUMO ligases and SUMO proteases in our RNA-seq experiment. DEG indicates genes that are differentially expressed in *siz1-2* at any of the time points (left), in WT on CIM 4 days compared to after cut (center), and in WT on SIM 4 days and 6 days compared to after cut (right) according to edgeR analysis (FDR < 0.05). Blue indicates genes downregulated and red indicates genes upregulated.

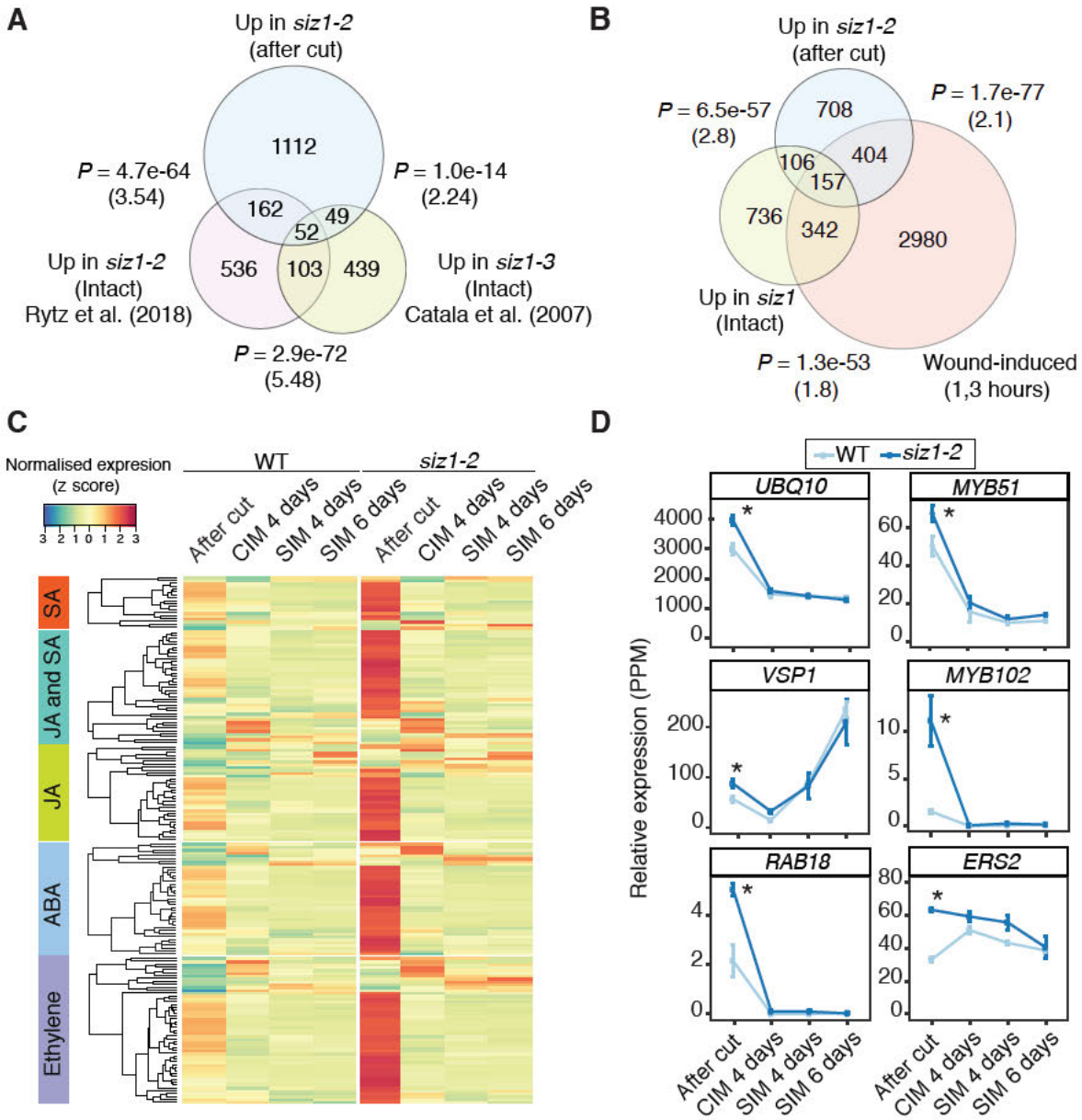

Figure 4-7. Many genes associated with stress-related hormone signalling are hyperactivated after wounding in *siz1-2*.

(A) Overlap between genes upregulated in *siz1-2* compared to WT after cut, based on our RNA-seq analysis, and those upregulated in intact siz1 mutant seedlings, as determined in previous studies (Catala et al., 2007; Rytz et al., 2018). The hypergeometric test was used to evaluate significance of overlap between pairs of gene sets. The calculated representation factor is shown in brackets. **(B)** Overlap between genes upregulated in *siz1-2* after cut, genes induced at 1 and/or 3 hours after wounding in hypocotyls (Ikeuchi et al., 2017) and genes upregulated in *siz1* intact plants (Catala et al., 2007; Rytz et al., 2018). The hypergeometric test was used to evaluate significance of overlap between pairs of gene sets. The calculated representation factor is shown in brackets. **(C)** Heatmap showing, based on the RNA-seq analysis, hyperactivation of genes after cut in *siz1-2* compared to WT which are also associated with a GO category containing one of the following words or phrases: “jasmonic acid” (JA), “salicylic acid” (SA), “ethylene” or “abscisic acid” (ABA). Normalized expression was calculated for each gene across all time points, using data from both genotypes. **(D)** Relative expression of a selection of genes which are associated with one or more of the phytohormone GO terms shown in **(C)** in *siz1-2* and in WT. Error bars represent +/- SE. *, $P < 0.05$ (EdgeR comparative analysis between WT and siz1-2).

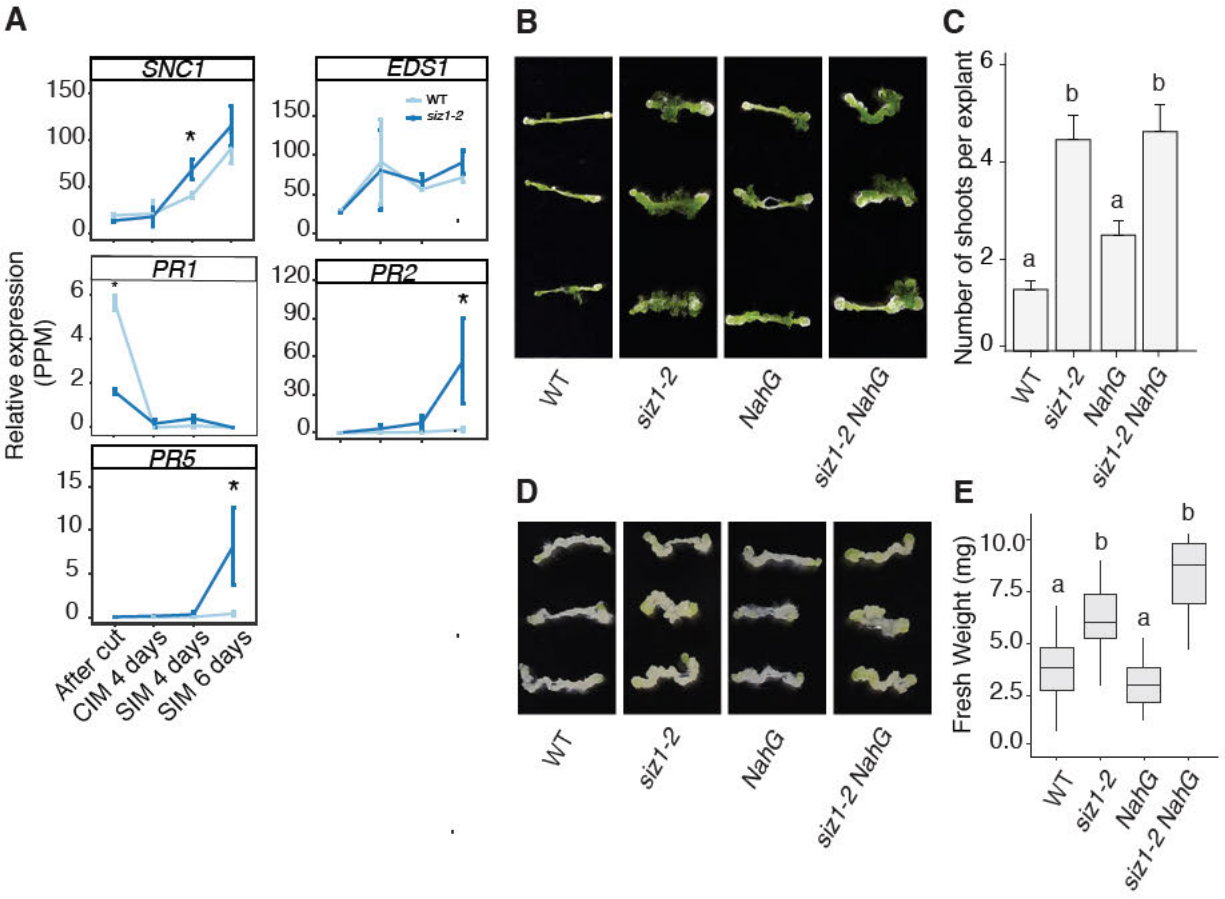

Figure 4-8. SIZ1 suppresses shoot regeneration and callus formation independent of salicylic acid.

(A) Expression of *SNC1* and other genes involved in SA-induced autoimmunity during shoot regeneration. Line plots show relative expression from RNA-seq analysis. Error bars represent +/- SE. *, $P < 0.05$ (edgeR comparative analysis between WT and *siz1-2*). **(B)** Representative images showing enhanced shoot regenertion in *siz1-2* and *siz1-2 NahG* explants compared to WT and *NahG*. Explants were incubated on callus inducing media (CIM) for 4 days and shoot inducing media (SIM) for 14 days. **(C)** Quantification of shoot regeneration in **(B)**. Values represent mean number of shoots produced per explant, and error bars represent standard error of the mean. Sample sizes are WT (n = 37), *siz1-2* (n = 44), *NahG* (n = 48) and *siz1-2 NahG* (n = 38). **(D)** Representative images showing enhanced callus formation in *siz1-2* and *siz1-2 NahG* explants compared to Col-0 wild-type and NahG. Explants were incubated on callus inducing media (CIM) for 17 days. **(E)** Quantification of callus formation in **(D)**. Values represent fresh weight of callus per explant. Sample sizes are WT (n = 35), *siz1-2* (n = 26), *NahG* (n = 21) and *siz1-2 NahG* (n = 21). Different letters indicate significant differences based on one-way ANOVA and post-hoc Tukey test ($P < 0.05$).

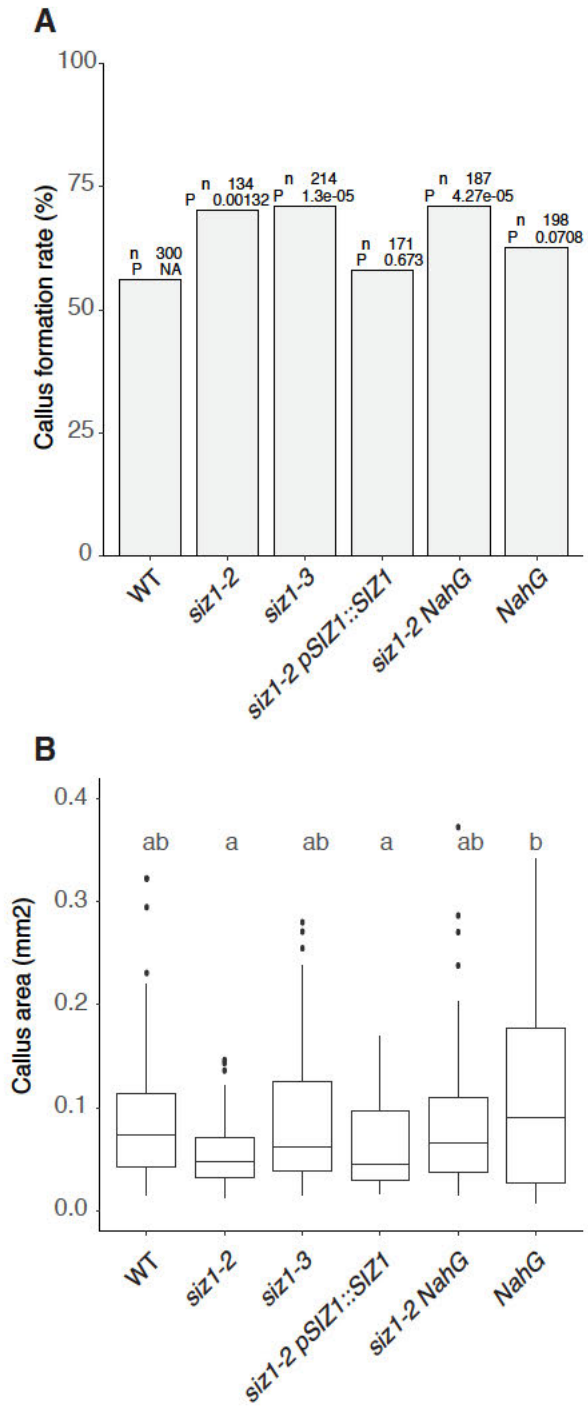

Figure 4-9. SIZ1 negatively regulates wound-induced callus formation.
(A) Proportion of hypocotyl explants that form callus within 1 week after cutting and incubation on MS. P-values (two-proportions z-test) of difference to WT. **(B)** Boxplot of projected area of callus formed after 10 days of incubation on MS reveals the area of callus is not affected by *siz1* mutation. Different letters in **(C)** and **(D)** indicate significant differences based on one-way ANOVA and post-hoc Tukey test ($P < 0.05$)

Chapter 3 will be submitted for publication mid 2020 to an appropriate journal

Chapter 3 will be submitted for publication mid 2020 to an appropriate journal

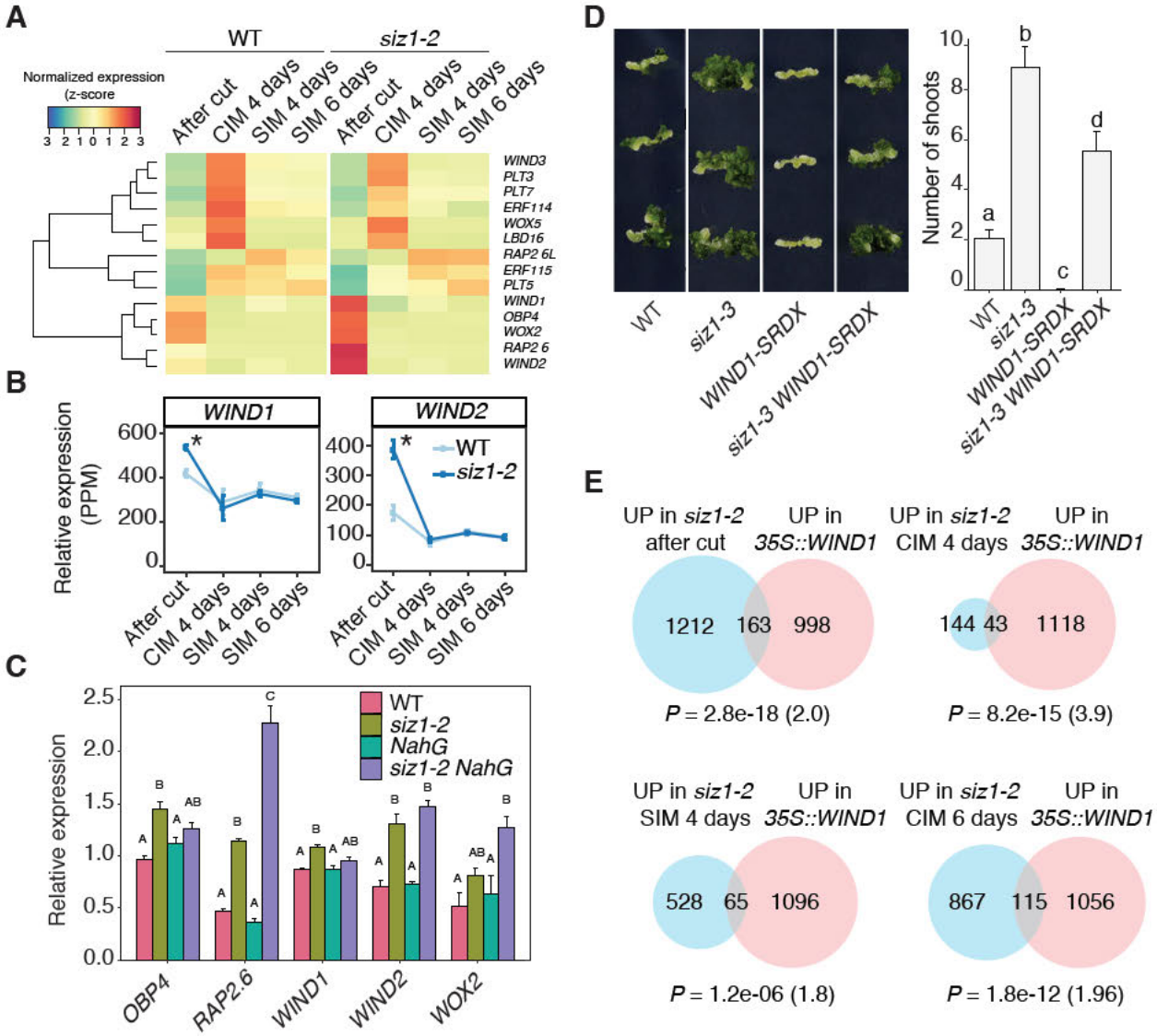
A
WT
siz1-2
Normalized expression (z-score)
3 2 1 0 1 2 3
After cut
CIM 4 days
SIM 4 days
SIM 6 days
WIND3
PLT3
PLT7
ERF114
WOX5
LBD16
RAP2 6L
ERF115
PLT5
WIND1
OBP4
WOX2
RAP2 6
WIND2
B
WIND1
WIND2
Relative expression (PPM)
WT
siz1-2
C
Relative expression
WT
siz1-2
NahG
siz1-2 NahG
OBP4
RAP2.6
WIND1
WIND2
WOX2
D
WT
siz1-3
WIND1-SRDX
siz1-3 WIND1-SRDX
Number of shoots
E
UP in siz1-2 after cut
UP in 35S::WIND1
1212
163
998
P = 2.8e-18 (2.0)
UP in siz1-2 CIM 4 days
UP in 35S::WIND1
144
43
1118
P = 8.2e-15 (3.9)
UP in siz1-2 SIM 4 days
UP in 35S::WIND1
528
65
1096
P = 1.2e-06 (1.8)
UP in siz1-2 CIM 6 days
UP in 35S::WIND1
867
115
1056
P = 1.8e-12 (1.96)

Figure 4-12. Elevated shoot regeneration in *siz1* is partially dependent on WIND1

(A) Heatmap showing relative expression, based on our RNA-seq analysis, of transcription factors identified as wound-inducible and involved in cellular reprograming (Ikeuchi et al., 2017). Normalized expression was calculated for each gene across all time points, using data from both genotypes. **(B)** *WIND1* and *WIND2* are upregulated in siz1-2 after cutting. Line plots show relative expression from RNA-seq analysis. Error bars represent +/- SE. *, $P < 0.05$ (edgeR comparative analysis between WT and *siz1-2*). **(C)** qRT-PCR analysis showing the expression of wound-induced transcription factors in WT, *siz1-2*, *NahG* and *siz1-2 NahG* hypocotyl explants after cut. Gene expression levels are normalized to *PP2A* (n = 3, biological replicates). Error bars represent +/- SE. Different letters indicate significant differences between genotypes for each gene based on one-way ANOVA and post-hoc Tukey test ($P < 0.05$). **(D)** Representative images (left) and quantification (right) of shoot regeneration from hypocotyl explants of WT, *siz1-3*, *WIND1-SRDX* (*pWIND1::WIND1-SRDX*), and *siz1-3 WIND1-SRDX*. All explants were incubated on CIM for 4 days then on SIM for 14 days. Values represent mean number of shoots produced per explant, and error bars represent +/- SE. Sample sizes are WT (n = 36), siz1-3 (n = 34), *WIND1-SRDX* (n = 36), *siz1-3 WIND1-SRDX* (n = 38). Different letters indicate significant differences based on one-way ANOVA and post-hoc Tukey test ($P < 0.05$). **(E)** Overlap between genes upregulated in siz1-2 at each time time point and *35S:WIND1* seedlings (Iwase et al., 2011). P-value was calculated by hypergeometric test and the representation factor is shown in brackets.

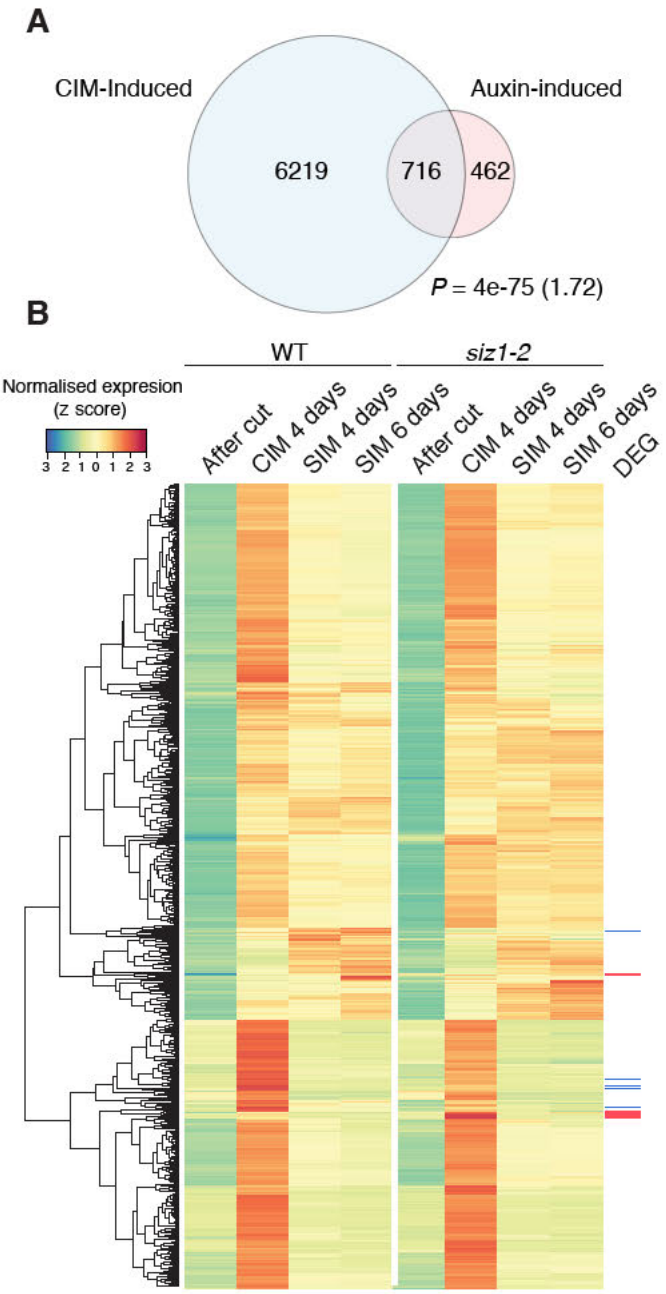

Figure 4-13. Expression of CIM-induced callus genes Is largely unchanged in *siz1-2*. **(A)** Venn diagram showing overlap between auxin inducible (IAA-induced) genes and CIM inducible genes. IAA-induced gene list was generated by combining datasets from Nemhauser et al., (2006) (430 genes), Omelyanchuk et al., (2017) (789 genes) and AtGeneExpress Goda et al., (2008) (ExpressionSet:1007965859) (103 genes). CIM induced genes are those upregulated in wild type at 4 days CIM compared to after cut (EdgeR, FDR < 0.01). **(B)** Heatmap showing no significant changes in expression between *siz1-2* and WT, based on our RNA-seq analysis, for genes inducible by both IAA and CIM identified in **(A)**. Normalised expression was calculated for each gene across all time points, using data from both genotypes. Differentially expressed genes (DEG) are marked in red for up-regulated genes in *siz1-2* at CIM 4 days and in blue for down-regulated genes.

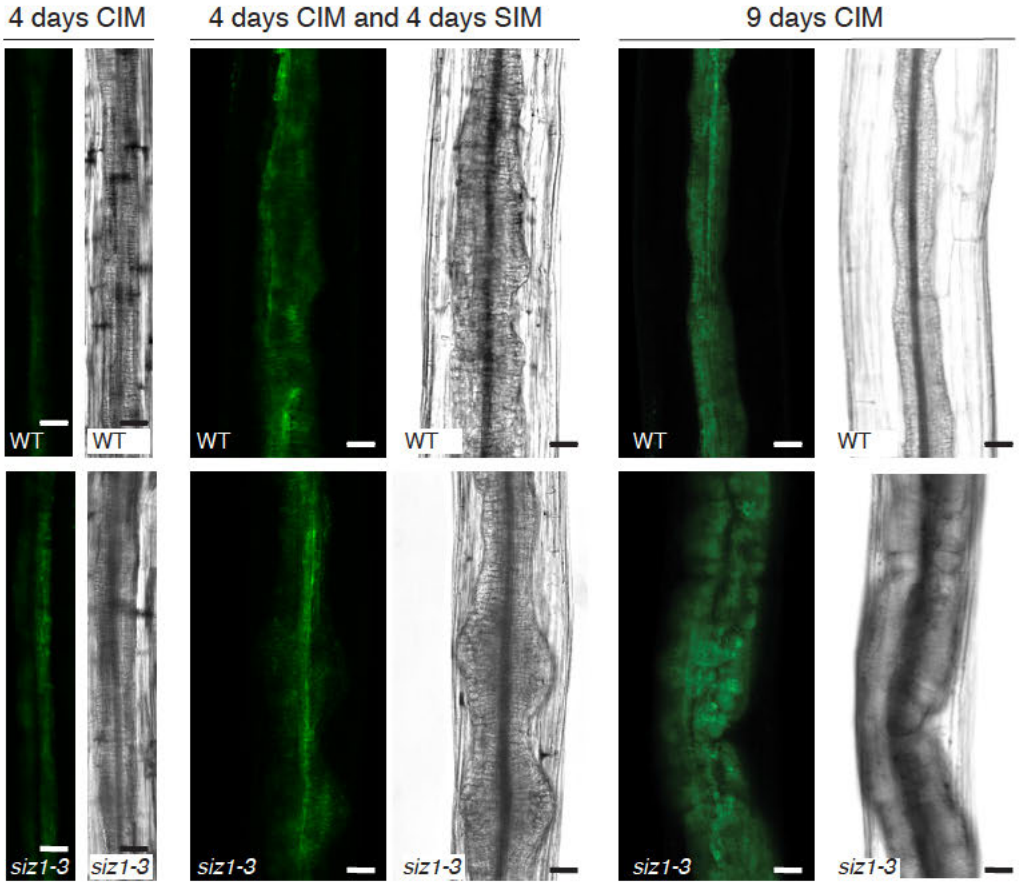

Figure 4-14. Observation of auxin-responsive marker *DR5rev::GFP* (*DR5-GFP*) in *siz1-3* during CIM and SIM incubation.
Representative images of *DR5-GFP* expressing hypocotyl explants incubated on CIM and SIM for the indicated period. At 4 days CIM the signal is weak in both WT and *siz1-3*. After transfer to SIM and incubation for 4 days there is no visable difference in the signal, while the area of *DR5-GFP* expressing cells and callus area is greater in *siz1-3* explants after 9 days on CIM. *DR5-GFP* (green) and brightfield images are shown. Scale bar = 50 μm.

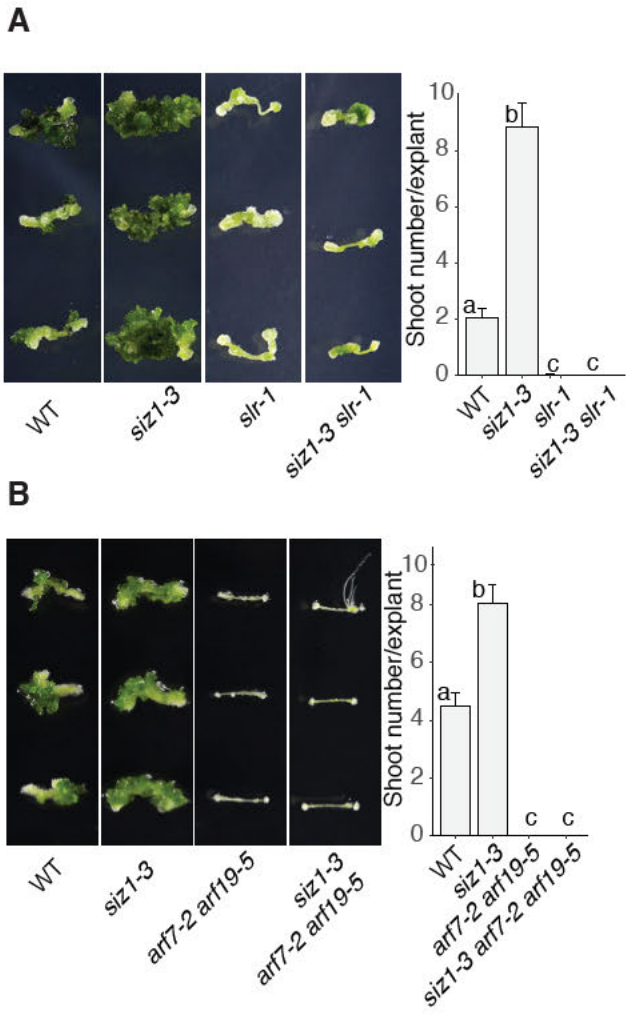

Figure 4-15. *ARF7* and *ARF19* are essential for shoot regeneration, even in *siz1-3* mutant.

(A) Enhanced shoot regeneration in *siz1-3* hypocotyl explants is dependent on ARF7/ARF19-mediated auxin signalling, loss of ARF7 and ARF19 function suppresses the *siz1-3* phenotype in hypocotyl explants of *siz1-3 slr-1* **(A)** and *siz1-3 arf7-2 arf19-5* **(B)**. Explants were incubated on CIM for 4 days followed by SIM for 14 days. Different letters indicate significant differences based on one-way ANOVA and post-hoc Tukey test ($P < 0.05$).

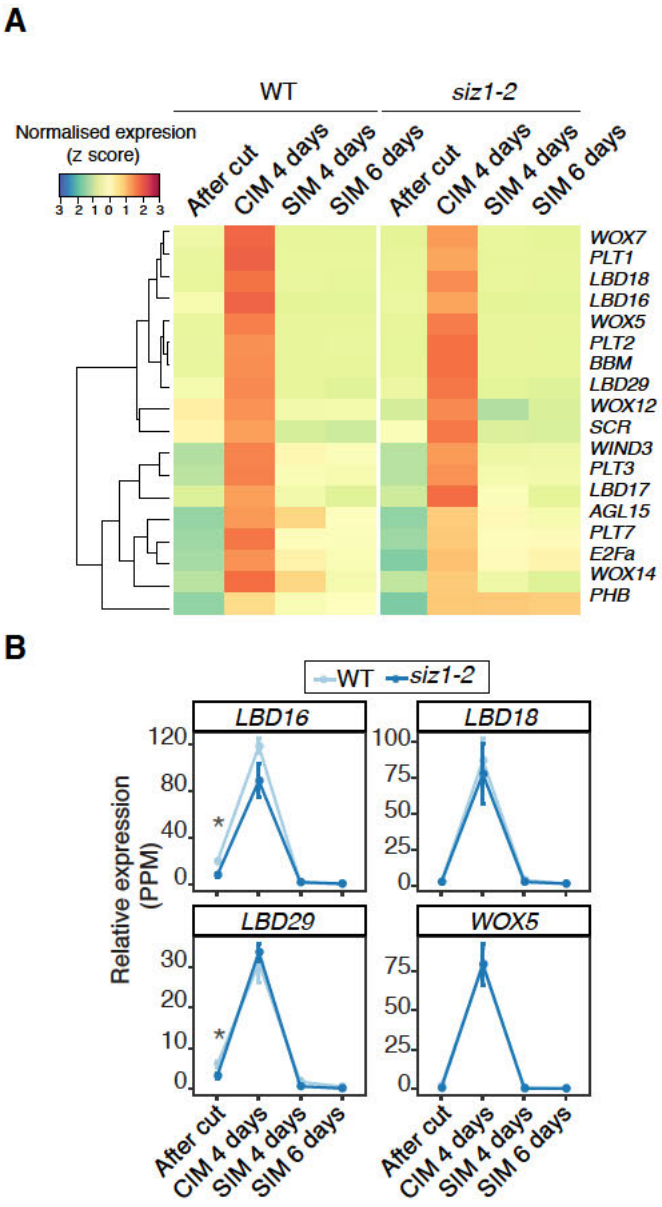

Figure 4-16. Expression of callus marker genes is largely unchanged in *siz1-2*.
(A) Heatmap showing an absence of significant changes in expression between *siz1-2* and WT for transcriptional regulators that are involved in callus formation and pluripotency acquisition according to Ikeuchi et al., (2019). Normalised expression was calculated for each gene across all time points, using data from both genotypes. **(B)** Relative expression (PPM) for a selection of genes from the heatmap in **(A)** in *siz1-2* vs WT. Statistical significance in the difference is indicated based on EdgeR analysis from the RNA-seq data (*; $P < 0.05$).

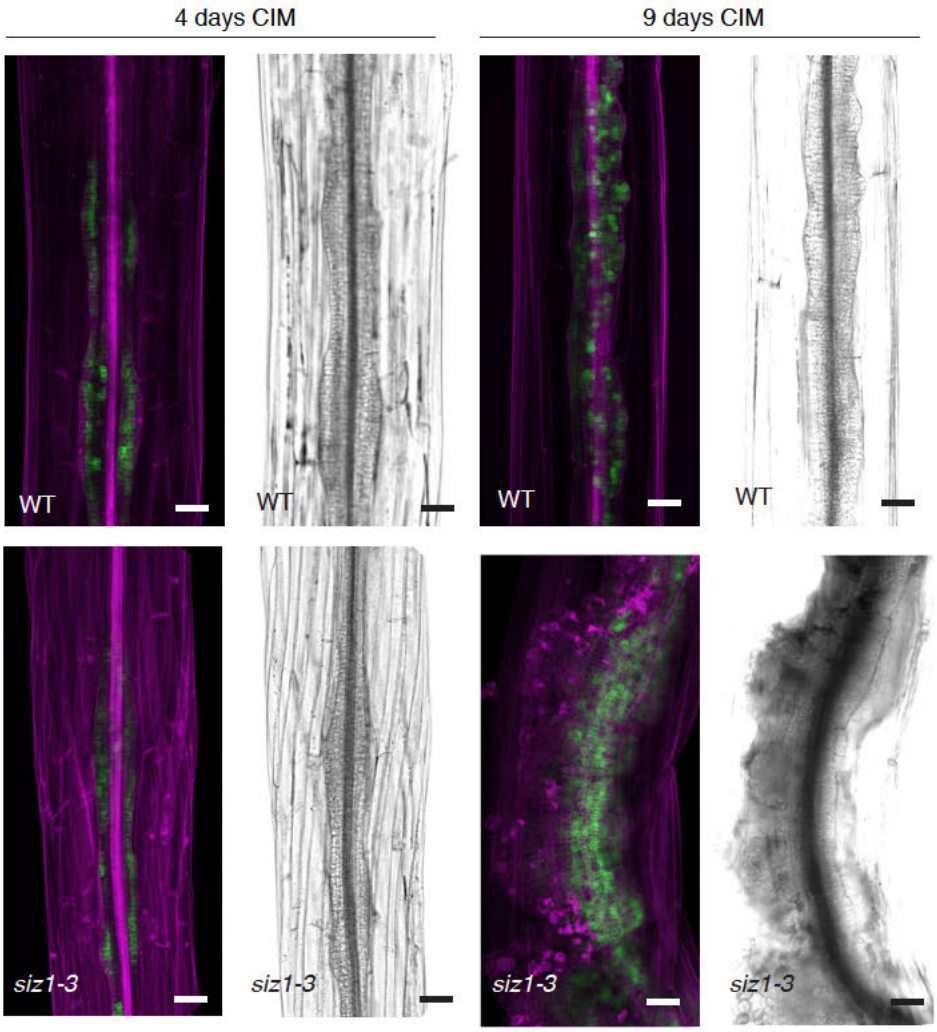

Figure 4-17. Observation of the root meristem regulator and auxin-induced callus marker *WOX5::ER-GFP* reporter during CIM incubation.
Fluorescence Microscopy image of *WOX5::ER-GFP* reporter (green) and callus (right) in *siz1-3* and WT hypocotyl explants after 4 days and 9 days on CIM. Samples were stained with propidium iodide (magenta) to stain cell walls. Brightfield image is shown on the right. Scale bar = 50 μm

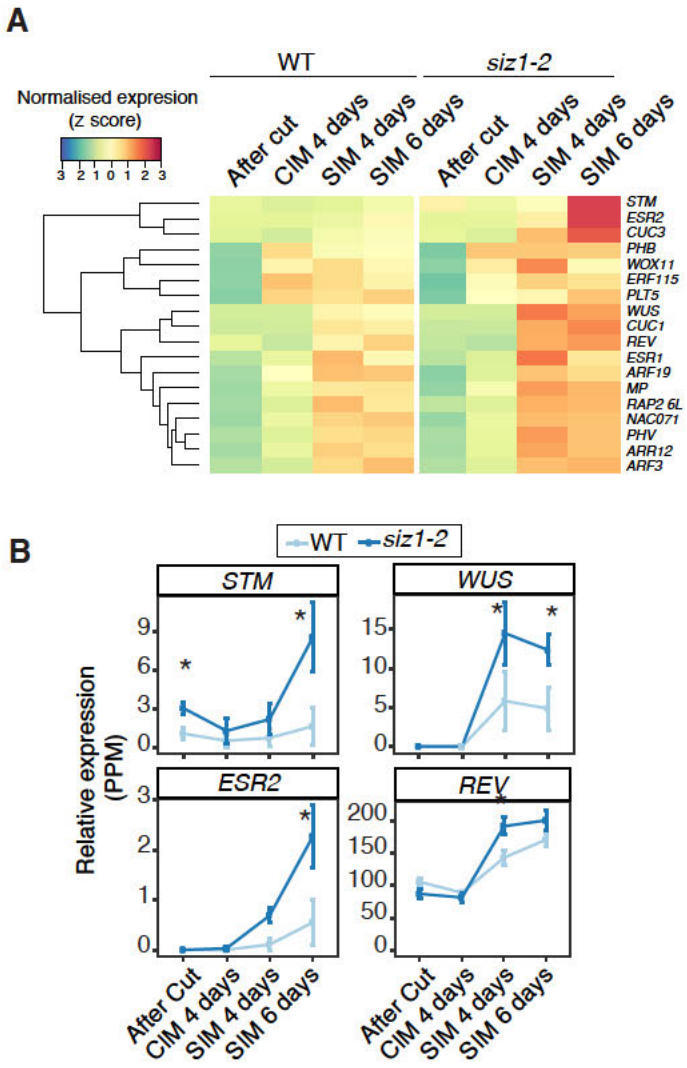

Figure 4-18. Shoot meristem regulators are up regulated in *siz1-2* on SIM.
(A) Heatmap showing that transcriptional regulators highly expressed on SIM that are also known to be involved in regeneration according to (Ikeuchi et al., 2019) are upregulated in *siz1-2*. Normalized expression was calculated for each gene across all time points, using data from both genotypes. **(B)** Relative expression (PPM) of selected shoot meristem genes from the heatmap in **(A)** in *siz1-2* vs wild type. Statistical significance in the difference is indicated based on EdgeR analysis from the RNA-seq data (*; $P < 0.05$).

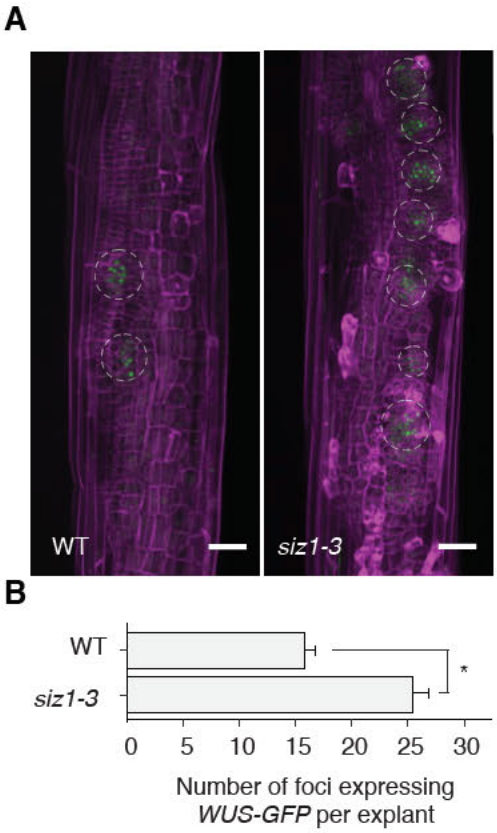

Figure 4-19. Observation of *WUS* expression pattern in WT and *siz1-3*.
(A) Confocal microscopy image of gWUS-GFP$_3$ (*WUS-GFP*) expressing hypocotyl explants explants after 4 days on CIM followed by 6 days on SIM, shows *WUS*-expressing cells (green) are more abundant than WT although individual *WUS*-expressing foci (circled) are not larger or more intense. Scale bar = 50 μm. Samples were stained with propidium iodide (magenta) to stain cell walls.
(B) Quantification of the number of *WUS-GFP*-expressing foci per explant after 6 days on SIM, as in **(A)**. Sample sizes are WT (n = 33) and *siz1-3* (n = 36). Significance was tested with two-tailed Welch Two Sample t-test (*P* = 2.9e-7).

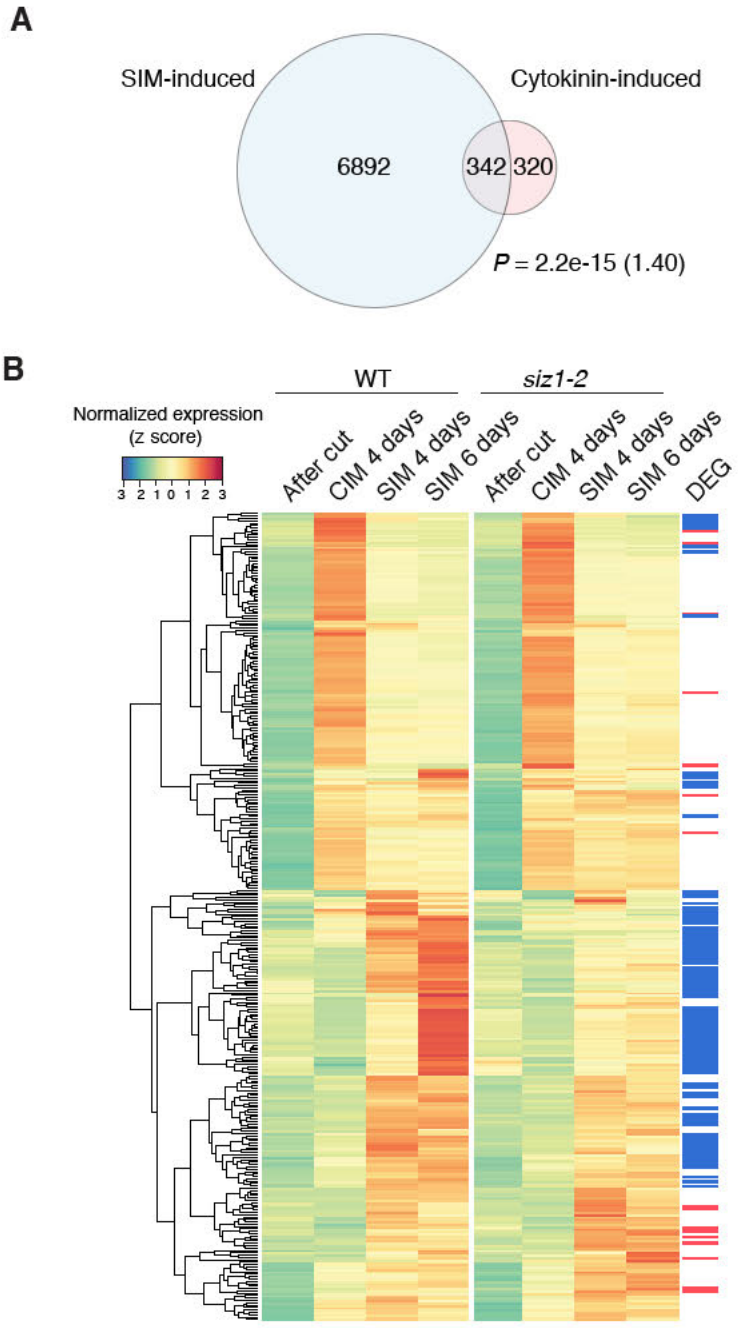

Figure 4-20. Gene expression of cytokinin and SIM-induced genes in *siz1-2*.
E) Venn diagram showing the overlap between cytokinin-inducible genes and SIM-inducible genes. The list of cytokinin-induced genes was created by combining data from Nemhauser et al. (2006) (332 genes), Bhargava et al. (2013) (422 genes) and AtGeneExpress (ExpressionSet:1008031453) (60 genes). SIM-inducible genes are those upregulated in WT after 4 or 6 days of incubation on SIM compared to after cut, based on our RNA-seq data (edgeR, FDR < 0.01). The significance of overlap between pairs of gene sets was evaluated by hypergeometric test. The calculated representation factor is shown in brackets. F) Heatmap showing the expression of genes which are both cytokinin-inducible and SIM-inducible, as identified in (E), in *siz1-2* and WT. Differentially expressed genes (DEG) are marked in red for up-regulated genes in *siz1-2* at SIM 4 days or 6 days and in blue for down-regulated genes.

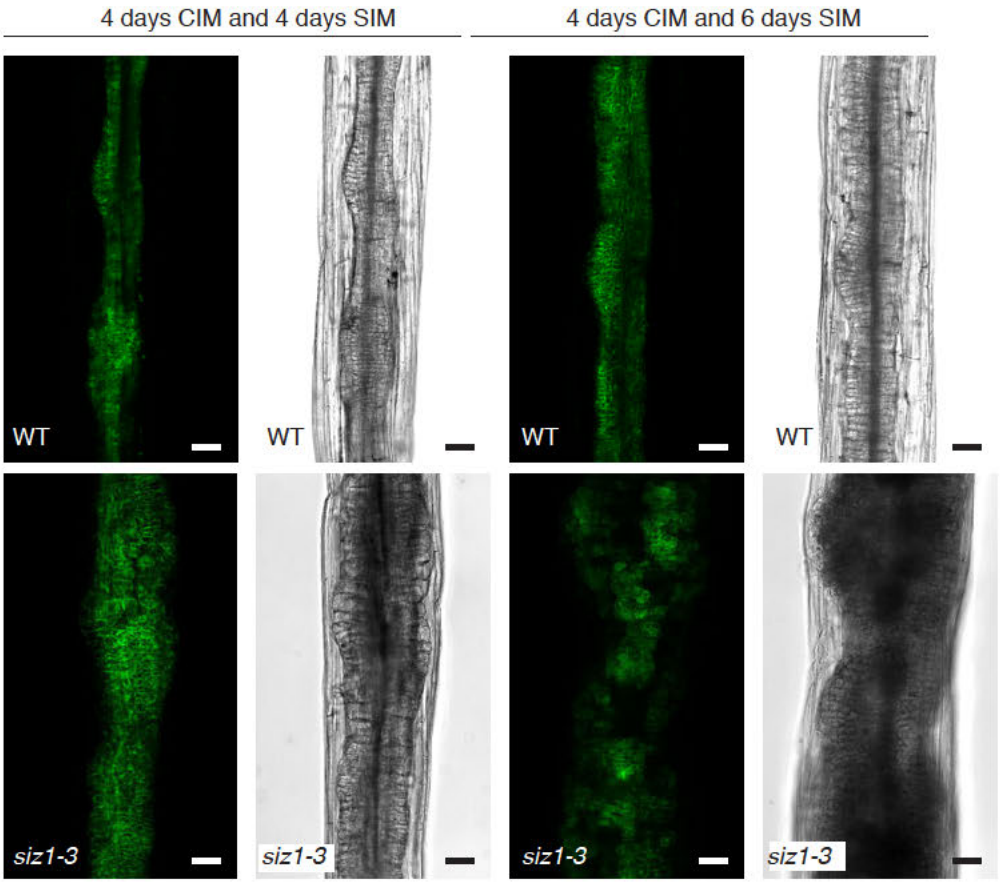

Figure 4-21. Observation of cytokinin-responsive marker *TCSn::GFP* (*TCS-GFP*) in *siz1-3* during CIM and SIM incubation.

Representative images of *TCS-GFP*-expressing explants after 4 days on CIM and 4 days on SIM show both WT and *siz1-3* strongly respond to cytokinin, and observed GFP signal becomes less uniform and callus size is comparitively larger in *siz1-3* after 6 days incubation on SIM. TCS-GFP (green) and brightfield images are shown. Hypocotyl explants were used. Scale bar = 50 μm.

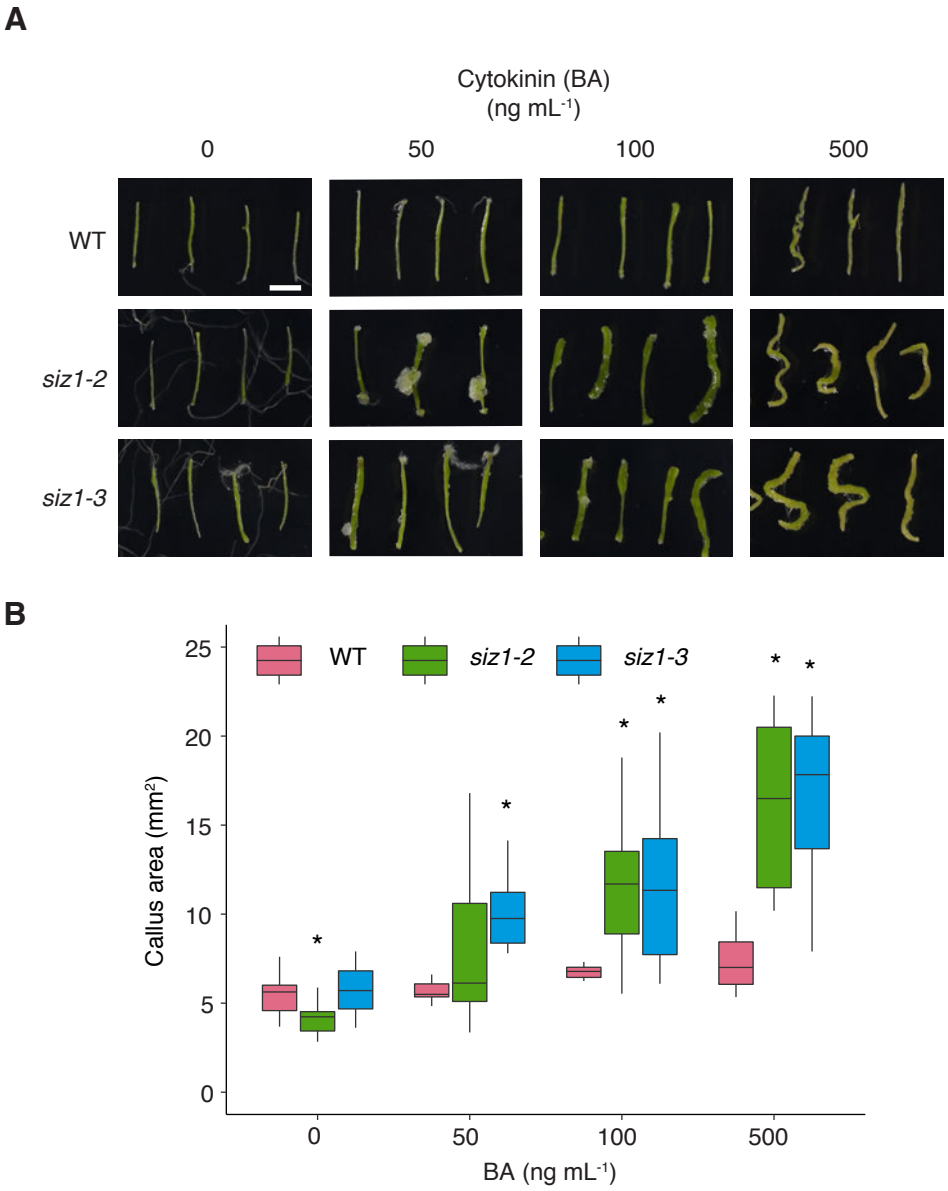

Figure 4-22. Callus formation induced by exogenously supplied BA.
A) Images of hypocotyl explants incubated on Gamborg B5 media containing 0 to 500 ng mL-1 6-benzylaminopurine (BA) for 27 days. Scale bar = 5 mm.
B) Boxplot showing the projected area of callus forming explants in (A). Sample sizes for each condition are (n = 12 - 16). Statistical difference of the mean between WT and each genotype within each concentration is indicated with an asterisk *, $P < 0.05$ (Wilcoxon rank sum test).

Chapter 3 will be submitted for publication mid 2020 to an appropriate journal

Table 4-1. Cytokinin and SIM-responsive genes that are differentially expressed in *siz1-2* on SIM 4 or 6 days in Fig. 4-20.

Upregulated in *siz1-2*		
AGI code	**Short Name**	**Annotation**
AT1G69040	ACR4	ACT domain repeat 4
AT3G61640	AGP20	arabinogalactan protein 20
AT1G48870	AT1G48870	Transducin/WD40 repeat-like superfamily protein
AT3G12860	AT3G12860	NOP56-like pre RNA processing ribonucleoprotein
AT3G13610	AT3G13610	2-oxoglutarate (2OG) and Fe(II)-dependent oxygenase superfamily protein
AT3G59670	AT3G59670	elongation factor
AT4G10500	AT4G10500	2-oxoglutarate (2OG) and Fe(II)-dependent oxygenase superfamily protein
AT4G15680	AT4G15680	Thioredoxin superfamily protein
AT4G15690	AT4G15690	Thioredoxin superfamily protein
AT4G34950	AT4G34950	Major facilitator superfamily protein
AT5G59240	AT5G59240	Ribosomal protein S8e family protein
AT5G59010	BSK5	kinase with tetratricopeptide repeat domain-containing protein
AT1G75450	CKX5	cytokinin oxidase 5
AT5G49480	CP1	Ca2 -binding protein 1
AT5G39760	HB23	homeobox protein 23
AT1G55020	LOX1	lipoxygenase 1
AT3G20860	NEK5	Serine/Threonine kinase catalytic domain protein
AT3G63130	RANGAP1	RAN GTPase activating protein 1
AT2G40670	RR16	response regulator 16
AT3G15990	SULTR3;4	sulfate transporter 3;4
AT1G78580	TPS1	trehalose-6-phosphate synthase
AT1G49320	USPL1	unknown seed protein like 1

Downregulated in *siz1-2*		
AGI code	**Short Name**	**Annotation**
AT4G21120	AAT1	amino acid transporter 1
AT5G19410	ABCG23	ABC-2 type transporter family protein
AT5G13580	ABCG6	ABC-2 type transporter family protein
AT3G21510	AHP1	histidine-containing phosphotransmitter 1
AT3G54720	AMP1	Peptidase M28 family protein
AT1G59940	ARR3	response regulator 3
AT1G19050	ARR7	response regulator 7
AT1G16530	ASL9	ASYMMETRIC LEAVES 2-like 9
AT1G03820	AT1G03820	E6-like protein
AT1G04360	AT1G04360	RING/U-box superfamily protein
AT1G11670	AT1G11670	MATE efflux family protein
AT1G14630	AT1G14630	XRI1-like protein
AT1G18980	AT1G18980	RmlC-like cupins superfamily protein
AT1G24430	AT1G24430	HXXXD-type acyl-transferase family protein
AT1G34520	AT1G34520	MBOAT (membrane bound O-acyl transferase) family protein
AT1G53060	AT1G53060	Legume lectin family protein
AT1G54540	AT1G54540	Late embryogenesis abundant (LEA) hydroxyproline-rich glycoprotein family
AT1G55990	AT1G55990	glycine-rich protein
AT1G56320	AT1G56320	hypothetical protein
AT1G58170	AT1G58170	Disease resistance-responsive (dirigent-like protein) family protein
AT1G68850	AT1G68850	Peroxidase superfamily protein
AT1G74460	AT1G74460	GDSL-like Lipase/Acylhydrolase superfamily protein
AT2G04100	AT2G04100	MATE efflux family protein
AT2G22510	AT2G22510	hydroxyproline-rich glycoprotein family protein
AT2G23540	AT2G23540	GDSL-like Lipase/Acylhydrolase superfamily protein

AT2G28510	AT2G28510	Dof-type zinc finger DNA-binding family protein
AT2G36295	AT2G36295	hypothetical protein
AT2G43470	AT2G43470	zinc finger CCCH domain protein, putative (DUF3755)
AT2G44230	AT2G44230	hypothetical protein (DUF946)
AT3G05770	AT3G05770	hypothetical protein
AT3G08030	AT3G08030	DNA-directed RNA polymerase subunit beta (Protein of unknown function, DUF642)
AT3G15810	AT3G15810	LURP-one-like protein (DUF567)
AT3G20370	AT3G20370	TRAF-like family protein
AT3G45070	AT3G45070	P-loop containing nucleoside triphosphate hydrolases superfamily protein
AT3G45080	AT3G45080	P-loop containing nucleoside triphosphate hydrolases superfamily protein
AT3G46690	AT3G46690	UDP-Glycosyltransferase superfamily protein
AT3G50300	AT3G50300	HXXXD-type acyl-transferase family protein
AT3G50400	AT3G50400	GDSL-like Lipase/Acylhydrolase superfamily protein
AT3G61930	AT3G61930	hypothetical protein
AT4G03610	AT4G03610	Metallo-hydrolase/oxidoreductase superfamily protein
AT4G18630	AT4G18630	hypothetical protein (DUF688)
AT4G20390	AT4G20390	Uncharacterized protein family (UPF0497)
AT4G22230	AT4G22230	defensin-like protein
AT4G23420	AT4G23420	NAD(P)-binding Rossmann-fold superfamily protein
AT4G24130	AT4G24130	DUF538 family protein (Protein of unknown function, DUF538)
AT4G24140	AT4G24140	alpha/beta-Hydrolases superfamily protein
AT4G25410	AT4G25410	basic helix-loop-helix (bHLH) DNA-binding superfamily protein
AT4G36610	AT4G36610	alpha/beta-Hydrolases superfamily protein
AT4G37409	AT4G37409	hypothetical protein
AT5G07475	AT5G07475	Cupredoxin superfamily protein
AT5G08250	AT5G08250	Cytochrome P450 superfamily protein
AT5G12420	AT5G12420	O-acyltransferase (WSD1-like) family protein
AT5G13900	AT5G13900	Bifunctional inhibitor/lipid-transfer protein/seed storage 2S albumin superfamily protein
AT5G14650	AT5G14650	Pectin lyase-like superfamily protein
AT5G16030	AT5G16030	mental retardation GTPase activating protein
AT5G19110	AT5G19110	Eukaryotic aspartyl protease family protein
AT5G23820	AT5G23820	MD-2-related lipid recognition domain-containing protein
AT5G23830	AT5G23830	MD-2-related lipid recognition domain-containing protein
AT5G26290	AT5G26290	TRAF-like family protein
AT5G37690	AT5G37690	SGNH hydrolase-type esterase superfamily protein
AT5G38020	AT5G38020	S-adenosyl-L-methionine-dependent methyltransferases superfamily protein
AT5G38030	AT5G38030	MATE efflux family protein
AT5G47980	AT5G47980	HXXXD-type acyl-transferase family protein
AT5G51780	AT5G51780	basic helix-loop-helix (bHLH) DNA-binding superfamily protein
AT3G13790	ATBFRUCT1	Glycosyl hydrolases family 32 protein
AT5G48850	ATSDI1	Tetratricopeptide repeat (TPR)-like superfamily protein
AT3G10960	AZG1	AZA-guanine resistant1
AT1G78950	BAS	Terpenoid cyclases family protein
AT2G44460	BGLU28	beta glucosidase 28
AT3G13380	BRL3	BRI1-like 3
AT2G17770	BZIP27	basic region/leucine zipper motif 27
AT4G39070	BZS1	B-box zinc finger family protein
AT4G39950	CYP79B2	cytochrome P450, family 79, subfamily B, polypeptide 2
AT4G37400	CYP81F3	cytochrome P450, family 81, subfamily F, polypeptide 3
AT4G37410	CYP81F4	cytochrome P450, family 81, subfamily F, polypeptide 4
AT5G23190	CYP86B1	cytochrome P450, family 86, subfamily B, polypeptide 1
AT1G12740	CYP87A2	cytochrome P450, family 87, subfamily A, polypeptide 2
AT4G39980	DHS1	3-deoxy-D-arabino-heptulosonate 7-phosphate synthase 1
AT3G01420	DOX1	Peroxidase superfamily protein
AT1G69530	EXPA1	expansin A1
AT2G03090	EXPA15	expansin A15
AT3G06020	FAF4	FANTASTIC four-like protein (DUF3049)
AT3G44540	FAR4	fatty acid reductase 4
AT3G44550	FAR5	fatty acid reductase 5
AT1G62570	FMO GS-OX4	flavin-monooxygenase glucosinolate S-oxygenase 4
AT3G11430	GPAT5	glycerol-3-phosphate acyltransferase 5

AT3G09270	GSTU8	glutathione S-transferase TAU 8
AT4G30850	HHP2	heptahelical transmembrane protein2
AT5G62630	HIPL2	hipl2 protein precursor
AT5G58910	LAC16	laccase 16
AT1G55020	LOX1	lipoxygenase 1
AT2G32510	MAPKKK17	mitogen-activated protein kinase kinase kinase 17
AT1G34670	MYB93	myb domain protein 93
AT3G18400	NAC058	NAC domain containing protein 58
AT2G22770	NAI1	basic helix-loop-helix (bHLH) DNA-binding superfamily protein
AT3G44320	NIT3	nitrilase 3
AT4G19030	NLM1	NOD26-like major intrinsic protein 1
AT5G09530	PELPK1	hydroxyproline-rich glycoprotein family protein
AT5G09520	PELPK2	hydroxyproline-rich glycoprotein family protein
AT2G38060	PHT4;2	phosphate transporter 4;2
AT3G29670	PMAT2	HXXXD-type acyl-transferase family protein
AT3G49120	PRXCB	peroxidase CB
AT1G26820	RNS3	ribonuclease 3
AT3G48100	RR5	response regulator 5
AT1G13420	ST4B	sulfotransferase 4B
AT4G23430	Tic32-IVa	NAD(P)-binding Rossmann-fold superfamily protein
AT5G65140	TPPJ	Haloacid dehalogenase-like hydrolase (HAD) superfamily protein
AT5G13930	TT4	Chalcone and stilbene synthase family protein
AT2G26480	UGT76D1	UDP-glucosyl transferase 76D1
AT4G15500	UGT84A4	UDP-Glycosyltransferase superfamily protein

Chapter 5 Discussion

Chapter 3 will be submitted for publication mid 2020 to an appropriate journal

Chapter 3 will be submitted for publication mid 2020 to an appropriate journal

Chapter 3 will be submitted for publication mid 2020 to an appropriate journal

Various biotic and/or abiotic stresses such as pathogen infection and exposure to heat are known to induce massive SUMOylation of proteins in plants (Kurepa et al., 2003; Catala et al., 2007; Castro et al., 2012; Miller et al., 2013). Given that loss-of-function mutants of SIZ1 are often hyper-sensitive to these stresses, SIZ1-mediated SUMOylation is thought to provide protection to limit the response of stress and maintain physiological homeostasis by post-translational regulation in plants exposed to stress conditions (Augustine and Vierstra, 2018). I find that *siz1* mutants have elevated expression of genes associated with wounding shortly after cutting (Fig. 4-7). For instance, SIZ1 is reported to suppress JA signaling and accordingly I saw a significant enrichment for JA-related genes and upregulation of JA receptor CORONATINE INSENSITIVE 1 (COI1)-dependent genes in *siz1* such as *VSP1* (Ellis and Turner, 2002; Srivastava et al., 2018). Furthermore, as JA-responsive genes are enriched at all timepoints in *siz1*, SIZ1 may be required to switch off the JA-response after exposure to stress.

Additionally, SIZ1-mediated regulation of ABA signaling might be involved in the response to wounding. As ABI5-dependent genes are transiently upregulated in *siz1-2* after cut, it is probable that SIZ1 negatively regulates this pathway after wounding. Although it is unclear if ABA plays a major role in the wound-response, it has been established in response to drought and oxidative stress (Shinozaki and Yamaguchi-Shinozaki, 1998; Finkelstein et al., 2002; Zhao et al., 2016). These stresses may also be experienced by the explant after cutting in this experiment, especially given that genes involved in response to drought are overexpressed in *siz1*

explants. Further analysis of mutants of *ABI5* or *ABA-RESPONSIVE ELEMENT BINDING (AREB)* transcription factors, which are major regulators of ABA signaling (Yoshida et al., 2010), could help elucidate the role of ABA in response to wounding. Although SUMOylation of proteins is known to accumulate in response to various stresses such as drought, hydrogen peroxide and heat (Kurepa et al., 2003; Catala et al., 2007; Castro et al., 2012; Miller et al., 2013), it is unclear if wounding can induce SUMOylation. Given that the transcript level of SIZ1 does not change markedly under my experimental conditions (Fig. 4-6), SIZ1-mediated SUMOylation is likely activated by post-transcriptional mechanisms. My data suggest that level of SUMOylated protein is stable over several hours after wounding, however, as wound stress generally elicits a local and transient response in plants (Bogre et al., 1997; Mousavi et al., 2013; Gilroy et al., 2014), it is possible that my experimental setup was not sensitive enough to detect subtle but physiologically relevant changes. Exposure to a short period of heat stress, for example, induces a transient accumulation of SUMOylated protein within minutes (Kurepa et al., 2003). A reduction of basal SUMOylation levels in *siz1* mutant may be relevant, as a number of wound-induced genes are already upregulated in intact *siz1* seedlings (Fig. 4-7B). SIZ1 may negatively regulate stress-associated genes under non-stressed conditions as well as dampening the response to stress.

5.3 Roles of SIZ1 in shoot regeneration

Various developmental phenotypes in *siz1* have been reported, including early flowering (Jin et al., 2008; Kong et al., 2017), reduced secondary cell wall thickening (Liu et al., 2019), reduced germination (Kim et al., 2016), and short hypocotyl growth (Lin et al., 2016; Hammoudi et al., 2018; Zhang et al., 2019b). In this study I find that the *siz1* mutation also causes enhanced shoot regeneration in tissue culture. I dissected the effect of *siz1* at each step of the procedure by RNA-seq analysis. Interestingly, prominent misexpression of distinct genes is observed immediately after cutting and upon incubation on SIM. This observation has led me to hypothesize that SIZ1 may act in suppressing the wound stress response and that the exaggerated wound response upon cutting in *siz1* may promote subsequent shoot regeneration. Part of the exaggerated response includes upregulation of genes related to stress-induced defense hormones SA, JA and ABA as well as many HSR genes. The role of

SIZ1 in suppressing SA response is well established and some aspects of *siz1* phenotype is due to the hyper-activation of SA (Lee et al., 2007; Miura et al., 2010). I provide genetic evidence, by expressing the SA-degrading enzyme *NahG* in *siz1-2* background, that the enhanced shoot regeneration phenotype of *siz1* is not due to accumulation of SA. This is also the case for the hypocotyl elongation phenotype and thermotolerance phenotype of *siz1* (Yoo et al., 2006; Lin et al., 2016). JA signaling is also negatively regulated by SUMOylation (Srivastava et al., 2018), and it is recently reported that pretreatment of JA before cutting and incubating explants on hormone-supplemented media promotes shoot regeneration, with *coi1* mutants showing reduced regeneration efficiency (Park et al., 2019). The importance of the SUMO-dependent regulation of COI1 in shoot regeneration would thus be worth investigating in further studies. Likewise, whether ABA is involved in shoot regeneration is not well established, though it does promote shoot regeneration from embryo explants for example (Paulraj et al., 2014). It is plausible that the shoot regeneration phenotype in *siz1* mutants is partially dependent on ABA or JA signaling.

It was previously reported that WIND1 regulates shoot regeneration *via* transcriptional activation of *ESR1* which is required for the induction of several shoot meristem regulators such as its paralog *ESR2*, *WUS* and *STM* (Matsuo et al., 2011; Iwase et al., 2017). Indeed, the expression levels of *WIND1*, *ESR2*, *WUS* and *STM* are elevated in *siz1* although I could not detect significantly different expression of *ESR1* between WT and *siz1* at the time points I tested. Since *ESR1* expression is generally very low and declines after several days on SIM (Iwase et al., 2017), further expression analysis at different time points may be necessary to detect a possible upregulation of *ESR1* in *siz1*. Genetic evidence nevertheless shows that WIND1 partly mediates the enhanced shoot regeneration phenotype observed in *siz1*. How SIZ1 regulates *WIND1* expression is not clear at this point but, [redacted]. Another possibility is through the ABA-mediated pathway since SIZ1 negatively regulates ABA signaling (Miura et al., 2009) and ABA induces *WIND1* expression within 30 minutes of application (Winter et al., 2007). Since incorporation of *WIND1-SRDX* does not fully suppress the shoot regeneration phenotype in *siz1*, I predict that SIZ1 additionally regulates other pathways that function in parallel to the

WIND1-mediated pathway. It is also possible that some factors acting downstream of WIND1 are repressed by SIZ1-dependent mechanisms since *WIND1-SRDX* plants regenerate shoots in the *siz1-3* background.

Transcriptome analysis and cytokinin-response marker analysis suggest many cytokinin-induced regulators of the shoot meristem are altered in *siz1*. Some type-B response regulators that are responsible for cytokinin signaling such as ARR1 and ARR2 have been identified as candidates of SUMOylation by proteomics (Rytz et al., 2018), thus the possibility that SIZ1 directly regulates cytokinin response should be further explored. These data demonstrated that auxin response is only marginally affected by *siz1* mutation during my time course RNA-seq experiment. Other studies have demonstrated that SUMOylation regulates auxin response in the context of nutrient deficiency (Miura et al., 2011) and water-induced lateral root formation (Orosa-Puente et al., 2018), suggesting that SIZ1 and SUMO regulation of auxin is context dependent. Although auxin-induced callus is enhanced in *siz1* mutant after prolonged incubation on CIM, it is unlikely the enhanced-shoot-regeneration phenotype of *siz1* is a result of increased callus growth. Future studies using inducible complementation of SIZ1 at stage-specific manner would reveal whether SIZ1 only regulates initial wound response which affects shoot regeneration afterwards or SIZ1 regulates both wound response and shoot formation on SIM.

Chapter 3 will be submitted for publication mid 2020 to an appropriate journal

Chapter 3 will be submitted for publication mid 2020 to an appropriate journal

5.5 Summary and significance

Previous studies in several model systems of organ regeneration have shown the molecular mechanism of cellular reprograming in plants involves a coordination of stress-responsive transcriptional regulators with phytohormones cytokinin and auxin signaling. In this study I investigated the role of two important stress-response regulators during *in vitro* shoot regeneration in Arabidopsis. [redacted]

Chapter 3 will be submitted for publication mid 2020 to an appropriate journal

understanding of the stress-induced cellular reprograming in the context of *de novo* organ regeneration. These new regulators of shoot regeneration provide a putative target for improvement of organ regeneration in important crop species.

Chapter 3 will be submitted for publication mid 2020 to an appropriate journal

References

Achard P, Gusti A, Cheminant S, Alioua M, Dhondt S, Coppens F, Beemster GTS, Genschik P (2009) Gibberellin signaling controls cell proliferation rate in Arabidopsis. Curr Biol **19**: 1188–1193

Ahmadi B, Shariatpanahi ME, Teixeira da Silva JA (2014) Efficient induction of microspore embryogenesis using abscisic acid, jasmonic acid and salicylic acid in Brassica napus L. Plant Cell Tissue Organ Cult **116**: 343–351

Aida M, Ishida T, Tasaka M (1999) Shoot apical meristem and cotyledon formation during Arabidopsis embryogenesis: Interaction among the CUP-SHAPED COTYLEDON and SHOOT MERISTEMLESS genes. Development **126**: 1563–1570

Åkerfelt M, Morimoto RI, Sistonen L (2010) Heat shock factors: integrators of cell stress, development and lifespan. **11**: 545–555

Albihlal WS, Irabonosi O, Blein T, Persad R, Chernukhin I, Crespi M, Bechtold U, Mullineaux PM (2018) Arabidopsis HEAT SHOCK TRANSCRIPTION FACTORA1b regulates multiple developmental genes under benign and stress conditions. J Exp Bot **69**: 2847–2862

Atta R, Laurens L, Boucheron-Dubuisson E, Guivarc'h A, Carnero E, Giraudat-Pautot V, Rech P, Chriqui D (2009) Pluripotency of Arabidopsis xylem pericycle underlies shoot regeneration from root and hypocotyl explants grown in vitro. Plant J **57**: 626–644

Augustine RC, Vierstra RD (2018) SUMOylation: re-wiring the plant nucleus during stress and development. Curr Opin Plant Biol **45**: 143–154

Bachmair A, Novatchkova M, Potuschak T, Eisenhaber F (2001) Ubiquitylation in plants: A post-genomic look at a post-translational modification. Trends Plant Sci **6**: 463–470

Banno H (2001) Overexpression of Arabidopsis ESR1 Induces Initiation of Shoot Regeneration. Plant Cell Online **13**: 2609–2618

Barlow P (1974) Regeneration of the cap of primary roots of Zea mays. New Phytol **73**: 937–954

Becker MG, Chan A, Mao X, Girard IJ, Lee S, Elhiti M, Stasolla C, Belmonte MF (2014) Vitamin C deficiency improves somatic embryo development through distinct gene regulatory networks in Arabidopsis. J Exp Bot **65**: 5903–5918

Bhargava A, Clabaugh I, To JP, Maxwell BB, Chiang YH, Schaller GE, Loraine A, Kieber JJ (2013) Identification of cytokinin-responsive genes using microarray meta-analysis and RNA-seq in Arabidopsis. Plant Physiol **162**: 272–294

Billou I, Xu J, Wildwater M, Willemsen V, Paponov I, Frimi J, Heldstra R, Aida M, Palme K, Scheres B (2005) The PIN auxin efflux facilitator network controls growth and patterning in Arabidopsis roots. Nature **433**: 39–44

Birkenmeier GF, Ryan CA (1998) Wound signaling in tomato plants: Evidence that ABA is not a primary signal for defense gene activation. Plant Physiol **117**: 687–693

Birnbaum KD, Alvarado AS (2008) Slicing across Kingdoms: Regeneration in Plants and Animals. Cell **132**: 697–710

Blanco F, Garretón V, Frey N, Dominguez C, Pérez-Acle T, Van Der Straeten D, Jordana X, Holuigue L (2005) Identification of NPR1-dependent and independent genes early induced by salicylic acid treatment in arabidopsis. Plant Mol Biol **59**: 927–944

Bloch R (1941) Wound healing in higher plants. Bot Rev **7**: 110

Bogre L, Ligterink W, Meskiene I, Barker P, Heberle-Bors E, Huskisson N, Hirt H (1997) Wounding induces the rapid and transient activation of a specific MAP kinase pathway. Plant Cell **9**: 75–83

Bostock RM, Stermer BA (1989) Perspectives on wound healing in resistance to pathogens. Annu Rev Phytopathol Vol 27 343–371

Brutus A, Sicilia F, Macone A, Cervone F, De Lorenzo G (2010) A domain swap approach reveals a role of the plant wall-associated kinase 1 (WAK1) as a receptor of oligogalacturonides. Proc Natl Acad Sci U S A **107**: 9452–9457

Bustillo-Avendaño E, Ibáñez S, Sanz O, Barross JAS, Gude I, Perianez-Rodriguez J, Micol JL, del Pozo JC, Moreno-Risueno MA, Perez-Perez JM (2017) Regulation of hormonal control, cell reprogramming and patterning during de novo root organogenesis. Plant Physiol **176**: 1709–1727

Carranco R, Prieto-Dapena P, Almoguera C, Jordano J (2017) SUMO-Dependent Synergism Involving Heat Shock Transcription Factors with Functions Linked to Seed Longevity and Desiccation Tolerance. Front Plant Sci **8**: 1–10

Castro PH, Tavares RM, Bejarano ER, Azevedo H (2012) SUMO,a heavyweight player in plant abiotic stress responses. Cell Mol Life Sci **69**: 3269–3283

Catala R, Ouyang J, Abreu IA, Hu Y, Seo H, Zhang X, Chua N-H (2007) The Arabidopsis E3 SUMO ligase SIZ1 regulates plant growth and drought responses. Plant Cell **19**: 2952–66

Charng Y, Chang S, Chi W, Liu N, Liu H, Wang C, Wang T (2006) A Heat-Inducible Transcription Factor, HsfA2, Is Required for Extension of Acquired Thermotolerance in Arabidopsis. Plant Physiol **143**: 251–262

Chassot C, Buchala A, Schoonbeek HJ, Métraux JP, Lamotte O (2008) Wounding of Arabidopsis leaves causes a powerful but transient protection against Botrytis infection. Plant J **55**: 555–567

Chatfield SP, Capron R, Severino A, Penttila P, Alfred S, Nahal H, Provart NJ (2013) Incipient stem cell niche conversion in tissue culture: using a systems approach to probe early events in WUSCHEL-dependent conversion of lateral root primordia into shoot meristems. Plant J **73**: 798–813

Che P, Lall S, Howell SH (2007) Developmental steps in acquiring competence for shoot development in Arabidopsis tissue culture. Planta **226**: 1183–1194

Che P, Lall S, Nettleton D, Howell SH (2006) Gene expression programs during shoot, root, and callus development in Arabidopsis tissue culture. Plant Physiol **141**: 620–637

Chen L, Tong J, Xiao L, Ruan Y, Liu J, Zeng M, Huang H, Wang JW, Xu L (2016) YUCCA-mediated auxin biogenesis is required for cell fate transition occurring during de novo root organogenesis in Arabidopsis. J Exp Bot **67**: 4273–4284

Cheng ZJ, Wang L, Sun W, Zhang Y, Zhou C, Su YH, Li W, Sun TT, Zhao XY, Li XG, et al (2013) Pattern of auxin and cytokinin responses for shoot meristem induction results from the regulation of cytokinin biosynthesis by AUXIN RESPONSE FACTOR 3. Plant Physiol **161**: 240–251

Cheong YH, Chang H-S, Gupta R, Wang X, Zhu T, Luan S (2002) Transcriptional profiling reveals novel interactions between wounding, pathogen, abiotic stress, and hormonal responses in Arabidopsis. Plant Physiol **129**: 661–677

Choi J, Tanaka K, Cao Y, Qi Y, Qiu J, Liang Y, Lee SY, Stacey G (2014) Identification of a plant receptor for extracellular ATP. Science **343**: 290–4

Clough SJ, Bent AF (1998) Floral dip: A simplified method for Agrobacterium-mediated transformation of Arabidopsis thaliana. Plant J **16**: 735–743

Cohen-Peer R, Schuster S, Meiri D, Breiman A, Avni A (2010) Sumoylation of Arabidopsis heat shock factor A2 (HsfA2) modifies its activity during acquired thermotholerance. Plant Mol Biol **74**: 33–45

Conti L, Nelis S, Zhang C, Woodcock A, Swarup R, Galbiati M, Tonelli C, Napier R, Hedden P, Bennett M, et al (2014) Small ubiquitin-like modifier protein SUMO enables plants to control growth independently of the phytohormone gibberellin. Dev Cell **28**: 102–110

Cordeiro J V, Jacinto A (2013) The role of transcription-independent damage signals in the initiation of epithelial wound healing. Nat Rev Mol Cell Biol **14**: 249–262

Cortijo S, Charoensawan V, Brestovitsky A, Buning R, Ravarani C, Rhodes D, van Noort J, Jaeger KE, Wigge PA (2017) Transcriptional regulation of the ambient temperature response by

H2A.Z nucleosomes and HSF1 transcription factors in Arabidopsis. Mol Plant **10**: 1258–1273

Daimon Y, Takabe K, Tasaka M (2003) The CUP-SHAPED COTYLEDON genes promote adventitious shoot formation on calli. Plant Cell Physiol **44**: 113–121

Davalos D, Grutzendler J, Yang G, Kim J V., Zuo Y, Jung S, Littman DR, Dustin ML, Gan WB (2005) ATP mediates rapid microglial response to local brain injury in vivo. Nat Neurosci **8**: 752–758

Devireddy AR, Zandalinas SI, Gómez-Cadenas A, Blumwald E, Mittler R (2018) Coordinating the overall stomatal response of plants: Rapid leaf-to-leaf communication during light stress. Sci Signal. doi: 10.1126/scisignal.aam9514

Dolcet-Sanjuan R, Claveria E (1995) Improved shoot-tip micropropagation of Pistacia vera L. and the beneficial effects of methyl jasmonate. J Am Soc Hortic Sci **120**: 938–942

Driedonks N, Xu J, Peters JL, Park S, Rieu I (2015) Multi-level interactions between heat shock factors, heat shock proteins, and the redox system regulate acclimation to heat. Front Plant Sci **6**: 1–9

Efroni I (2017) A conceptual framework for cell identity transitions in plants. Plant Cell Physiol **0**: 1–11

Efroni I, Mello A, Nawy T, Ip PL, Rahni R, Delrose N, Powers A, Satija R, Birnbaum KD (2016) Root Regeneration Triggers an Embryo-like Sequence Guided by Hormonal Interactions. Cell **165**: 1721–1733

Ellis C, Turner JG (2002) A conditionally fertile coi1 allele indicates cross-talk between plant hormone signalling pathways in Arabidopsis thaliana seeds and young seedlings. Planta **215**: 549–556

Evans MJ, Choi W-G, Gilroy S, Morris RJ (2016) A ROS-Assisted Calcium Wave Dependent on the AtRBOHD NADPH Oxidase and TPC1 Cation Channel Propagates the Systemic Response to Salt Stress. Plant Physiol **171**: 1771–1784

Fan M, Xu C, Xu K, Hu Y (2012) LATERAL ORGAN BOUNDARIES DOMAIN transcription factors direct callus formation in Arabidopsis regeneration. Cell Res **22**: 1169–1180

Feldman LJ (1976) The de novo origin of the quiescent center regenerating root apices of Zea mays. Planta **128**: 207–212

Finkelstein RR, Gampala SSL, Rock CD (2002) Abscisic acid signaling in seeds and seedlings. Plant Cell **14**: 15–46

Frerigmann H, Gigolashvili T (2014) MYB34, MYB51, and MYB122 distinctly regulate indolic glucosinolate biosynthesis in arabidopsis Thaliana. Mol Plant **7**: 814–828

Gallois J-L, Nora FR, Mizukami Y, Sablowski R (2004) WUSCHEL induces shoot stem cell activity and developmental plasticity in the root meristem. Genes Dev **18**: 375–380

Gilroy S, Suzuki N, Miller G, Choi WG, Toyota M, Devireddy AR, Mittler R (2014) A tidal wave of signals: Calcium and ROS at the forefront of rapid systemic signaling. Trends Plant Sci **19**: 623–630

Goda H, Sasaki E, Akiyama K, Maruyama-Nakashita A, Nakabayashi K, Li W, Ogawa M, Yamauchi Y, Preston J, Aoki K, et al (2008) The AtGenExpress hormone and chemical treatment data set: Experimental design, data evaluation, model data analysis and data access. Plant J **55**: 526–542

Goh T, Joi S, Mimura T, Fukaki H (2012) The establishment of asymmetry in Arabidopsis lateral root founder cells is regulated by LBD16/ASL18 and related LBD/ASL proteins. Development **139**: 883–893

Gou M, Huang Q, Qian W, Zhang Z, Jia Z, Hua J (2017) Sumoylation E3 ligase SIZ1 modulates plant immunity partly through the immune receptor gene SNC1 in arabidopsis. Mol Plant-Microbe Interact **30**: 334–342

Gravino M, Savatin DV, MacOne A, De Lorenzo G (2015) Ethylene production in Botrytis cinerea- and oligogalacturonide-induced immunity requires calcium-dependent protein kinases. Plant J **84**: 1073–1086

Guerra D, Crosatti C, Khoshro HH, Mastrangelo AM, Mica E, Mazzucotelli E (2015) Post-transcriptional and post-translational regulations of drought and heat response in plants: A spider's web of mechanisms. Front Plant Sci **6**: 1–14

Hammoudi V, Fokkens L, Beerens B, Vlachakis G, Chatterjee S, Arroyo-Mateos M, Wackers PFK, Jonker MJ, van den Burg HA (2018) The Arabidopsis SUMO E3 ligase SIZ1 mediates the temperature dependent trade-off between plant immunity and growth. PLoS Genet **14**: 1–26

Hander T, Fernández-Fernández ÁD, Kumpf RP, Willems P, Schatowitz H, Rombaut D, Staes A, Nolf J, Pottie R, Yao P, et al (2019) Damage on plants activates Ca 2+ -dependent metacaspases for release of immunomodulatory peptides. Science (80-). doi: 10.1126/science.aar7486

Heyman J, Cools T, Canher B, Shavialenka S, Traas J, Vercauteren I, Van den Daele H, Persiau G, De Jaeger G, Sugimoto K (2016) The heterodimeric transcription factor complex ERF115–PAT1 grants regeneration competence. Nat plants **2**: 16165

Heyman J, Cools T, Vandenbussche F, Heyndrickx KS, Van Leene J, Vercauteren I, Vanderauwera S, Vandepoele K, De Jaeger G, Van Der Straeten D (2013) ERF115 controls root quiescent center cell division and stem cell replenishment. Science (80-) **342**: 860–863

Hietakangas V, Ahlskog JK, Jakobsson AM, Hellesuo M, Sahlberg NM, Holmberg CI, Mikhailov A, Palvimo JJ, Pirkkala L, Sistonen L (2003) Phosphorylation of serine 303 is a prerequisite for the stress-inducible SUMO modification of heat shock factor 1. Mol Cell Biol **23**: 2953–68

Hietakangas V, Anckar J, Blomster HA, Fujimoto M, Palvimo JJ, Nakai A, Sistonen L (2005) PDSM, a motif for phosphorylation-dependent SUMO modification. Proc Natl Acad Sci **103**: 45–50

Hoermayer L, Friml J (2019) Targeted cell ablation-based insights into wound healing and restorative patterning. Curr Opin Plant Biol **52**: 124–130

Holmberg CI, Hietakangas V, Mikhailov A, Rantanen JO, Kallio M, Meinander A, Hellman J, Morrice N, MacKintosh C, Morimoto RI, et al (2001) Phosphorylation of serine 230 promotes inducible transcriptional activity of heat shock factor 1. EMBO J **20**: 3800–3810

Ikeda M, Mitsuda N, Ohme-Takagi M (2011) Arabidopsis HsfB1 and HsfB2b act as repressors of the expression of heat-Inducible Hsfs but positively regulate the acquired Thermotolerance. Plant Physiol **157**: 1243–1254

Ikeda Y, Banno H, Niu QW, Howell SH, Chua NH (2006) The ENHANCER of SHOOT REGENERATION 2 gene in Arabidopsis regulates CUP-SHAPED COTYLEDON 1 at the transcriptional level and controls cotyledon development. Plant Cell Physiol **47**: 1443–1456

Ikeuchi M, Favero DS, Sakamoto Y, Iwase A, Coleman D, Rymen B, Sugimoto K (2019) Molecular Mechanisms of Plant Regeneration. Annu Rev Plant Biol 1–30

Ikeuchi M, Iwase A, Rymen B, Lambolez A, Kojima M, Takebayashi Y, Heyman J, Watanabe S, Seo M, De Veylder L, et al (2017) Wounding triggers callus formation via dynamic hormonal and transcriptional changes. Plant Physiol **175**: 1158–1174

Ikeuchi M, Ogawa Y, Iwase A, Sugimoto K (2016) Plant regeneration: cellular origins and molecular mechanisms. Development **143**: 1442–1451

Ikeuchi M, Shibata M, Rymen B, Iwase A, Bågman A-M, Watt L, Coleman D, Favero DS, Takahashi T, Ahnert SE, et al (2018) A gene regulatory network for cellular reprogramming in plant regeneration. Plant Cell Physiol 1–13

Ikeuchi M, Sugimoto K, Iwase A (2013) Plant callus: mechanisms of induction and repression. Plant Cell **25**: 3159–73

Ishida T, Fujiwara S, Miura K, Stacey N, Yoshimura M, Schneider K, Adachi S, Minamisawa K, Umeda M, Sugimoto K (2009) SUMO E3 ligase HIGH PLOIDY2 regulates endocycle onset and meristem maintenance in Arabidopsis. Plant Cell **21**: 2284–2297

Ishida T, Yoshimura M, Miura K, Sugimoto K (2012) MMS21/HPY2 and SIZ1, two Arabidopsis SUMO E3 Ligases, have Distinct functions in development. PLoS One **7**: 1–10

Ishikawa M, Murata T, Sato Y, Nishiyama T, Hiwatashi Y, Imai A, Kimura M, Sugimoto N, Akita A, Oguri Y (2011) Physcomitrella cyclin-dependent kinase A links cell cycle reactivation to other cellular changes during reprogramming of leaf cells. Plant Cell **23**: 2924–2938

Iwase A, Harashima H, Ikeuchi M, Rymen B, Ohnuma M, Komaki S, Morohashi K, Kurata T, Nakata M, Ohme-Takagi M, et al (2017) WIND1 promotes shoot regeneration through transcriptional activation of ENHANCER OF SHOOT REGENERATION1 in Arabidopsis. Plant Cell **29**: 54–69

Iwase A, Mita K, Nonaka S, Ikeuchi M, Koizuka C, Ohnuma M, Ezura H, Imamura J, Sugimoto K (2015) WIND1-based acquisition of regeneration competency in Arabidopsis and rapeseed. J Plant Res **128**: 389–397

Iwase A, Mitsuda N, Koyama T, Hiratsu K, Kojima M, Arai T, Inoue Y, Seki M, Sakakibara H, Sugimoto K, et al (2011) The AP2/ERF transcription factor WIND1 controls cell dedifferentiation in arabidopsis. Curr Biol **21**: 508–514

Jin JB, Jin YH, Lee J, Miura K, Yoo CY, Kim WY, Van Oosten M, Hyun Y, Somers DE, Lee I, et al (2008) The SUMO E3 ligase, AtSIZ1, regulates flowering by controlling a salicylic acid-mediated floral promotion pathway and through affects on FLC chromatin structure. Plant J **53**: 530–540

Kamada H, Kobayashi K, Kiyosue T, Harada H (1989) Stress induced somatic embryogenesis in carrot and its application to synthetic seed production. Vitr Cell Dev Biol - Anim **25**: 1163–1166

Kamada H, Tachikawa Y, Saitou T, Harada H (1994) Heat Stress Induction of Carrot Somatic Embryogenesis. Plant Tissue Cult Lett **11**: 229–232

Kareem A, Durgaprasad K, Sugimoto K, Du Y, Pulianmackal AJ, Trivedi ZB, Abhayadev P V., Pinon V, Meyerowitz EM, Scheres B, et al (2015) PLETHORA genes control regeneration by a two-step mechanism. Curr Biol **25**: 1017–1030

Kareem A, Roy M V, Radhakrishnan D, Sugimoto K, Sondhi Y, Aiyaz M, Prasad K (2016) De novo assembly of plant body plan : a step ahead of Deadpool. 182–197

Keller WA, Armstrong KC (1979) Stimulation of embryogenesis and haploid production in Brassica campestris anther cultures by elevated temperature treatments. Theor Appl Genet **55**: 65–67

Kikuchi A, Sanuki N, Higashi K, Koshiba T, Kamada H (2006) Abscisic acid and stress treatment are essential for the acquisition of embryogenic competence by carrot somatic cells. Planta **223**: 637–645

Kim J, Yang W, Forner J, Lohmann JU, Noh B, Noh Y (2018) Epigenetic reprogramming by histone acetyltransferase HAG1/AtGCN5 is required for pluripotency acquisition in *Arabidopsis*. EMBO J e98726

Kim JY, Song JT, Seo HS (2017) Post-translational modifications of Arabidopsis E3 SUMO ligase AtSIZ1 are controlled by environmental conditions. FEBS Open Bio **7**: 1622–1634

Kim M, McGinnis W (2011) Phosphorylation of Grainy head by ERK is essential for wound-dependent regeneration but not for development of an epidermal barrier. Proc Natl Acad Sci U S A **108**: 650–5

Kim S Il, Kwak JS, Song JT, Seo HS (2016) The E3 SUMO ligase AtSIZ1 functions in seed germination in Arabidopsis. Physiol Plant **158**: 256–271

Kiyosue T, Kamada H, Harada H (1989) Induction of somatic embryogenesis by salt stress in carrot. Plant Tissue Cult Lett **6**: 162–164

Kobayashi M, Ohura I, Kawakita K, Yokota N, Fujiwara M, Shimamoto K, Doke N, Yoshioka H (2007) Calcium-Dependent Protein Kinases Regulate the Production of Reactive Oxygen Species by Potato NADPH Oxidase. Plant Cell Online **19**: 1065–1080

Kong X, Luo X, Qu GP, Liu P, Jin JB (2017) Arabidopsis SUMO protease ASP1 positively regulates flowering time partially through regulating FLC stability. J Integr Plant Biol **59**: 15–29

Koo AJK, Gao X, Daniel Jones A, Howe GA (2009) A rapid wound signal activates the systemic synthesis of bioactive jasmonates in Arabidopsis. Plant J **59**: 974–986

Kotak S, Larkindale J, Lee U, von Koskull-Döring P, Vierling E, Scharf KD (2007) Complexity of the heat stress response in plants. Curr Opin Plant Biol **10**: 310–316

Kraft E, Stone SL, Ma L, Su N, Gao Y, Lau O, Deng X, Callis J, Kraft E, Stone SL, et al (2016) Genome Analysis and Functional Characterization of the E2 and RING-Type E3 Ligase Ubiquitination Enzymes of Arabidopsis. **139**: 1597–1611

Kurepa J, Walker JM, Smalle J, Gosink MM, Davis SJ, Durham TL, Sung D-Y, Vierstra RD (2003) The small ubiquitin-like modifier (SUMO) protein modification system in Arabidopsis. J Biol Chem **278**: 6862–6872

Kwak JS, Son GH, Kim S-I, Song JT, Seo HS (2016) Arabidopsis HIGH PLOIDY2 Sumoylates and Stabilizes Flowering Locus C through Its E3 Ligase Activity. Front Plant Sci **7**: 1–9

Langmead B, Salzberg SL (2012) Fast gapped-read alignment with Bowtie 2. Nat Methods **9**: 357–359

Lee J, Nam J, Park HC, Na G, Miura K, Jin JB, Yoo CY, Baek D, Kim DH, Jeong JC, et al (2007) Salicylic acid-mediated innate immunity in Arabidopsis is regulated by SIZ1 SUMO E3 ligase. Plant J **49**: 79–90

León J, Rojo E, Sánchez-Serrano JJ (2001) Wound signalling in plants. J Exp Bot **52**: 1–9

Lin XL, Niu D, Hu ZL, Kim DH, Jin YH, Cai B, Liu P, Miura K, Yun DJ, Kim WY, et al (2016) An Arabidopsis SUMO E3 Ligase, SIZ1, negatively regulates photomorphogenesis by promoting COP1 activity. PLoS Genet **12**: 1–21

Liu C, Yu H, Li L (2019) SUMO modification of LBD30 by SIZ1 regulates secondary cell wall formation in Arabidopsis Thaliana. PLoS Genet **15**: 1–19

Liu H, Charng Y (2013) Common and Distinct Functions of Arabidopsis Class A1 and A2 Heat Shock Factors in Diverse Abiotic Stress Responses and Development. Plant Physiol **163**: 276–290

Liu HC, Liao HT, Charng YY (2011) The role of class A1 heat shock factors (HSFA1s) in response to heat and other stresses in Arabidopsis. Plant, Cell Environ **34**: 738–751

Liu HT, Gao F, Li GL, Han JL, Liu DL, Sun DY, Zhou RG (2008) The calmodulin-binding protein kinase 3 is part of heat-shock signal transduction in Arabidopsis thaliana. Plant J **55**: 760–773

Liu J, Hu X, Qin P, Prasad K, Hu Y, Xu L (2018a) The WOX11 - LBD16 pathway promotes pluripotency acquisition in callus cells during de novo shoot regeneration in tissue culture. Plant Cell Physiol **59**: 734–743

Liu J, Sheng L, Xu Y, Li J, Yang Z, Huang H, Xu L (2014) WOX11 and 12 Are Involved in the First-Step Cell Fate Transition during de Novo Root Organogenesis in Arabidopsis. Plant Cell **26**: 1081–1093

Liu W, Yu J, Ge Y, Qin P, Xu L (2018b) Pivotal role of LBD16 in root and root-like organ initiation. Cell Mol Life Sci **75**: 3329–3338

Liu Y, Lai J, Yu M, Wang F, Zhang J, Jiang J, Hu H, Wu Q, Lu G, Xu P, et al (2016) The Arabidopsis SUMO E3 ligase AtMMS21 dissociates the E2Fa/DPa complex in cell cycle regulation. Plant Cell **28**: 2225–2237

Lomelí H, Vázquez M (2011) Emerging roles of the SUMO pathway in development. Cell Mol Life Sci **68**: 4045–4064

Mace KA, Pearson JC, McGinnis W (2005) An epidermal barrier wound repair pathway in *Drosophila* is mediated by grainy head. Science (80-) **308**: 381–385

Marhava P, Hoermayer L, Yoshida S, Marhavý P, Benková E, Friml J (2019) Re-activation of stem cell pathways for pattern restoration in plant wound healing. Cell 957–969

Matsuo N, Makino M, Banno H (2011) Arabidopsis ENHANCER OF SHOOT REGENERATION (ESR)1 and ESR2 regulate in vitro shoot regeneration and their expressions are differentially regulated. Plant Sci **181**: 39–46

Mattei B, Spinelli F, Pontiggia D, De Lorenzo G (2016) Comprehensive Analysis of the Membrane

Phosphoproteome Regulated by Oligogalacturonides in Arabidopsis thaliana. Front Plant Sci **7**: 1107

Mazzucotelli E, Mastrangelo AM, Crosatti C, Guerra D, Stanca AM, Cattivelli L (2008) Abiotic stress response in plants: When post-transcriptional and post-translational regulations control transcription. Plant Sci **174**: 420–431

Mcconn M, Creelman RA, Bell E, Mullet JE, Browse J (1997) Jasmonate is essential for insect defense in Arabidopsis. Proc Natl Acad Sci U S A **94**: 5473–5477

Meng WJ, Cheng ZJ, Sang YL, Zhang MM, Rong XF, Wang ZW, Tang YY, Zhang XS (2017) Type-B ARABIDOPSIS RESPONSE REGULATORs Specify the Shoot Stem Cell Niche by Dual Regulation of WUSCHEL Plant Cell **29**: 1357 LP – 1372

Miller G, Mittler R (2006) Could heat shock transcription factors function as hydrogen peroxide sensors in plants? Ann Bot **98**: 279–288

Miller G, Schlauch K, Tam R, Cortes D, Torres MA, Shulaev V, Dangl JL, Mittler R (2009) The plant NADPH oxidase RBOHD mediates rapid systemic signaling in response to diverse stimuli. Sci Signal **2**: ra45–ra45

Miller MJ, Barrett-Wilt GA, Hua Z, Vierstra RD (2010) Proteomic analyses identify a diverse array of nuclear processes affected by small ubiquitin-like modifier conjugation in Arabidopsis. Proc Natl Acad Sci U S A **107**: 16512–16517

Miller MJ, Scalf M, Rytz TC, Hubler SL, Smith LM, Vierstra RD (2013) Quantitative Proteomics Reveals Factors Regulating RNA Biology as Dynamic Targets of Stress-induced SUMOylation in *Arabidopsis*. Mol Cell Proteomics **12**: 449–463

Miura K, Lee J, Gong Q, Ma S, Jin JB, Yoo CY, Miura T, Sato A, Bohnert HJ, Hasegawa PM (2011) SIZ1 regulation of phosphate starvation-induced root architecture remodeling involves the control of auxin accumulation. Plant Physiol **155**: 1000–1012

Miura K, Lee J, Jin JB, Yoo CY, Miura T, Hasegawa PM (2009) Sumoylation of ABI5 by the Arabidopsis SUMO E3 ligase SIZ1 negatively regulates abscisic acid signaling. Proc Natl Acad Sci U S A **106**: 5418–23

Miura K, Lee J, Miura T, Hasegawa PM (2010) SIZ1 controls cell growth and plant development in arabidopsis through salicylic acid. Plant Cell Physiol **51**: 103–113

Motte H, Vereecke D, Geelen D, Werbrouck S (2014) The molecular path to in vitro shoot regeneration. Biotechnol Adv **32**: 107–121

Mousavi SAR, Chauvin A, Pascaud F, Kellenberger S, Farmer EE (2013) GLUTAMATE RECEPTOR-LIKE genes mediate leaf-to-leaf wound signalling. Nature **500**: 422–426

Mozgová I, Muñoz-Viana R, Hennig L (2017) PRC2 Represses Hormone-Induced Somatic Embryogenesis in Vegetative Tissue of Arabidopsis thaliana. PLoS Genet **13**: 1–27

Nemhauser JL, Hong F, Chory J (2006) Different Plant Hormones Regulate Similar Processes through Largely Nonoverlapping Transcriptional Responses. Cell **126**: 467–475

Niethammer P (2016) The early wound signals. Curr Opin Genet Dev **40**: 17–22

Niethammer P, Grabher C, Look AT, Mitchison TJ (2009) A tissue-scale gradient of hydrogen peroxide mediates rapid wound detection in zebrafish. Nature **459**: 996–999

Nishizawa A, Yabuta Y, Yoshida E, Maruta T, Yoshimura K, Shigeoka S (2006) Arabidopsis heat shock transcription factor A2 as a key regulator in response to several types of environmental stress. Plant J **48**: 535–547

Niu D, Lin XL, Kong X, Qu GP, Cai B, Lee J, Jin JB (2019) SIZ1-Mediated SUMOylation of TPR1 Suppresses Plant Immunity in Arabidopsis. Mol Plant **12**: 215–228

Ogawa D, Yamaguchi K, Nishiuchi T (2007) High-level overexpression of the Arabidopsis HsfA2 gene confers not only increased themotolerance but also salt/osmotic stress tolerance and enhanced callus growth. J Exp Bot **58**: 3373–3383

Ogawa T, Ara T, Aoki K, Suzuki H, Shibata D (2010) Transient increase in salicylic acid and its glucose conjugates after wounding in Arabidopsis leaves. Plant Biotechnol **27**: 205–209

Ohama N, Kusakabe K, Mizoi J, Zhao H, Kidokoro S, Koizumi S, Takahashi F, Ishida T, Yanagisawa S, Shinozaki K, et al (2016a) The transcriptional cascade in the heat stress response of Arabidopsis is strictly regulated at the expression levels of transcription factors. Plant Cell. doi: 10.1105/tpc.15.00435

Ohama N, Sato H, Shinozaki K, Yamaguchi-Shinozaki K (2016b) Transcriptional Regulatory Network of Plant Heat Stress Response. Trends Plant Sci **22**: 53–65

Olate E, Jiménez-gómez JM, Holuigue L, Salinas J (2018) NPR1 mediates a novel regulatory pathway in cold acclimation by interacting with HSFA1 factors. Nat Plants. doi: 10.1038/s41477-018-0254-2

Omelyanchuk NA, Wiebe DS, Novikova DD, Levitsky VG, Klimova N, Gorelova V, Weinholdt C, Vasiliev G V., Zemlyanskaya E V., Kolchanov NA, et al (2017) Auxin regulates functional gene groups in a fold-change-specific manner in Arabidopsis thaliana roots. Sci Rep **7**: 1–11

Orosa-Puente B, Leftley N, von Wangenheim D, Banda J, Srivastava AK, Hill K, Truskina J, Bhosale R, Morris E, Srivastava M, et al (2018) Root branching toward water involves posttranslational modification of transcription factor ARF7. Science (80-) **362**: 1407–1410

Papdi C, Ábrahám E, Joseph MP, Popescu C, Koncz C, Szabados L (2008) Functional identification of Arabidopsis stress regulatory genes using the controlled cDNA overexpression system. Plant Physiol **147**: 528–542

Park OS, Bae SH, Kim SG, Seo PJ (2019) JA-pretreated hypocotyl explants potentiate de novo shoot regeneration in Arabidopsis. Plant Signal Behav **14**: 1–3

Paulraj S, Lopez-Villalobos A, Yeung EC (2014) Abscisic acid promotes shoot regeneration in Arabidopsis zygotic embryo explants. Vitr Cell Dev Biol - Plant **50**: 627–637

Pernas M, Ryan E, Dolan L (2010) SCHIZORIZA controls tissue system complexity in plants. Curr Biol **20**: 818–823

Porco S, Larrieu A, Du Y, Gaudinier A, Goh T, Swarup K, Swarup R, Kuempers B, Bishopp A, Lavenus J, et al (2016) Lateral root emergence in Arabidopsis is dependent on transcription factor LBD29 regulation of auxin influx carrier LAX3. Dev **143**: 3340–3349

Qi Z, Stephens NR, Spalding EP (2006) Calcium entry mediated by GLR3.3, an Arabidopsis gutamate receptor with a broad agonist profile. Plant Physiol **142**: 963–971

Rau A, Gallopin M, Celeux G, Jaffrézic F (2013) Data-based filtering for replicated high-throughput transcriptome sequencing experiments. Bioinformatics **29**: 2146–2152

Reindl a, Schöffl F, Schell J, Koncz C, Bakó L (1997) Phosphorylation by a cyclin-dependent kinase modulates DNA binding of the Arabidopsis heat-shock transcription factor HSF1 in vitro. Plant Physiol **115**: 93–100

Reinhardt D, Frenz M, Mandel T, Kuhlemeier C (2003) Microsurgical and laser ablation analysis of interactions between the zones and layers of the tomato shoot apical meristem. Development **130**: 4073–4083

Reymond P, Grünberger S, Paul K, Müller M, Farmer EE (1995) Oligogalacturonide defense signals in plants: Large fragments interact with the plasma membrane in vitro. Proc Natl Acad Sci U S A **92**: 4145–4149

Reymond P, Weber H, Damond M, Farmer EE (2000) Differential gene expression in response to mechanical wounding and insect feeding in Arabidopsis. Plant Cell **12**: 707–719

Richter K, Haslbeck M, Buchner J (2010) The heat shock response: life on the verge of death. Mol Cell **40**: 253–266

Robinson MD, McCarthy DJ, Smyth GK (2009) edgeR: A Bioconductor package for differential expression analysis of digital gene expression data. Bioinformatics **26**: 139–140

Rojo E, León J, Sánchez-Serrano JJ (1999) Cross-talk between wound signalling pathways determines local versus systemic gene expression in Arabidopsis thaliana. Plant J **20**: 135–142

Rosspopoff O, Chelysheva L, Saffar J, Lecorgne L, Gey D, Caillieux E, Colot V, Roudier F, Hilson P, Berthomé R, et al (2017) Direct conversion of root primordium into shoot meristem relies on timing of stem cell niche development. Development **144**: 1187–1200

Rymen B, Kawamura A, Lambolez A, Inagaki S, Takebayashi A, Iwase A, Sakamoto Y, Sako K, Favero DS, Ikeuchi M, et al (2019) Histone acetylation orchestrates wound-induced transcriptional activation and cellular reprogramming in Arabidopsis. Commun Biol **2**: 1–15

Rytz TC, Miller MJ, McLoughlin F, Augustine RC, Marshall RS, Juan YT, Charng YY, Scalf M, Smith LM, Vierstra RD (2018) SUMOylome profiling reveals a diverse array of nuclear targets modified by the SUMO ligase SIZ1 during heat stress. Plant Cell **30**: 1077–1099

Sadanandom A, Ádám É, Orosa B, Viczián A, Klose C, Zhang C, Josse E-M, Kozma-Bognár L, Nagy F (2015) SUMOylation of phytochrome-B negatively regulates light-induced signaling in *Arabidopsis thaliana*. Proc Natl Acad Sci **112**: 11108–11113

Saracco SA, Miller MJ, Kurepa J, Vierstra RD (2007) Genetic analysis of SUMOylation in Arabidopsis: Conjugation of SUMO1 and SUMO2 to nuclear proteins is essential. Plant Physiol **145**: 119–134

Scheres B (2007) Stem-cell niches: Nursery rhymes across kingdoms. Nat Rev Mol Cell Biol **8**: 345–354

Schmidt R, Schippers JHM (2015) ROS-mediated redox signaling during cell differentiation in plants. Biochim Biophys Acta - Gen Subj **1850**: 1497–1508

Schmollinger S, Schulz-Raffelt M, Strenkert D, Veyel D, Vallon O, Schroda M (2013) Dissecting the heat stress response in chlamydomonas by pharmaceutical and RNAi approaches reveals conserved and novel aspects. Mol Plant **6**: 1795–1813

Sena G, Wang X, Liu H-Y, Hofhuis H, Birnbaum KD (2009) Organ regeneration does not require a functional stem cell niche in plants. Nature **457**: 1150

Shibata M, Breuer C, Kawamura A, Clark NM, Rymen B, Braidwood L, Morohashi K, Busch W, Benfey PN, Sozzani R, et al (2018) GTL1 and DF1 regulate root hair growth through transcriptional repression of *ROOT HAIR DEFECTIVE 6-LIKE 4* in *Arabidopsis*. Development **145**: dev159707

Shiio Y, Eisenman RN (2003) Histone sumoylation is associated with transcriptional repression. Proc Natl Acad Sci **100**: 13225–13230

Shinozaki K, Yamaguchi-Shinozaki K (1998) Molecular responses to drought stress. Stress Responses Photosynth Org 149–163

Srivastava AK, Orosa B, Singh P, Cummins I, Walsh C, Zhang C, Grant M, Roberts MR, Anand GS, Fitches E, et al (2018) SUMO suppresses the activity of the jasmonic acid receptor CORONATINE INSENSITIVE 1. Plant Cell **1**: tpc.00036.2018

Stobbe H, Schmitt U, Eckstein D, Dujesiefken D (2002) Developmental stages and fine structure of surface callus formed after debarking of living lime trees (Tilia sp.). Ann Bot **89**: 773–782

Su YH, Zhao XY, Liu YB, Zhang CL, O'Neill SD, Zhang XS (2009) Auxin-induced WUS expression is essential for embryonic stem cell renewal during somatic embryogenesis in Arabidopsis. Plant J **59**: 448–460

Sugimoto K, Gordon SP, Meyerowitz EM (2011) Regeneration in plants and animals: Dedifferentiation, transdifferentiation, or just differentiation? Trends Cell Biol **21**: 212–218

Sugimoto K, Jiao Y, Meyerowitz EM (2010) Arabidopsis Regeneration from multiple tissues occurs via a root development pathway. Dev Cell **18**: 463–471

Sugiyama M (2015) Historical review of research on plant cell dedifferentiation. J Plant Res **128**: 349–359

Sukumar P, Maloney G, Muday GK (2013) Localized induction of the ATP-Binding cassette B19 auxin transporter enhances adventitious root formation in Arabidopsis. Plant Physiol **162**: 1392–1405

Sun JQ, Jiang HL, Li CY (2011) Systemin/jasmonate-mediated systemic defense signaling in tomato. Mol Plant **4**: 607–615

Sussex IM (1964) The permanence of meristems: developmental organizers or reactors to exogenous stimuli. Brookhaven Symp Biol. pp 1–12

Suzuki N, Miller G, Salazar C, Mondal HA, Shulaev E, Cortes DF, Shuman JL, Luo X, Shah J, Schlauch K, et al (2013) Temporal-spatial interaction between reactive oxygen species and abscisic acid regulates rapid systemic acclimation in plants. Plant Cell **25**: 3553–3569

Szechyńska-Hebda M, Skrzypek E, Dabrowska G, Wędzony M, van Lammeren A (2012) The effect of endogenous hydrogen peroxide induced by cold treatment in the improvement of tissue regeneration efficiency. Acta Physiol Plant **34**: 547–560

Tampe PA, Reid DM, Thorpe TA (2001) Jasmonic acid inhibition of in vitro shoot organogenesis in Pinus radiata cotyledons. J Plant Physiol **158**: 607–611

Tanaka K, Choi J, Cao Y, Stacey G (2014) Extracellular ATP acts as a damage-associated molecular pattern (DAMP) signal in plants. Front Plant Sci **5**: 446

Toyota M, Spencer D, Sawai-Toyota S, Jiaqi W, Zhang T, Koo AJ, Howe GA, Gilroy S (2018) Glutamate triggers long-distance, calcium-based plant defense signaling. Science (80-) **361**: 1112–1115

Tucker MR, Hinze A, Tucker EJ, Takada S, Jürgens G, Laux T (2008) Vascular signalling mediated by ZWILLE potentiates WUSCHEL function during shoot meristem stem cell development in the Arabidopsis embryo. Development **135**: 2839–2843

Valvekens D, Van Montagu M, Van Lijsebettens M (1988) Agrobacterium tumefaciens-mediated transformation of Arabidopsis thaliana root explants by using kanamycin selection. Proc Natl Acad Sci U S A **85**: 5536–40

Volkov RA, Panchuk II, Mullineaux PM, Schöffl F (2006) Heat stress-induced H2O2 is required for effective expression of heat shock genes in Arabidopsis. Plant Mol Biol **61**: 733–746

Vu LD, Gevaert K, De Smet I (2018) Feeling the heat: searching for plant thermosensors. Trends Plant Sci **xx**: 1–10

Walden R, Wingender R (1995) Gene-transfer and plant-regeneration (techniques). Trends Biotechnol **13**: 324–331

Wang KLC, Li H, Ecker JR (2002) Ethylene biosynthesis and signaling networks. Plant Cell **14**: 131–152

Wickham H (2016) ggplot2: elegant graphics for data analysis. Springer

Winter D, Vinegar B, Nahal H, Ammar R, Wilson G V., Provart NJ (2007) An "electronic fluorescent pictograph" Browser for exploring and analyzing large-scale biological data sets. PLoS One **2**: 1–12

Xu J, Hofhuis H, Heidstra R, Sauer M, Friml J, Scheres B (2006) A Molecular Framework for Plant Regeneration. Science (80-) **311**: 385–388

Xuan Y, Zhou S, Wang L, Cheng Y, Zhao L (2010) Nitric oxide functions as a signal and acts upstream of atCaM3 in thermotolerance in arabidopsis seedlings. Plant Physiol **153**: 1895–1906

Yamada K, Nishimura M, Hara-Nishimura I (2004) The slow wound-response of γVPE is regulated by endogenous salicylic acid in Arabidopsis. Planta **218**: 599–605

Yin J, Xu K, Zhang J, Kumar A, Yu F-SX (2007) Wound-induced ATP release and EGF receptor activation in epithelial cells. J Cell Sci **120**: 815–825

Yoo CY, Miura K, Jin JB, Lee J, Park HC, Salt DE, Yun D-J, Bressan RA, Hasegawa PM (2006) SIZ1 small ubiquitin-like modifier E3 ligase facilitates basal thermotolerance in Arabidopsis independent of salicylic acid. Plant Physiol **142**: 1548–1558

Yoo SK, Freisinger CM, LeBert DC, Huttenlocher A (2012) Early redox, Src family kinase, and calcium signaling integrate wound responses and tissue regeneration in zebrafish. J Cell Biol **199**: 225–234

Yoshida T, Fujita Y, Sayama H, Kidokoro S, Maruyama K, Mizoi J, Shinozaki K, Yamaguchi-Shinozaki K (2010) AREB1, AREB2, and ABF3 are master transcription factors that cooperatively regulate ABRE-dependent ABA signaling involved in drought stress tolerance and require ABA for full activation. Plant J **61**: 672–685

Yoshida T, Ohama N, Nakajima J, Kidokoro S, Mizoi J, Nakashima K, Maruyama K, Kim JM, Seki M, Todaka D, et al (2011) Arabidopsis HsfA1 transcription factors function as the main positive regulators in heat shock-responsive gene expression. Mol Genet Genomics **286**: 321–332

Yoshida T, Sakuma Y, Todaka D, Maruyama K, Qin F, Mizoi J, Kidokoro S, Fujita Y, Shinozaki K, Yamaguchi-Shinozaki K (2008) Functional analysis of an Arabidopsis heat-shock transcription factor HsfA3 in the transcriptional cascade downstream of the DREB2A stress-regulatory system. Biochem Biophys Res Commun **368**: 515–521

Yu G, Wang L-G, Han Y, He Q-Y (2012) clusterProfiler: an R Package for Comparing Biological Themes Among Gene Clusters. Omi A J Integr Biol **16**: 284–287

Zandalinas SI, Sengupta S, Burks D, Azad RK, Mittler R (2019) Identification and characterization of a core set of ROS wave-associated transcripts involved in the systemic acquired acclimation response of Arabidopsis to excess light. Plant J **98**: 126–141

Zhang G, Zhao F, Chen L, Pan Y, Sun L, Bao N, Zhang T, Cui CX, Qiu Z, Zhang Y, et al (2019a) Jasmonate-mediated wound signalling promotes plant regeneration. Nat Plants **5**: 491–497

Zhang L, Han Q, Xiong J, Zheng T, Han J, Zhou H, Lin H, Yin Y, Zhang D (2019b) Sumoylation of BRI1-EMS-SUPPRESSOR 1 (BES1) by the SUMO E3 Ligase SIZ1 Negatively Regulates Brassinosteroids Signaling in Arabidopsis thaliana. Plant Cell Physiol **1**: 1–11

Zhang S, Wang S, Lv J, Liu Z, Wang Y, Ma N, Meng Q (2018) SUMO E3 Ligase SlSIZ1 Facilitates Heat Tolerance in Tomato. Plant Cell Physiol **59**: 58–71

Zhang T-Q, Lian H, Zhou C-M, Xu L, Jiao Y, Wang J-W (2017) A two-step model for de novo activation of WUSCHEL during plant shoot regeneration. Plant Cell tpc-00863

Zhao Y, Chan Z, Gao J, Xing L, Cao M, Yu C, Hu Y, You J, Shi H, Zhu Y, et al (2016) ABA receptor PYL9 promotes drought resistance and leaf senescence. Proc Natl Acad Sci U S A **113**: 1949–1954

Zhou W, Lozano-Torres JL, Blilou I, Zhang X, Zhai Q, Smant G, Li C, Scheres B (2019) A jasmonate signaling network activates root stem cells and promotes regeneration. Cell **177**: 942-956.e14

Zuo J, Niu QW, Chua NH (2000) An estrogen receptor-based transactivator XVE mediates highly inducible gene expression in transgenic plants. Plant J. doi: 10.1046/j.1365-313X.2000.00868.x

Zürcher E, Tavor-Deslex D, Lituiev D, Enkerli K, Tarr PT, Müller B (2013) A robust and sensitive synthetic sensor to monitor the transcriptional output of the cytokinin signaling network in planta. Plant Physiol **161**: 1066–1075